Investigating cellular reconstruction of the cornea in inherited disease

James McKelvie

A thesis submitted in partial fulfillment of the requirements for the degree of Doctor of Philosophy,

Department of Ophthalmology,

The University of Auckland, 2011.

Abstract

Corneal blindness affects 10 million people worldwide and has a significant detrimental impact on quality of life. One cause of corneal blindness is keratoconus, a corneal ectasia that is over represented in New Zealand Maori and Pacific populations. For the most severe forms of keratoconus the only effective treatment is corneal transplantation and currently Keratoconus represents the single largest indication for corneal transplantation in New Zealand. Despite the excellent results following corneal transplantation, there is a worldwide shortage of donor corneal tissue which is commonly the rate limiting step for timely treatment both in New Zealand and Internationally.

The aim of this research was to investigate the potential for using cultured-corneal-stromal-cell-sphere implants as an alternative to traditional corneal transplantation in early keratoconus.

Stromal cells were isolated from human corneal rims and cultured in a sphere-forming culture system. Isolated cells were sorted using fluorescence activated cell sorting (FACS) and the sphere forming capability of side population (SP) and non-SP cells was determined. The mechanisms and temporal sequence of sphere formation were investigated using live-cell, dark field, scanning electron and confocal imaging. Live keratocytes were labelled and tracked using quantum dots, azito labelled sugars and nucleotides and investigated using immunocytochemistry to monitor collagen subtype and glycoprotein expression in conjunction with cell division during sphere formation. Isolated cells were sorted using FACS before and after sphere formation and gene expression was analysed using quantitative microfluidic arrays and real time PCR. The ability for cultured stromal cells to migrate on

collagen gels and within human stromal tissue was determined using live cell labelling and time-lapse confocal microscopy.

SP and non-SP cells were capable of forming spheres in culture. Early sphere formation occurred predominantly from cell migration/aggregation. As sphere formation progressed cell proliferation played an increasing contribution in late sphere development. Primary spheroid cultures remained stable for up to 6 months and demonstrated up-regulated expression of extracellular matrix genes including the stromal collagen subtypes and proteoglycans including keratocan. Immunohistochemistry confirmed expression of collagen subtypes and keratocan in cultured spheres and deposition of azito labelled glycoproteins were detected in cultured spheres following cell aggregation during early and late sphere formation. Migration of sphere cells was observed on collagen gels and following implantation of labelled spheres into corneal stroma.

Human corneal stromal cells can be isolated and cultured using a sphere-based serum-free culture system that maintains the keratocyte phenotype. The mechanism of sphere formation and the ability to migrate and express keratocyte specific extracellular matrix indicate that stromal cell sphere implants may be an effective treatment for early keratoconus.

Acknowledgements

The past three years spent completing this PhD have been extremely exciting, challenging and rewarding. This project would not have been possible without the significant contribution of many people.

I would like to give a special thanks to my supervisors. First and foremost I would like to acknowledge my primary supervisor Professor McGhee without whom this project would not have existed. Professor McGhee has been an inspirational mentor and supervisor and I am extremely grateful for all the time and energy he has put into this project. He has given me countless hours of one-on-one teaching and advice, and I have benefited from his incredible insight into research, clinical ophthalmology and life in general, which has been pivotal over the course of my PhD and in planning my career pathway. In addition, I am very appreciative for all of the funding that Professor McGhee has arranged and assisted in obtaining so that I could concentrate on completing my studies, and present my results at numerous overseas conferences over the past three years. I could not have hoped for a better supervisor or mentor.

I am also incredibly grateful to my other supervisors, Associate Professors Dipika Patel and Trevor Sherwin. I am very thankful for all the help, support, supervision and teaching that Associate Professor Patel has given me over the duration of my PhD. From the generous project funding and ethics approval already in place at the commencement of my PhD to the meticulous editing of numerous revisions of my thesis manuscript, and brilliant (plus patient) surgical teaching, I am constantly impressed by Associate Professor Patel's efficiency and high standards. I am very grateful for all her tremendous support in completing this research project and furthering my career. Associate Professor Sherwin has also been exceptionally supportive during my PhD and I am equally grateful for his contribution. Associate Professor Sherwin has given me expert insight and advice on my experimental work, which has allowed me to successfully traverse many of the difficulties I have

faced in the laboratory during this project. He has also been very encouraging and supportive on a personal level when I have needed it most, and for this I am very appreciative.

I would like to extend my thanks to the Maurice and Phyllis Paykel Trust for providing my stipend and a travel grant to present my research overseas over the past three years during my time as a Corneal Research fellow. This generous contribution made it possible for me to study full time and provide for the needs of my family.

The incredible donation by all of the tissue donors and their families deserves a special mention. This gift of human tissue is greatly appreciated and has been essential for conducting this research. I am also thankful to all of the New Zealand National Eye Bank Staff for their help.

There are many others I would also like to thank including Jane McGhee for her technical help and advice in the laboratory, Professor Helen Danesh-Meyer for all her clinical teaching and support, Michael Plunket for his work during two summer studentships, and thanks also to co-students Stuti Misra and Isabella Chung for their friendship and encouragement over the past three years.

Finally, I cannot finish without mentioning the wonderful support and understanding that my wife Adele and children Hamish and Claire have given me throughout this PhD.

Table of Contents

List of Figures

List of Tables

Chapter 1. Corneal anatomy and biology

1.1. Gross anatomy of the cornea

The cornea is the convex, transparent, avascular structure that comprises the anterior most aspect of the eye and 16% of the total surface area of the globe.[1, 2] Viewed from the anterior aspect, the cornea is slightly elliptical with a horizontal diameter of approximately 11.9mm[3] and a vertical diameter of approximately 10.6mm (**Figure 1.1**).[2] In normal subjects central corneal thickness is approximately 0.56mm [3] and peripherally the cornea is slightly thicker at approximately 0.7mm. [2] Although there is slight individual variation in the parameters of the cornea, the anterior surface has a radius of curvature of approximately 7.7mm and the posterior surface has a radius of curvature of approximately 6.9mm. [2] The radius of corneal curvature, in combination with the indices of refraction (1.000 in air, 1.376 in cornea, and 1.336 in aqueous humor) produces a refractive power of approximately 44.4 Dioptres, comprising two thirds of the eye's focusing power.[4]

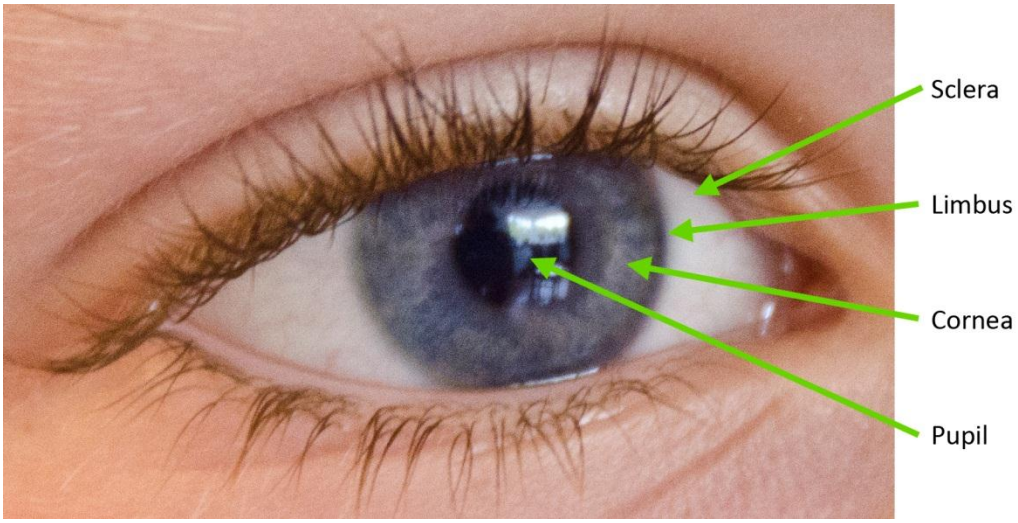

Figure 1.1 The cornea forms the transparent anterior aspect of the eye. It is elliptical with the horizontal diameter approximately 1mm greater than the vertical diameter.

1.2. The layers of the cornea

The cornea is arranged in five distinct layers. From anterior to posterior they are the epithelium, Bowman's layer, the stroma, Descemet's membrane, and the endothelium (**Figure 1.2**).

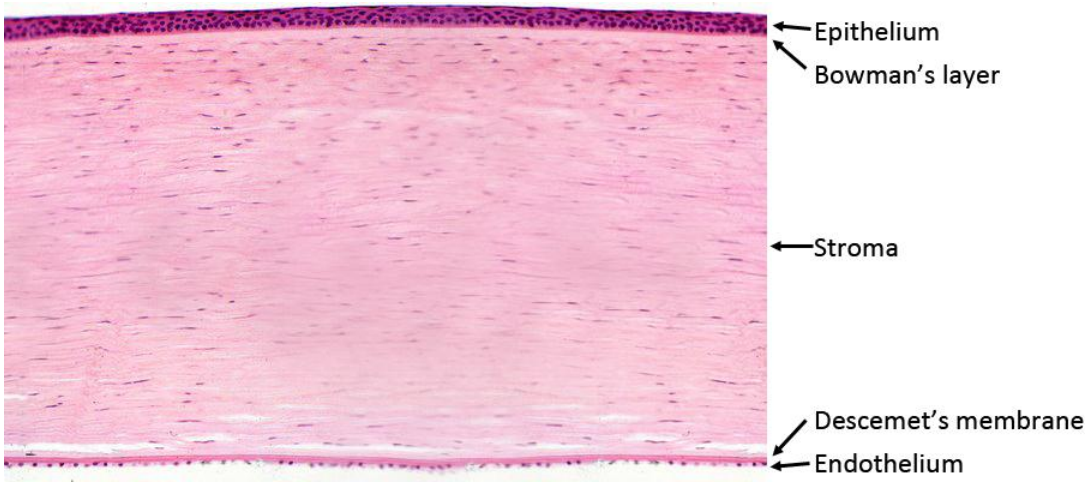

Figure 1.2 Haematoxylin and eosin labelled full thickness corneal section demonstrating the layers of the cornea. The entire section measures approximately 560µm vertically (the thickness of a normal cornea).

1.2.1. The epithelium

The epithelium is 40-50µm thick, consists of five layers of cells, is extremely uniform, and functions as the outermost barrier to the eye in combination with the tear film. [2, 5] Epithelial cells have a relatively rapid turnover with a lifespan of 7-10 days before apoptotic involution and replacement. [5] The superficial layers of epithelial cells are stratified squamous, nucleated and non-keratinized, however, the basal epithelial cells differ from the more superficial layers in that they are arranged in columnar configuration and are adherent to the underlying basement membrane and Bowman's layer. [2] The superficial epithelial cells are flattened and adhere to one another *via* tight junctions to resist tear penetration. The slightly deeper epithelial cells that comprise the central three epithelial cell layers are known as wing cells which have a less flattened appearance and also are attached with tight junctions.[3] The basal epithelial cells are 20µm thick and are adhered to one another with gap junctions and to the underlying basement membrane and the associated anchoring fibrils with hemidesmosomes. These basal epithelial cells are mitotically active giving rise to new wing and superficial epithelial cells as part of normal cell turnover. [1, 3]

1.2.2. Bowman's layer

Bowman's layer is an acellular membranous condensation of the anterior stroma that forms a smooth layer between the epithelium and the stroma. Bowman's layer is approximately 10-12µm thick and is comprised of extracellular matrix including collagen fibres in a relatively random arrangement and associated proteoglycans. [3]

1.2.3. The stroma

The corneal stroma, or substantia propria, makes up 80-90% of the total corneal thickness and is the major structural element responsible for maintaining the shape and integrity of the cornea.[3, 6, 7] The stroma is composed of extracellular matrix (ECM), cells and approximately 78% water.[5] The extracellular matrix component, which provides the structural framework for the cornea, is a combination of collagen and proteoglycans.

Collagen molecules exist as homo or hetero trimeric complexes of 1-3 different collagen α peptides which associate through an α-helical domain. [8] To date there are 28 subtypes of collagen that have been identified,[8] however, only 10 of these subtypes are expressed in the cornea.[9] The predominant stromal collagens are types I, V, and VI which are arranged as a dense regular array of parallel bundles or fibrils that form with extensive post translational modification and cross linking of the trimeric collagen subunits.[10] The size, spacing and regularity of the collagen fibrils in combination with other components of the ECM reduces light scattering and allows the cornea to remain transparent.[5, 9-11] The collagen fibrils are 21-65nm in diameter and are arranged in parallel relatively orthogonal arrays or lamellae throughout the cornea.[2] There are 200-250 lamellae within the central corneal stroma that contain fibrils of relatively anisotropic arrangement in the anterior stroma, increasingly regular orthogonal arrangement towards the posterior stroma, and circumferential arrangement in the peripheral stroma.[2, 12-16] The consequence of this differential fibril architecture throughout the stroma is increased structural integrity with the effect that stromal oedema, when

present, is directed posteriorly and results in flattening of the posterior cornea and characteristic folds in the underlying Descemet's membrane.[5]

Proteoglycans comprise the other major constituent of the stromal ECM aside from collagen. Proteoglycans are less abundant than collagen in the stroma, however the two molecules have integrated functions in the regulation of fibril production, assembly and overall structural integrity of the stromal ECM.[11, 17-19] Stromal proteoglycans consist of a protein core with glycosaminoglycan residues attached and are involved in collagen fibril assembly.[11] There are two major types of proteoglycans in the corneal stroma; either with keratan sulphate side chains (mimecan, keratocan and lumican) or with dermatan sulphate side chains (decorin).[9]

The predominant cell type residing in the corneal stroma is the keratocyte which arises from neural crest cells during development.[11] The stroma contains approximately 2-3.5 million keratocytes distributed throughout the stroma.[20] These specialised cells produce and maintain structural homeostasis within the stromal ECM *via* synthesis and deposition of collagens, proteoglycans and matrix metalloproteinases.[5] Keratocytes have a dendritic like morphology with a compact cell body and cytoplasmic lamellapodia that form an interconnecting network between neighbouring keratocytes enabling cell-to-cell communication (**Figure 1.3**).[11] In addition to production and maintenance of the ECM, stromal keratocytes are able to express cell adhesion molecules and chemotactic factors to signal and activate neutrophil and other immune cells.[21, 22] Keratocytes although relatively quiescent in the stroma under normal conditions can undergo activation, migration and myo/fibroblastic transdifferentiation with scar tissue deposition within the stroma in response to wounding and other stimuli.[11, 21-29]

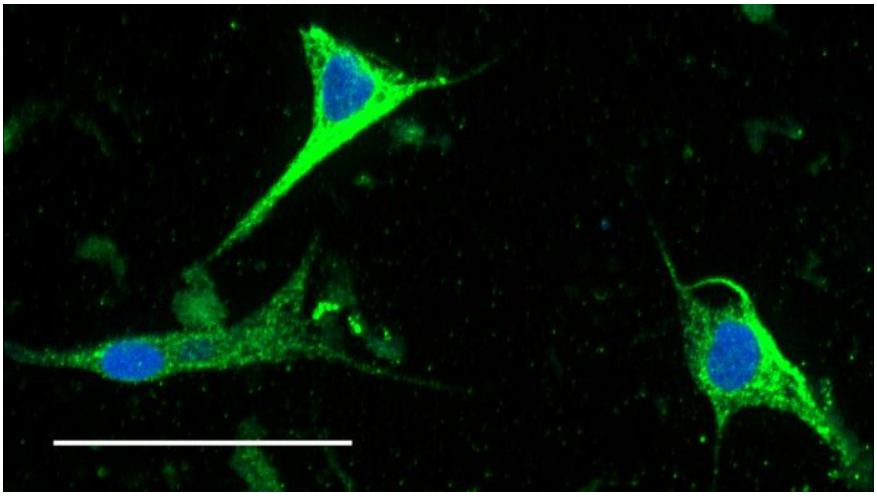

Figure 1.3 Confocal image of isolated human keratocytes demonstrating their characteristic dendritic morphology. Keratocytes nuclei are labelled blue and the cytoplasm is labelled green. In the corneal stroma these keratocytes form an interconnecting network throughout the stroma. Scale = 40 µm.

In addition to keratocytes there are several other cell types that reside within the corneal stroma. Quiescent keratocyte stem and progenitor cells, although relatively low in number compared with keratocytes are thought to act as a reservoir for regeneration of keratocytes within the stroma.[30-32]

The cornea is one of the most densely innervated tissues of the entire body and is supplied by the nasocillary branch of the ophthalmic division of the trigeminal nerve.[5] Nerve fibres enter the stroma from the periphery in radial bundles to form the subepithelial nerve plexus between the anterior stroma and Bowman's layer. Nerve fibres then penetrate Bowman's layer mostly in the region of the mid periphery and form an extensive sub basal nerve plexus beneath the basal epithelium.[2, 33]

1.2.4. Descemet's membrane

Descemet's membrane is composed of type IV collagen fibrils that are continuously secreted by the endothelial cells throughout life and acts as a basement membrane for the endothelium.[2] The membrane measures up to 10µm in thickness and is arranged in two layers that correspond to that which is deposited in utero starting at 8 weeks (the anterior layer, 3µm thickness) and that which is

deposited later in life (posterior layer).[5, 34] Descemet's membrane is distinct from the corneal stroma and can be dissected away from the stromal ECM (with intact endothelium) with relative ease.[2]

1.2.5. The endothelium

The deepest layer of the cornea is the endothelium which functions to keep the stromal ECM in a state of relative dehydration to maintain transparency. The endothelium is composed of a single layer of flattened polygonal cells that form a hexagonal honeycomb array. This monolayer of cells is of neural crest origin and originally is arranged as a 10μm thick cuboidal monolayer that eventually flattens to achieve a thickness of approximately 4μm.[2, 5] The endothelial cells actively dehydrate the stroma *via* the endothelial-membrane-bound Na^+/K^+ATPase ion transporter and the intracellular carbonic anhydrase pathway to establish an osmotic gradient to draw fluid out of the stroma and into the anterior chamber.[5] Neighbouring endothelial cells are adhered to one another by tight junctions to arrest the bulk flow of aqueous into the stroma.[2, 5] There is no cell division or reservoir for renewal of endothelial cells so following birth a gradual and progressive decline in the density of endothelial cells is observed. At birth the density of endothelial cells is approximately 3,500/mm^2 and at the normal rate of decline of 0.6% per year this is more than enough to last for a normal lifespan.[5] Once the endothelial cell density drops below approximately 500/mm^2, the remaining endothelial cells are unable to maintain the relative stromal dehydration, and stromal oedema with an associated decrease in corneal transparency and visual acuity ensues.

1.3. Conclusions

The cornea is one of the most remarkable organs in the human body. At the size and thickness of a fingernail it is able to provide most people with a lifetime of vision while maintaining transparency and protecting the delicate contents of the eye. The cornea has incredibly sophisticated mechanical structural arrangement unparalleled elsewhere in the body, and is composed of the most intricate array of specialised cells and materials that achieve an incredible balance of form and function.

1.4. References

1. Anthony JB, Bron AJ. Wolff's anatomy of the eye and orbit / anthony j. Bron, ramesh c. Tripathi, brenda j. Tripathi: London : Chapman & Hall Medical, 1997., 1997.
2. Richard SS, Snell RS. Clinical anatomy of the eye / richard s. Snell, michael a. Lemp: Malden, Mass. : Blackwell Science, c1998., 1998.
3. Sanchis-Gimeno JA, Sanchez-Zuriaga D, Martinez-Soriano F. White-to-white corneal diameter, pupil diameter, central corneal thickness and thinnest corneal thickness values of emmetropic subjects. Surgical and radiologic anatomy : SRA 2011.
4. KhabazKhoob M, Hashemi H, Yazdani K, et al. Keratometry measurements, corneal astigmatism and irregularity in a normal population: The tehran eye study. Ophthalmic & physiological optics : the journal of the British College of Ophthalmic Opticians 2010;30(6):800-5.
5. DelMonte DW, Kim T. Anatomy and physiology of the cornea. Journal of Cataract and Refractive Surgery 2011;37(3):588-98.
6. Corneal surgery : Theory, technique and tissue / lead editor, frederick s. Brightbill ... [et al.] ; illustrated by laurel cook lhowe: St. Louis, Mo. ; London : Mosby, c2009., 2009.
7. Bergmanson JP. Clinical anatomy of the external eye. Journal of the American Optometric Association 1990;61(6 Suppl):S7-15.
8. Gordon MK, Hahn RA. Collagens. Cell and Tissue Research 2010;339(1):247-57.
9. Zieske JD. Extracellular matrix and wound healing. Current Opinion in Ophthalmology 2001;12(4):237-41.
10. Michelacci YM. Collagens and proteoglycans of the corneal extracellular matrix. Brazilian Journal of Medical and Biological Research 2003;36(8):1037-46.
11. Hassell JR, Birk DE. The molecular basis of corneal transparency. Experimental Eye Research 2010;91(3):326-35.

12. Abahussin M, Hayes S, Knox Cartwright NE, et al. 3d collagen orientation study of the human cornea using x-ray diffraction and femtosecond laser technology. Investigative Ophthalmology and Visual Science 2009;50(11):5159-64.

13. Boote C, Hayes S, Abahussin M, Meek KM. Mapping collagen organization in the human cornea: Left and right eyes are structurally distinct. Investigative Ophthalmology and Visual Science 2006;47(3):901-8.

14. Boote C, Kamma-Lorger CS, Hayes S, et al. Quantification of collagen organization in the peripheral human cornea at micron-scale resolution. Biophysical Journal 2011;101(1):33-42.

15. Kamma-Lorger CS, Boote C, Hayes S, et al. Collagen and mature elastic fibre organisation as a function of depth in the human cornea and limbus. Journal of Structural Biology 2010;169(3):424-30.

16. Young RD, Swamynathan SK, Boote C, et al. Stromal edema in klf4 conditional null mouse cornea is associated with altered collagen fibril organization and reduced proteoglycans. Investigative Ophthalmology and Visual Science 2009;50(9):4155-61.

17. Beales MP, Funderburgh JL, Jester JV, Hassell JR. Proteoglycan synthesis by bovine keratocytes and corneal fibroblasts: Maintenance of the keratocyte phenotype in culture. Investigative Ophthalmology and Visual Science 1999;40(8):1658-63.

18. Hassell JR, Schrecengost PK, Rada JA, et al. Biosynthesis of stromal matrix proteoglycans and basement membrane components by human corneal fibroblasts. Investigative Ophthalmology and Visual Science 1992;33(3):547-57.

19. Musselmann K, Kane B, Alexandrou B, Hassell JR. Stimulation of collagen synthesis by insulin and proteoglycan accumulation by ascorbate in bovine keratocytes in vitro. Investigative Ophthalmology and Visual Science 2006;47(12):5260-6.

20. Moller-Pedersen T. Keratocyte reflectivity and corneal haze. Experimental Eye Research 2004;78(3):553-60.

21. Burns AR, Li Z, Smith CW. Neutrophil migration in the wounded cornea: The role of the keratocyte. Ocular Surface 2005;3(4 Suppl):S173-6.

22. Gagen D, Laubinger S, Li Z, et al. Icam-1 mediates surface contact between neutrophils and keratocytes following corneal epithelial abrasion in the mouse. Experimental Eye Research 2010;91(5):676-84.

23. Carlson EC, Wang IJ, Liu CY, et al. Altered kspg expression by keratocytes following corneal injury. Molecular Vision 2003;9:615-23.

24. Funderburgh JL, Mann MM, Funderburgh ML. Keratocyte phenotype mediates proteoglycan structure: A role for fibroblasts in corneal fibrosis. Journal of Biological Chemistry 2003;278(46):45629-37.

25. Kim A, Lakshman N, Karamichos D, Petroll WM. Growth factor regulation of corneal keratocyte differentiation and migration in compressed collagen matrices. Investigative Ophthalmology and Visual Science 2010;51(2):864-75.

26. Maatta M, Vaisanen T, Vaisanen MR, et al. Altered expression of type xiii collagen in keratoconus and scarred human cornea: Increased expression in scarred cornea is associated with myofibroblast transformation. Cornea 2006;25(4):448-53.

27. Wilson SE, Chaurasia SS, Medeiros FW. Apoptosis in the initiation, modulation and termination of the corneal wound healing response. Experimental Eye Research 2007;85(3):305-11.

28. Anderson KI, Cross R. Contact dynamics during keratocyte motility. Current Biology 2000;10(5):253-60.

29. Andresen JL, Ledet T, Ehlers N. Keratocyte migration and peptide growth factors: The effect of pdgf, bfgf, egf, igf-i, afgf and tgf-beta on human keratocyte migration in a collagen gel. Current Eye Research 1997;16(6):605-13.

30. Chen YH, Wang IJ, Young TH. Formation of keratocyte spheroids on chitosan-coated surface can maintain keratocyte phenotypes. Tissue Engineering Part A 2009;15(8):2001-13.

31. Du Y, Funderburgh ML, Mann MM, et al. Multipotent stem cells in human corneal stroma. Stem Cells 2005;23(9):1266-75.

32. Funderburgh ML, Du Y, Mann MM, et al. Pax6 expression identifies progenitor cells for corneal keratocytes. FASEB Journal 2005;19(10):1371-3.

33. Patel DV, McGhee CN. Mapping of the normal human corneal sub-basal nerve plexus by in vivo laser scanning confocal microscopy. Investigative Ophthalmology and Visual Science 2005;46(12):4485-8.

34. Murphy C, Alvarado J, Juster R. Prenatal and postnatal growth of the human descemet's membrane. Investigative Ophthalmology and Visual Science 1984;25(12):1402-15.

Chapter 2. Keratoconus: traditional management and the possibility for a new paradigm in corneal transplantation

2.1. Introduction

Corneal blindness is a significant problem worldwide and currently affects approximately 10 million people with millions more suffering from less severe, but significant, degrees of visual impairment.[1] The aetiology of corneal blindness is varied and the prevalence of individual disorders typically differs between countries. Regardless of the aetiology, corneal blindness has a significant impact on the quality of life of those affected.[1]

Keratoconus is a non-inflammatory, progressive ectasia of the cornea that typically manifests with progressively deteriorating vision in the second and third decades of life.[2] Visual impairment or blindness in keratoconic patients is associated with a profound decrease in quality of life that is disproportionate to what may be clinically expected when compared to other causes of blindness such as age related macular degeneration (AMD).[3-7] The extent of the impact of deteriorating vision on quality of life in keratoconus is most likely related to the timing of disease manifestation and progression – striking patients at a young age which is a particularly formative period in respect to educational achievement, as well as financial, emotional and social wellbeing.[5] People with keratoconus typically report higher rates of dependency and mental health issues,[3] and lower quality of life scores[4] including long term impacts on financial and social health that are progressive over time.[5, 6, 8]

Although the majority of keratoconic patients are successfully managed with contact lenses, surgical intervention with corneal transplantation by expert trained ophthalmologists is currently the most, and indeed often only, effective treatment for the majority of corneal blindness and severe keratoconus.[9] Successful transplantation, however, requires a reliable source of high quality donor corneal tissue and significant postoperative care and follow-up. Unfortunately, corneal transplantation is not a cost effective option in many developing nations.[1]

2.2. Keratoconus: a corneal dystrophy

Keratoconus is a bilateral non-inflammatory corneal ectasia that is characterised by progressive corneal thinning and steepening.[9-12] The prevalence of keratoconus is reported to be approximately 4-55 per 100,000,[13, 14] however, New Zealand is believed to have one of the highest rates of keratoconus in the world in particular within Maori and Pacific populations.[15]

The precise aetiology of keratoconus remains elusive and is likely to be multifactorial or a common phenotype resulting from the convergence of several genetic and environmental mechanisms.[11] Although the majority of keratoconus is sporadic, there is evidence for a genetic contribution with a positive family history of keratoconus in some patients and an association with other genetic disorders such as Down's and Marfan's syndromes.[11] The genetics of keratoconus are not straightforward and no single causative gene has been identified as yet, although reports have confirmed at least 13 sets of monozygotic twins with keratoconus.[11, 16] Interestingly, in these twins variable penetrance was typically observed with topographic discordance between twins suggesting environmental factors remain central to disease progression and severity.[11, 17] Additional evidence to support environmental factors in the aetiology of keratoconus includes a strong association with atopy (including asthma, eczema and hayfever) and a history of eye rubbing.[12, 15, 18, 19]

The pathogenesis of keratoconus has been extensively studied. Keratoconus is predominantly a disease of the corneal stroma, although in advanced stages it affects all layers of the cornea. [20] Stromal thinning, loss of collagen fibrils and keratocytes and a subsequently increased ratio of proteoglycans in keratoconic corneas have all been reported despite an as yet unidentified underlying mechanism.[20] Keratoconic corneas have several well characterised cellular abnormalities including increased rates of keratocyte apoptosis,[21] decreased keratocyte density that correlates with disease severity, and decreased corneal innervation[22-24] It is still unknown if keratocyte viability/density is the cause or effect of keratoconus as there are other mechanisms in the cornea that can increase keratocyte apoptosis including corneal transplantation and surgery,[25] epithelial

injury,[26] and corneal collagen crosslinking.[27] It has been postulated that keratoconic keratocytes may be sensitised to apoptosis as they express four times the interleukin 1 (IL-1) receptors that normal keratocytes do and IL-1 is known to stimulate apoptosis (*via* Fas ligand).[21, 26] Indeed, IL-1 mediated apoptosis has been suggested as a possible link between atopy, eye rubbing and decreased keratocyte density in keratoconus; and further, may potentially contribute to corneal ectasia with the release of proteases that degrade the stromal extracellular matrix (ECM) following keratocyte apoptosis.[21, 28-30]

Keratoconus typically presents with progressively worsening myopia, irregular astigmatism and higher order aberrations resulting in decreased visual acuity which cannot be fully corrected with spectacles or contact lenses.[9, 11, 12] The clinical signs include Munson's sign with characteristic bulging of the lower lid on downgaze, corneal haemosiderin iron deposits in a 'Fleisher ring' arrangement at the base of the cone, 'Vogt's striae', prominent corneal stromal nerves, central corneal thinning and occasionally scarring.[9, 12, 18, 31, 32] Severe keratoconus is associated with corneal hydrops, subsequent apical scarring and a loss of best corrected visual acuity.[12]

The treatment of keratoconus varies depending on the severity of the disease and rate of progression. The main objectives of treatment are to halt progression and to maximise visual acuity.[33] Mild keratoconus is typically managed with spectacles or soft contact lenses and steeper cones, indicating more advanced disease, generally require rigid gas permeable (RGP) contact lenses for stable refractive correction.[33]

Eventually as keratoconus progresses, RGP contact lens fitting becomes difficult or impossible and alternative strategies need to be considered. In these cases Intracorneal ring segments (Intacs) can be beneficial to help flatten the cornea, improve refractive error and temporarily reinstate contact lens tolerance.[34] Intacs are small ring segments that are inserted into manually dissected or femtosecond laser cut intrastromal channels.[34] Although intacs are relatively safe, they are not used

routinely by most clinicians as they do not halt the progression and therefore seldom represent a definitive treatment for keratoconus.

Rapid progression is often a poor prognostic indicator in keratoconus and one of the most recent advances in the treatment of keratoconus, collagen cross linking using riboflavin and ultraviolet A irradiation, specifically acts to slow progression in keratoconic patients.[35] This treatment modality was developed following the observation that diabetic patients had lower than expected rates of keratoconus which was later attributed to advanced-glycation-end-product mediated collagen cross linking in the cornea.[35, 36] Although corneal cross linking is a relatively new modality for treating keratoconus, early results from animal and human clinical trials suggest that this treatment improves corneal rigidity, slows keratoconus progression, and improves maximum keratometry readings and refractive error.[36] Studies suggest that corneal cross linking is relatively safe with relatively few reports of corneal scarring and stromal haze and rare episodes of postoperative microbial keratitis.[35, 36] Although keratocyte apoptosis does occur in the anterior stroma following crosslinking, it appears to be a transient effect with keratocyte repopulation occurring 3-6 months following the procedure.[36] Although the initial reports for corneal cross linking appear promising, the future of this treatment modality will be dependent on the long term clinical outcomes which as yet remain unknown.

Typically up to 20% of keratoconic patients will eventually require a corneal transplant to regain functional vision once other conservative treatments are exhausted.[33] Although 80% of keratoconic patients are successfully managed using conservative treatments such as contact lenses, keratoconus requiring corneal transplantation currently represents the largest single indication for corneal transplantation in New Zealand over the past decade, comprising 41.2% of all corneal transplants nationally.[37]

2.3. Corneal transplantation strategies for keratoconus

Given the stromal changes observed in keratoconus it is not surprising, from a conceptual perspective, that *en bloc* replacement of the central cornea in the form of a full thickness penetrating keratoplasty (PKP) has been the treatment of choice for severe keratoconus. Although PKP has been the gold standard for keratoconic patients requiring corneal transplantation and generally achieves excellent optical outcomes with graft survival rates of approximately 95% at five years and 89% at 10 years, there are still complications associated with PKP in addition to the limitations of tissue availability and postoperative follow-up.[33]

The most significant complication of PKP, and the most common cause of graft failure, is allograft rejection which affects up to 20% of patients within 5 years of transplantation.[38-40] The most common type of corneal allograft rejection is endothelial rejection.[12, 41] To circumvent this problem, in certain patients it is possible to transplant the anterior cornea only as conducted in a deep anterior lamellar keratoplasty (DALK) – leaving the host endothelium in place and greatly reducing the risk of rejection (**Figure 2.1**). DALK is a technically challenging surgery that is only suitable for a subset of patients that do not have excessive deep stromal scarring or damage to Descemet's membrane; however, despite the limitations this technique generally provides better long term graft survival with shorter durations of clinical follow up and topical corticosteroid treatment required, and similar refractive outcomes when compared with PKP.[37, 42-45]

In addition to DALK there are other lamellar corneal transplants such as Descemet's stripping endothelial keratoplasty (DSEK) (and variations thereof) that involve transplanting the posterior stroma and endothelium and leaving the host epithelium and stroma intact (**Figure 2.1**). Although this is typically not a transplant technique that is used as a primary transplant for treating keratoconus, occasionally it may be a useful treatment strategy in the context of a decompensated PKP following an episode of rejection in an eye that achieved excellent vision with minimal refractive correction. Despite the current practice of using one donor cornea to treat one patient, lamellar

keratoplasty techniques allow for the possibility of using one donor cornea to treat two or three patients requiring different lamellar procedures.[46]

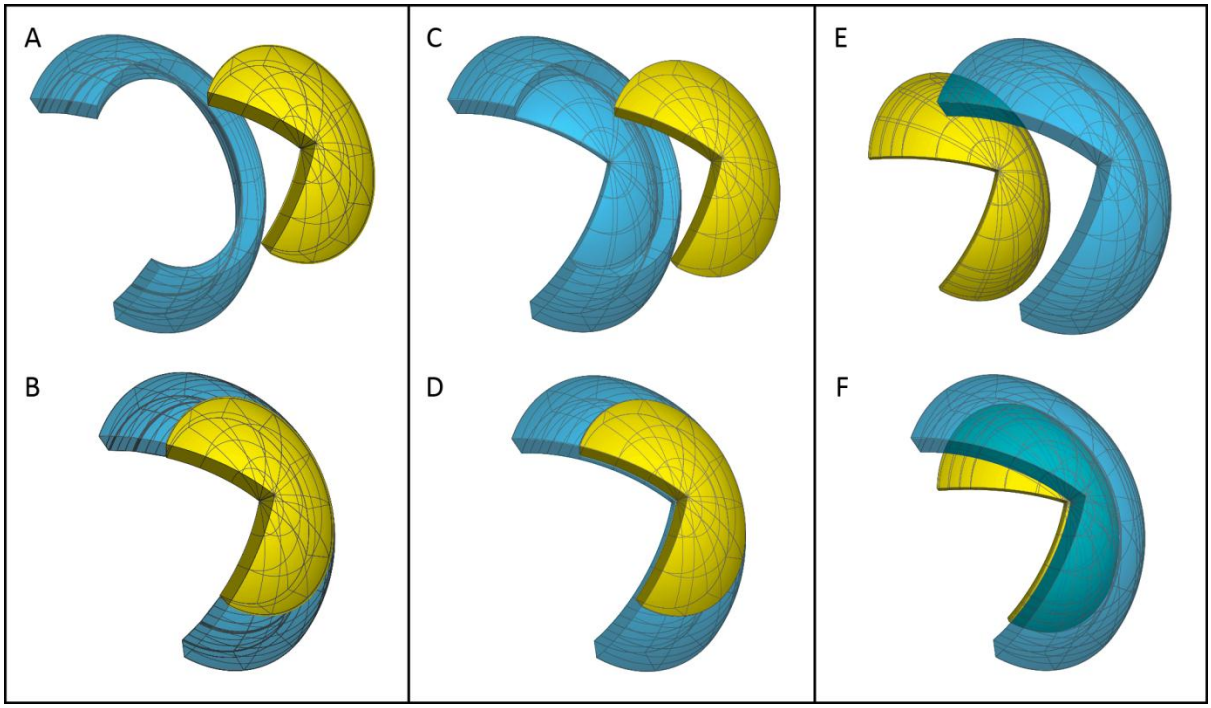

Figure 2.1 Lamellar variations of corneal transplantation. The host/recipient tissue is labelled blue and the donor tissue labelled yellow. A penetrating keratoplasty (PKP) utilises a full thickness donor 'button' that is sutured into the host cornea once a full thickness trephine cut is made (A). The completed transplant has a fully integrated donor button in the host cornea (B). A deep anterior lamellar keratoplasty (DALK) retains the host cornea endothelium and Descemet's membrane with often a small amount of residual posterior stroma (C). The donor button has the endothelium removed and is sutured into the host cornea (D). A Descemet's stripping endothelial keratoplasty (DSEK) has the host endothelium removed before inserting the transplant comprised of endothelium and a small amount of posterior stroma (E). The donor button is held in place with an air bubble until the tissue adheres to the exposed posterior stroma of the host cornea (F).

2.4. Alternatives to traditional corneal transplantation to address donor shortages

The demand for donor tissue for corneal transplantation greatly outstrips supply, especially in Asian countries where patients currently wait listed for corneal transplantation exceed 300,000 in India and 4 million in China.[47] Despite this massive demand, corneal allotransplantation rates remain at less than 20,000 per year in both of these countries combined.[47] In New Zealand there are similar, although less severe, challenges in respect to the supply of corneal tissue for transplantation and current waiting times are up to 12 months for a corneal transplant due to tissue shortages.[48]

With the worldwide shortage of corneal tissue for transplantation there has been growing interest in alternative tissue sources. Xenotransplantation offers one potential solution, and corneal transplants into humans with donor corneas sourced from pigs, sheep, dogs, rabbits, gibbons, cows and fish have been previously attempted with limited success.[47, 49-51] The most significant obstacle to xenotransplantation is that despite promising results with xenotransplantation into animal models, most transplants fail due to hyperacute rejection within a month or two of transplantation into human recipients.[47] Xenograft rejection is mediated by a number of mechanisms including CD4+ T-cell and to a lesser extent CD8+ T-cell mediated processes in combination with natural antibodies to xenoantigens such as the porcine Galα1,3Gal surface molecule.[47, 52] Although significant progress has been made in genetic manipulation of pigs to remove these immune stimulating antigens,[47, 52] to date there have been no studies to evaluate the potential benefit for corneal transplantation. Additionally, the technology remains prohibitively expensive for widespread use at present. Even if the technical and biological aspects for xenotransplantation of corneas into human recipients are overcome, it is likely that a large proportion of patients may refuse these transplants on the basis of religious or ethical grounds[53] as observed with porcine heart valve xenotransplants and other animal derived surgical products.[54]

Keratoprosthesis is an alternative to corneal allotransplantation that has been used with variable success over the past 200 years.[55] There are several commercially available keratoprostheses

currently used in clinical practice. Although these implants are particularly suited to certain clinical situations (such as extremely hostile ocular surface environments that would contribute to premature allograft failure), significant complications and poor visual outcomes preclude their routine use for patients that are candidates for allotransplantation.[55]

Animal models have recently demonstrated some promising results using a novel strategy – cell based corneal transplants.[56, 57] Both studies have used human derived cells for phenotypic rescue of lumican knockout mice that are associated with characteristically opaque corneas. The first study used human cultured stromal stem cells, and the second study used human umbilical mesenchymal stem cells injected into mice corneas. In both cases transplantation of human cells into the opaque mouse corneas did not elicit rejection and corneas demonstrated improvement in the organisation of the corneal extracellular matrix and in transparency over a three month period.[56, 57]

2.5. Hypothesis: The potential for cell based transplantation for treatment of early keratoconus

We hypothesise that it is possible to isolate, culture and transplant human corneal stromal cells to treat early keratoconus. The prerequisites for this cell based transplant strategy to be successful as a therapeutic intervention for the treatment of keratoconus are:

1. Transplanted cells should express healthy extracellular matrix (ECM) material at similar ratios to that seen in the human cornea in order to stabilize the cornea and halt the progression of the keratoconic phenotype.
2. The transplanted cells must contain a proportion of stem or progenitor cells for a prolonged effect and to repopulate the host cornea.
3. Transplanted cells must be able to divide and proliferate in order to provide cell numbers able to support healthy ECM production and maintenance throughout the host cornea.
4. Transplanted cells must be able to migrate within the host cornea to distribute and produce ECM throughout the entire host cornea.

2.6. Conclusions

Keratoconus is a corneal dystrophy that is probably caused by a combination of genetic predisposition and environmental influences. New Zealand has one of the highest rates of keratoconus in the world and there is differential ethnic prevalence with highest rates in Maori and Pacific populations. Despite successful conservative management in the majority of patients, a substantial proportion of patients require corneal transplantation. Even with the excellent results obtained with corneal transplantation, availability of donor tissue remains the limiting factor for timely treatment.

Recently, trends in corneal transplant surgery have seen a rise in popularity in lamellar techniques – transplanting less tissue is associated with similar optical outcomes and better long term survival of the graft. Following the natural evolution of this trend it should be possible to use cell based corneal

transplants for treating corneal dystrophies such as early keratoconus. Cell based implants have the potential to treat many patients with one donor cornea, may reduce the risk of rejection as observed in lamellar transplants, and if used in early keratoconus could prevent disease progression and the associated patient morbidity and ultimately may reduce or eliminate the requirement for traditional corneal transplantation.

2.7. References

1. Whitcher JP, Srinivasan M, Upadhyay MP. Corneal blindness: A global perspective. Bulletin of the World Health Organization 2001;79(3):214-21.
2. Olivares Jimenez JL, Guerrero Jurado JC, Bermudez Rodriguez FJ, Serrano Laborda D. Keratoconus: Age of onset and natural history. Optometry and Vision Science 1997;74(3):147-51.
3. Cesnekova T, Skorkovska K, Petrova S, Cermakova S. [visual functions and quality of life in patients with keratoconus]. Ceska a slovenska oftalmologie : casopis Ceske oftalmologicke spolecnosti a Slovenske oftalmologicke spolecnosti 2011;67(2):51-4.
4. de Freitas Santos Paranhos J, Avila MP, Paranhos A, Jr., Schor P. Evaluation of the impact of intracorneal ring segments implantation on the quality of life of patients with keratoconus using the nei-rql (national eye institute refractive error quality of life) instrument. British Journal of Ophthalmology 2010;94(1):101-5.
5. Kymes SM, Walline JJ, Zadnik K, Gordon MO. Quality of life in keratoconus. American Journal of Ophthalmology 2004;138(4):527-35.
6. Kymes SM, Walline JJ, Zadnik K, et al. Changes in the quality-of-life of people with keratoconus. American Journal of Ophthalmology 2008;145(4):611-7.
7. Yildiz EH, Cohen EJ, Virdi AS, et al. Quality of life in keratoconus patients after penetrating keratoplasty. American Journal of Ophthalmology 2010;149(3):416-22 e1-2.
8. Rebenitsch RL, Kymes SM, Walline JJ, Gordon MO. The lifetime economic burden of keratoconus: A decision analysis using a markov model. American Journal of Ophthalmology 2011;151(5):768-73 e2.
9. Romero-Jimenez M, Santodomingo-Rubido J, Wolffsohn JS. Keratoconus: A review. Contact lens & anterior eye : the journal of the British Contact Lens Association 2010;33(4):157-66; quiz 205.

10. Arne JL, Fournie P. [keratoconus, the most common corneal dystrophy. Can keratoplasty be avoided?]. Bulletin de l'Academie Nationale de Medecine 2011;195(1):113-29.

11. Edwards M, McGhee CN, Dean S. The genetics of keratoconus. Clinical and Experimental Ophthalmology 2001;29(6):345-51.

12. McGhee CN. 2008 sir norman mcalister gregg lecture: 150 years of practical observations on the conical cornea--what have we learned? Clinical and Experimental Ophthalmology 2009;37(2):160-76.

13. Hofstetter HW. A keratoscopic survey of 13,395 eyes. American Journal of Optometry and Archives of American Academy of Optometry 1959;36(1):3-11.

14. Kennedy RH, Bourne WM, Dyer JA. A 48-year clinical and epidemiologic study of keratoconus. American Journal of Ophthalmology 1986;101(3):267-73.

15. Jordan CA, Zamri A, Wheeldon C, et al. Computerized corneal tomography and associated features in a large new zealand keratoconic population. Journal of Cataract and Refractive Surgery 2011;37(8):1493-501.

16. Nowak DM, Gajecka M. The genetics of keratoconus. Middle East African Journal of Ophthalmology 2011;18(1):2-6.

17. Weed KH, MacEwen CJ, McGhee CN. The variable expression of keratoconus within monozygotic twins: Dundee university scottish keratoconus study (dusks). Contact Lens and Anterior Eye 2006;29(3):123-6.

18. Weed KH, MacEwen CJ, Giles T, et al. The dundee university scottish keratoconus study: Demographics, corneal signs, associated diseases, and eye rubbing. Eye 2008;22(4):534-41.

19. Owens H, Gamble G. A profile of keratoconus in new zealand. Cornea 2003;22(2):122-5.

20. Ambekar R, Toussaint KC, Jr., Wagoner Johnson A. The effect of keratoconus on the structural, mechanical, and optical properties of the cornea. Journal of the Mechanical Behavior of Biomedical Materials 2011;4(3):223-36.

21. Kim WJ, Rabinowitz YS, Meisler DM, Wilson SE. Keratocyte apoptosis associated with keratoconus. Experimental Eye Research 1999;69(5):475-81.

22. Patel DV, Ku JY, Johnson R, McGhee CN. Laser scanning in vivo confocal microscopy and quantitative aesthesiometry reveal decreased corneal innervation and sensation in keratoconus. Eye 2009;23(3):586-92.

23. Patel DV, McGhee CN. Mapping the corneal sub-basal nerve plexus in keratoconus by in vivo laser scanning confocal microscopy. Investigative Ophthalmology and Visual Science 2006;47(4):1348-51.

24. Ku JY, Niederer RL, Patel DV, et al. Laser scanning in vivo confocal analysis of keratocyte density in keratoconus. Ophthalmology 2008;115(5):845-50.

25. Ohno K, Mitooka K, Nelson LR, et al. Keratocyte activation and apoptosis in transplanted human corneas in a xenograft model. Investigative Ophthalmology and Visual Science 2002;43(4):1025-31.

26. Wilson SE, Kim WJ. Keratocyte apoptosis: Implications on corneal wound healing, tissue organization, and disease. Investigative Ophthalmology and Visual Science 1998;39(2):220-6.

27. Wollensak G, Spoerl E, Wilsch M, Seiler T. Keratocyte apoptosis after corneal collagen cross-linking using riboflavin/uva treatment. Cornea 2004;23(1):43-9.

28. Chwa M, Atilano SR, Reddy V, et al. Increased stress-induced generation of reactive oxygen species and apoptosis in human keratoconus fibroblasts. Investigative Ophthalmology and Visual Science 2006;47(5):1902-10.

29. Matthews FJ, Cook SD, Majid MA, et al. Changes in the balance of the tissue inhibitor of matrix metalloproteinases (timps)-1 and -3 may promote keratocyte apoptosis in keratoconus. Experimental Eye Research 2007;84(6):1125-34.

30. Sevost'ianov EN, Giniatullin RU, Gorskova EN, Teplova SN. [keratocyte apoptosis in keratoconus]. Vestnik Oftalmologii 2002;118(4):36-8.

31. Zadnik K, Barr JT, Gordon MO, Edrington TB. Biomicroscopic signs and disease severity in keratoconus. Collaborative longitudinal evaluation of keratoconus (clek) study group. Cornea 1996;15(2):139-46.

32. Li X, Yang H, Rabinowitz YS. Keratoconus: Classification scheme based on videokeratography and clinical signs. Journal of Cataract and Refractive Surgery 2009;35(9):1597-603.

33. Jhanji V, Sharma N, Vajpayee RB. Management of keratoconus: Current scenario. British Journal of Ophthalmology 2011;95(8):1044-50.

34. Pinero DP, Alio JL. Intracorneal ring segments in ectatic corneal disease - a review. Clinical and Experimental Ophthalmology 2010;38(2):154-67.

35. Keating A, Pineda R, 2nd, Colby K. Corneal cross linking for keratoconus. Seminars in Ophthalmology 2010;25(5-6):249-55.

36. Ashwin PT, McDonnell PJ. Collagen cross-linkage: A comprehensive review and directions for future research. British Journal of Ophthalmology 2010;94(8):965-70.

37. Cunningham WJ, Brookes NH, Twohill HC, et al. Trends in the distribution of donor corneal tissue and indications for corneal transplantation: The new zealand national eye bank study 2000-2009. Clinical and Experimental Ophthalmology 2011.

38. Rahman I, Huang MC, Carley F, et al. The influence of donor and recipient factors in allograft rejection of the human cornea. Eye 2010;24(2):334-9.

39. Wagoner MD, Gonnah el S, Al-Towerki AE. Outcome of primary adult penetrating keratoplasty in a saudi arabian population. Cornea 2009;28(8):882-90.

40. Patel HY, Ormonde S, Brookes NH, et al. The new zealand national eye bank: Survival and visual outcome 1 year after penetrating keratoplasty. Cornea 2011;30(7):760-4.

41. Klebe S, Coster DJ, Williams KA. Rejection and acceptance of corneal allografts. Current opinion in organ transplantation 2009;14(1):4-9.

42. Terry MA, Ousley PJ. Deep lamellar endothelial keratoplasty visual acuity, astigmatism, and endothelial survival in a large prospective series. Ophthalmology 2005;112(9):1541-8.

43. Han DC, Mehta JS, Por YM, et al. Comparison of outcomes of lamellar keratoplasty and penetrating keratoplasty in keratoconus. American Journal of Ophthalmology 2009;148(5):744-51 e1.

44. Jones MN, Armitage WJ, Ayliffe W, et al. Penetrating and deep anterior lamellar keratoplasty for keratoconus: A comparison of graft outcomes in the united kingdom. Investigative Ophthalmology and Visual Science 2009;50(12):5625-9.

45. Karimian F, Feizi S. Deep anterior lamellar keratoplasty: Indications, surgical techniques and complications. Middle East African Journal of Ophthalmology 2010;17(1):28-37.

46. Vajpayee RB, Sharma N, Jhanji V, et al. One donor cornea for 3 recipients: A new concept for corneal transplantation surgery. Archives of Ophthalmology 2007;125(4):552-4.

47. Hara H, Cooper DK. Xenotransplantation--the future of corneal transplantation? Cornea 2011;30(4):371-8.

48. Moffatt L. Wait list for corneal transplant in new zealand. In: McKelvie J, ed. Auckland, 2011.

49. Haq M. Fish cornea for grafting. British Medical Journal 1972;2(5815):712-3.

50. Watts GT. Fish cornea for grafting. British Medical Journal 1973;1(5853):615.

51. Durrani KM, Kirmani TH, Hassan MM, et al. Penetrating keratoplasty with purified bovine collagen: Report of a coordinated trial on fifteen human cases. Annals of Ophthalmology 1974;6(6):639-46.

52. Kim MK, Wee WR, Park CG, Kim SJ. Xenocorneal transplantation. Current Opinion in Organ Transplantation 2011;16(2):231-6.

53. Jorqui-Azofra M, Romeo-Casabona CM. Some ethical aspects of xenotransplantation in light of the proposed european directive on the protection of animals used for scientific purposes. Transplantation Proceedings 2010;42(6):2122-5.

54. Easterbrook C, Maddern G. Porcine and bovine surgical products: Jewish, muslim, and hindu perspectives. Archives of Surgery 2008;143(4):366-70; discussion 70.

55. Gomaa A, Comyn O, Liu C. Keratoprostheses in clinical practice - a review. Clinical and Experimental Ophthalmology 2010;38(2):211-24.

56. Du Y, Carlson EC, Funderburgh ML, et al. Stem cell therapy restores transparency to defective murine corneas. Stem Cells 2009;27(7):1635-42.

57. Liu H, Zhang J, Liu CY, et al. Cell therapy of congenital corneal diseases with umbilical mesenchymal stem cells: Lumican null mice. PLoS ONE 2010;5(5):e10707.

Chapter 3. Materials and methods

3.1. Tissue for research

3.1.1. Human corneal tissue procurement

Post-mortem human corneal tissue with research consent was obtained from the New Zealand National Eye Bank (Auckland, NZ). Corneal tissue was either in the form of limbal rims remaining after transplantation surgery or whole corneas that were not suitable for transplantation because the cause of death was unknown or due to an underlying systemic disease in the donor. Donor corneas were maintained in organ culture (Eagles MEM, 2% FCS, 2mM L-Glut, 1x Anti anti) for an average of 9 days prior to transfer to transport medium (Eagles MEM, 2% FCS, 2mM L-Glutamine, 1x Anti anti, Dextran 50g/L). Approval for all human tissue-based research was obtained from the Northern X Regional Human Ethics Committee. All research procedures were developed in accordance with the Declaration of Helsinki.

A total of 31 human corneas/corneal rims were used for the research outlined in this thesis.

3.1.2. Animal corneal tissue procurement

Post-mortem porcine corneal tissue was obtained from Freshpork Northern Ltd, 10 Miami Parade, Onehunga, Auckland**,** New Zealand**.** Whole eyes were obtained within 12 hours post mortem and were sterilised using 4% povidone iodine solution prior to removal of intact corneas by dissection around the limbus. Isolated corneal tissue was used immediately. All research procedures were developed in accordance with the Declaration of Helsinki.

3.2. Corneal stromal cell isolation and culture

3.2.1. Corneal stromal cell isolation

Descemet's membrane and the endothelium were removed from the corneal stroma by peeling with fine forceps under a dissecting microscope. The epithelium was denuded by careful scraping with a scalpel blade. Residual cells and culture media were removed with a sterilised cotton bud or surgical spear/sponge prior to rinsing in phosphate buffered saline (PBS). The clear stromal tissue was carefully dissected away from the sclera.

Dissected corneal stromal tissue was placed in digest mix consisting of Dulbecco's modified Eagle's medium (DMEM) (Life Technologies, Carlsbad, CA, USA) with type II collagenase 2.0mg/ml (Life Technologies, Carlsbad, Ca, USA), type 1S hyaluronidase 0.5mg/ml (Sigma-Aldrich, St Louis, MO, USA) and digested overnight at 37°C with gentle rocking before passing through a 40 micrometer cell strainer to remove undigested stromal tissue and cell aggregates. The digest mix was removed by pelleting cells with centrifugation at 1500 rpm for 7 minutes and discarding supernatant. Cells were rinsed twice in PBS with repeat centrifugation between rinses and then placed in culture media.

3.2.2. Corneal stromal cell culture and culture media

Isolated stromal cells were re-suspended in culture medium (see below for media formulation). Cells were incubated at 37°C with 5% CO_2 with media changes every 3 days (unless otherwise specified).

3.2.3. Stem cell growth media

DMEM/MCDB-201 (Life Technologies, Carlsbad, Ca, USA), Fetal bovine serum 2% (Life Technologies, Carlsbad, Ca, USA), epidermal growth factor (EGF) 10ng/ml (Life Technologies, Carlsbad, Ca, USA), Platelet-derived growth factor (PDGF-BB) 10ng/ml (Life Technologies, Carlsbad, Ca, USA), Insulin 5ug/ml (Life Technologies, Carlsbad, Ca, USA), transferrin 5ug/ml (Life Technologies, Carlsbad, Ca, USA), selenous acid 5ng/ml (Life Technologies, Carlsbad, Ca, USA), Leukemia inhibitory factor (LIF) 1000U/ml (Life Technologies, Carlsbad, Ca, USA), Linoleic acid -bovine serum albumin (LA-BSA) x1,

Ascorbic acid-2-phosphate 0.1mM (Life Technologies, Carlsbad, Ca, USA), Dexamethasone 10-8M (Life Technologies, Carlsbad, Ca, USA), Penicillin 100IU/ml, Streptomycin 100ug/ml, Amphotericin B 1.25ug/ml (Life Technologies, Carlsbad, Ca, USA).

3.2.4. Basal growth media

Advanced DMEM (Life Technologies, Carlsbad, Ca, USA), 2 ng/ml EGF (Life technologies, Carlsbad, Ca, USA), and 1ng/ml basic fibroblast growth factor (bFGF)(Life technologies, Carlsbad, Ca, USA), L-glutamine (Life technologies, Carlsbad, Ca, USA) and Antibiotic-Antimycotic (Anti-Anti)(Life technologies, Carlsbad, Ca, USA).

3.3. Cytokine expression analysis

3.3.1. Cell preparation for cytokine analysis

Cytokine analysis was conducted using the RayBio Human Cytokine Antibody Array C Series 1000 kit with all supplied buffers and reagents as per manufacturer protocols (combination of array VI and VII, RayBiotech Inc., Norcross, GA, USA). Cells were rinsed twice in phosphate buffered saline and each sample was homogenised in 1ml 1x Cell Lysis buffer to extract proteins from the stromal-cell samples. Each sample was centrifuged and the protein concentration of the supernatant was determined using the Bio-Rad DC Protein Assay (Bio-Rad Laboratories, Hercules, CA, USA).

Cytokine array membranes (VI and VII) were prepared according to the manufacturer's protocol. All array membranes were treated with 30 minute incubation in 1x Blocking Buffer at room temperature. Blocked array membranes were incubated with 100 µg protein samples in 1x Blocking Buffer for 2 hours at room temperature.

Array membranes were washed three times for five minutes in 2ml 1x Wash Buffer I, then twice for five minutes in 2ml 1x Wash Buffer II at room temperature with shaking. Each array membrane (VI and VII) was then incubated with 1ml of the corresponding (VI and VII) biotin-conjugated antibodies in 1x Blocking Buffer for 2 hours at room temperature. Following incubation each membrane was washed again as outlined above. Array membranes were incubated separately in 2ml of 1:200,000 HRP-conjugated streptavidin for 2 hours at room temperature and washed again as outlined above. Each array membrane was incubated in freshly prepared detection buffer (250uL of Detection Buffer A and 250 µL of Detection Buffer B per membrane) for 1 minute at room temperature. Array membranes were removed from the Detection Buffers, drained and placed between plastic sheets ready for signal detection with the Fuji Chemiluminescence Imaging System (Fugifilm LAS3000 Scanner, Tokyo, Japan).

Signal detection using chemiluminescence intensity was conducted using Fujifilm Multigauge Ver. 3.0 software (Fuji Photo Film, Tokyo, Japan) and signal intensity values were imported into RayBio

Antibody Array Analysis Tool (RayBiotech Inc., Norcross, GA, USA) to normalise and compare signal intensities and the relative expression of individual cytokines between samples.

3.4. Fluorescence activated cell sorting (FACS)

3.4.1. Cell preparation and analysis using FACS

Isolated stromal cells were prepared for fluorescence activated cell sorting (FACS) by suspending in 5ml DMEM medium (Life Technologies, Carlsbad, Ca, USA) with Hoechst 33341 (Life Technologies, Carlsbad, Ca, USA) at 5µg/ml for 90mins at 37°C. Cells were then centrifuged at 1500 rpm for 7 minutes and re-suspended in 1ml DMEM with 2µg/ml propidium iodide (Life Technologies, Carlsbad, Ca, USA) added immediately prior to sorting. To inhibit transport of Hoechst 33342 out of ABCG2 positive cells, control cells were pre-incubated for 20 minutes with 50 µg/ml verapamil (Sigma-Aldrich, St. Louis, MO, USA) prior to Hoechst 33342 incubation. Twenty percent of cells were set aside as an unstained control in order to calibrate the cell sorter prior to sorting the labelled cells. Cells were sorted using a Becton Dickinson FACSAria II, Becton Dickinson LSR II, or Becton Dickinson FACSVantage fluorescence activated cell sorter (Franklin Lakes, NJ, USA). Cell sorting was analysed using Becton Dickinson FACSDiva v.6.1 and BD CellQuest Pro software (version 3.5.1, Franklin Lakes, NJ, USA).

3.5. Histological analysis

3.5.1. Quantum dot nanocrystal (Qtracker) labelling

For stromal cell fluorescent quantum dot nanocrystal labelling, 10nM labelling solution of Qtracker 525 and 605 (Life technologies, Carlsbad, CA, USA) were used by combining 1µL of Qtracker nanocrystals with 1µL of Qtracker carrier and incubating at room temperature for 5 minutes before adding 200µL of basal growth medium and vortexing. The labelling solution was then added to digested stromal cells after centrifugation and removal of supernatant and the cells were incubated at 37°C for 60 minutes before washing in growth medium twice and then culturing in basal growth medium and imaging.

3.5.2. Tissue preparation for immunocytochemistry

Tissue samples were embedded in Optimal Cutting Temperature (OCT) compound and then snap frozen in liquid nitrogen. Frozen tissue was then sectioned using the Microm HM550 Cryostat (Thermo-Scientific, Waltham, MA, USA) and mounted on Superfrost Plus electrostatic slides (Menzel-Glenser, Braunscchweig, Germany).

3.5.3. Immunohistochemical and immunocytochemical analysis

Tissue and cell preparations were prepared as outlined in section 3.5.2 and warmed to room temperature to enable removal of OCT compound by washing in phosphate buffered saline (PBS) twice for 5 minutes prior to labelling. Non-specific binding was then blocked with 10% normal goat serum (Invitrogen Corp., Carlsbad, CA, USA) in PBS for 1 hour at room temperature. Tissue sections were labelled with primary antibodies (see

Table 3.1 for details and dilutions). Primary antibodies were incubated at 4 °C overnight.

Following primary antibody incubation, samples were rinsed in PBS three times (for 5 minutes each rinse) to remove unbound antibodies. Secondary antibodies with conjugated fluorophores were then added to tissue sections and incubated at room temperature for 2 hours before rinsing in PBS three times (for 15 minutes each rinse). Tissue sections were counterstained with the DNA binding

fluorescent label 4',6-diamidino-2-phenylindole (DAPI) (Life Technologies, Carlsbad, Ca, USA) at 0.1 g/ml for 10 minutes at room temperature. Slides were rinsed in PBS again and mounted using Citiflour (Agar Scientific, Essex, UK) prior to viewing with fluorescent or confocal microscopy.

For intracellular targets, samples were incubated in ice cold methanol for 10 minutes at 4 °C to permeabilise the cell membrane prior to labelling with the primary antibody. For DNA targeting antibodies such as anti bromodeoxyuridine (BrdU), DNA was denatured using 2M HCl at 37 °C for 45 minutes then neutralised with 0.1M borate buffer at pH8.5 for 10 minutes at room temperature prior to antibody labelling.

3.5.4. Primary and secondary antibodies

All primary and secondary antibodies were sourced and incubated at the dilutions as indicated in **Table 3.1**.

Antibody target	Supplier	Dilution	Catalog number	Target organism
Keratocan	Santa Cruz Biotechnology Inc. (Santa Cruz, Ca. USA)	1:50	(H-50): sc-66941	Human
Collagen I	Abcam (Cambridge, UK)	1:500	ab6308	Human
Collagen IV	Sigma Aldrich (St. Louis, Mo, USA)	1:2000	C1926	Human
Collagen V	Abcam (Cambridge, UK)	1:500	ab19812	Human
Collagen VI	Freddie Sherwin (custom)	1:500	na	Human
ABCG2	Calbiochem, Merck (Darmstadt, Germany)	1:50	BXP-21	Human
Alexa 488	Life Technologies (Carlsbad, Ca, USA)	1:400	A11034	Goat anti-rabbit
Alexa 488	Life Technologies (Carlsbad, Ca, USA)	1:400	A11029	Goat anti-mouse

Table 3.1 Details of all antibodies, suppliers and dilutions used.

3.6. Live cell labelling

3.6.1. Light and time lapse microscopy

Time lapse microscopy was conducted using the Biostation IM (Nikon corp. Tokyo, Japan). Isolated stromal cells from a single cornea were divided into two equal aliquots and labelled with either Qtracker 525 or 605 and then combined and incubated at 37°C with 5% CO_2 and phase and fluorescence images were captured using the Biostation IM software version 2.10 (Nikon corp. Tokyo, Japan) over a 72 hour period. Spheres were imaged on a Leica DIL inverted microscope with a Nikon digital camera attachment and Nikon NIS Elements 3.0 software (Nikon corp. Tokyo, Japan) for image acquisition.

3.7. Live cell imaging

3.7.1. Immunohistochemistry

Cultured spheres were removed from culture-plate wells using a pipette and inverted microscope at 10x magnification, and placed in 0.5ml microfuge tubes. Optimal cutting temperature compound (OCT) was added, and the tubes were centrifuged. Tubes were snap-frozen in liquid nitrogen, and their contents embedded in mounting wells containing OCT, and snap-frozen again. Embedded spheres were sectioned at 16µm thickness with a cryostat.

Sphere sections were washed in PBS for 5 minutes twice. Non-specific binding was blocked with 10% normal goat serum in PBS for 1 hour. Sections were incubated at 4°C overnight with specific primary antibodies. Sections were washed three times in PBS and incubated with secondary antibodies (Alexa 488) at room temperature for 2 hours. Sections were washed a further three times in PBS to remove unbound secondary antibody. Sections were mounted in Prolong Gold reagent (Life Technologies, Carlsbad, Ca, USA) with 4',6-diamidino-2-phenylindole (DAPI) to counterstain for nuclei. Negative controls were treated in the same manner as labelled sphere sections; however, these sections were incubated overnight with PBS instead of specific primary antibodies.

Human corneal rims were dissected into pieces and embedded in mounting wells containing OCT and snap-frozen in liquid nitrogen. Samples were sectioned at 16um thickness. These sections were labelled as described above.

Stained sections were viewed and images acquired using either a Leica DMRA fluorescence microscope with a Nikon DS-5Mc digital camera attachment or the Olympus FV1000 confocal microscope.

3.7.2. Collagen coating coverslips for live cell migration assays

Glass coverslips were placed in an ultrasound sonicator with detergent and tap water and sonicated twice to clean the glass surface of any contaminants. Sonicated coverslips were placed in filtered water and autoclaved to sterilise. A 2ml solution of collagen was prepared for coating the coverslips by combining 20 microliters of type I collagen (Gibco rat tail collagen I - catalog number A10483-01, Life technologies, Carlsbad, Ca, USA.) with 1980 microliters of 0.02M sterilised acetic acid. Sterilised coverslips were incubated in the prepared collagen I solution at room temperature for one hour. Coverslips were rinsed in sterilised PBS five times prior to use.

3.8. Quantitative gene expression analysis

3.8.1. RNA extraction from stromal tissue and stromal cells

Total RNA was isolated from digested and cultured stromal cells using the RNeasy mini kit and manufacturer specified protocols (Qiagen, Venlo, Netherlands). RNA quantification was conducted using the Nanodrop 2000 spectrophotometer (Thermo Fisher Scientific, Waltham, Ma, USA).

3.8.2. cDNA production

cDNA was synthesised using reverse transcription of mRNA with the SuperScript® VILO™ cDNA synthesis kit and the manufacturer specified protocols using 20µl reactions (Life Technologies, Carlsbad, Ca, USA).

3.8.3. Primer design/selection

All primer sequences were sourced from previously published studies and oligonucleotides were synthesised by GeneWorks (Adelaide, SA, Australia). All primer sets were validated individually using a variety of template concentrations to ensure the validity of the results and specificity of the amplicon using a previously published methodology[1] as recommended by Rotorgene technical support (Roche, Applied Science, Penzberg, Germany).

Gene target	Primer sequence	Reference
ABCG2	Forward: TGCAACATGTACTGGCGAAGA Reverse: TCTTCCACAAGCCCCAGG	[2]
Beta-actin	Forward: AACTCCATCATGAAGTGTGACG Reverse: GATCCACATCTGCTGGAAGG	
Collagen I	Forward: ATGCCTGGTGAACGTGGT Reverse:AGGAGAGCCATCAGCACCT	[3]
Collagen II	Forward: CCGGGCAGAGGGCAATAGCAGGTT Reverse: CAATGATGGGGAGGCGTGAG	[2]
ColIVA1	Forward: ATGTCAATGCACCCATC Reverse: CTTCAAGGTGGACGGCGT	[4]
Col6A1	Forward: GACCTCGGACCTGTTGGGTAC Reverse: TACCCCATCTCCCCCTTCAC	[5]
Keratin 12	Forward: CTACCTGGATAAGGTGCGAGCT Reverse: TCTCGCATTGTCAATCTGCA	[2]
Keratocan	Forward: ATCTGCAGCACCTTCACCTT Reverse: CATTGGAATTGGTGGTTTGA	[2]
Neurofilament	Forward: GAGGAACACCAAGTGGGAGA Reverse: CTCCTCCTCTTTGGCCTCTT	[2]
Pax6	Forward: CAATCAAAACGTGTCCAACG Reverse: TAGCCAGGTTGCGAAGAACT	[2]

Table 3.2 Details of the primers used for gene expression analysis on the Rotorgene platform and published references for the source of the sequences.

3.8.4. Quantitative gene expression analysis using the Rotorgene

All polymerase chain reactions (PCR) reaction volumes were 10µL and consisted of 2x concentrated FastStart SYBR Green Master (Rox) (Roche Applied Science, Penzberg, Germany), forward and reverse primers at a final concentration of 300nM, and 1uL of cDNA at an optimized concentration. Each assay was performed in triplicate. Amplification of beta-actin was performed for each cDNA sample in triplicate as a housekeeping gene to provide normalisation of RNA content. All PCR samples was thermocycled at 95°C for 10 minutes followed by 40 cycles of 15 seconds at 95°C and 60 seconds at 60°C. Relative quantification of target template concentration was calculated using the delta delta Ct analysis as described previously.[1]

3.8.5. Quantitative gene expression analysis using the ABI 7900 Real-Time Polymerase Chain Reaction platform.

cDNA samples were then loaded into the micro fluidic array cards and cycled on the 7900HT RT-PCR machine (Life Technologies, Carlsbad, Ca, USA). Quantitative gene expression analysis was conducted using the SDS RQ Manager, version 1.2 (Life technologies, Carlsbad, Ca, USA).

3.8.6. TaqMan microfluidic array analysis

A customised TaqMan microfluidic array card (Life technologies, Carlsbad, Ca, USA) was designed for quantitative gene expression of key keratocyte genes using the manufacturer predesigned gene expression assays. Total RNA was isolated from digested and cultured stromal cells using the RNeasy kit (Qiagen, Venlo, Netherlands). RNA quantification was conducted using the Nanodrop 2000 spectrophotometer (Thermo Fisher Scientific, Waltham, Ma, USA). cDNA was produced from transcription of mRNA using the SuperScript® VILO™ cDNA synthesis kit (Life Technologies, Carlsbad, Ca, USA). cDNA samples were then loaded into the micro fluidic array cards with master mix (Life Technologies, Carlsbad, Ca, USA) and cycled on the 7900HT RT-PCR machine (Life Technologies Carlsbad, Ca, USA). Quantitative gene expression analysis was conducted using the SDS RQ Manager, version 1.2 (Life technologies Carlsbad, Ca, USA).

3.9. Cell division and glycoprotein production

3.9.1. EDU and GalNAz labelling

Isolated stromal cells were labelled by culturing in basal culture medium containing either 10uM 5-ethynyl-2´-Deoxyuridine (EDU)(Life Technologies, CA, USA) to detect cells that have divided, or 50uM tetraacetylated N-azidoacetylgalactosamine (GalNAz)(Life Technologies, Carlsbad, Ca, USA) to detect newly synthesized glycoproteins. Media was changed every three days and cell division/glycoprotein production was detected using the Click-iT™ detection assay (Life Technologies, Carlsbad, Ca, USA) at days 3, 7, 10, and 14. Labelled cells were imaged using confocal microscopy.

3.10. Scanning electron microscopy

3.10.1. Sample preparation and imaging of stromal cell spheres

Spheres were cultured on a sterilised glass coverslip in the bottom of a six well plate. Culture media was gently aspirated leaving just a thin film on the coverslip to ensure the spheres did not dry or dislodge. Cover slips were submerged in 2.5% glutaraldehyde (EM grade) in 0.1M phosphate buffer pH 7.4 and rocked gently for 20 minutes at room temperature. Coverslips were rinsed twice for 5 minutes with 0.1M phosphate buffer. Phosphate buffer was aspirated leaving a thin film on the coverslip. Two or three drops of 1% aqueous OsO_4 was added to each coverslip (just enough to cover them) and left at room temperature in a fume hood for 20 minutes.

Coverslips were rinsed in deionised water twice to remove residual OsO_4 and 1% aqueous uranyl acetate was then added to the coverslip for 20 minutes at room temperature. Spheres were dehydrated with a graded ethanol series: 30%, 50%, 70%, 90%, 100%, 100% for 5 minutes each and critical point dried prior to imaging. Samples were imaged using a Philips XL30 scanning electron microscope.

3.11. References

1. Livak KJ, Schmittgen TD. Analysis of relative gene expression data using real-time quantitative pcr and the 2(-delta delta c(t)) method. Methods 2001;25(4):402-8.
2. Du Y, Funderburgh ML, Mann MM, et al. Multipotent stem cells in human corneal stroma. Stem Cells 2005;23(9):1266-75.
3. Marlovits S, Hombauer M, Truppe M, et al. Changes in the ratio of type-i and type-ii collagen expression during monolayer culture of human chondrocytes. Journal of Bone and Joint Surgery 2004;86(2):286-95.
4. Lam S, van der Geest RN, Verhagen NA, et al. Secretion of collagen type iv by human renal fibroblasts is increased by high glucose via a tgf-beta-independent pathway. Nephrology, Dialysis, Transplantation 2004;19(7):1694-701.
5. Schnoor M, Cullen P, Lorkowski J, et al. Production of type vi collagen by human macrophages: A new dimension in macrophage functional heterogeneity. Journal of Immunology 2008;180(8):5707-19.

Chapter 4. The production and effect of growth factors and cytokines on corneal stromal cells

4.1. Introduction

Keratocytes in the corneal stroma are exposed to a variety of growth factors and cytokines that are likely to regulate activation from a quiescent state as well as cell migration, differentiation and proliferation.[1, 2] Although cytokines are likely to have wide ranging actions on keratocytes, the precise effects of individual growth factors such as epidermal growth factor (EGF) and basic fibroblast growth factor (bFGF, also known as FGF2) remain largely unknown. Studies investigating *in vitro* keratocyte biology typically use different concentrations and constituents for culture media supplementation making comparison between studies and interpretation of results challenging.

Growth factors including EGF are likely to play a central role in regulating wound healing in the cornea. EGF is expressed within all layers of the cornea and appears to have a role in stimulating keratocyte proliferation in a dose dependant manner, at least in serum containing media.[3-7] In addition, EGF improves wound strength when applied to wounded corneas.[2] The effect of EGF is likely to be modulated not only by EGF concentration but also by regulation of the EGF receptor. Following injury in rat corneas EFG levels remain static, however, levels of EGF receptor mRNA increase seven days following injury.[8] Despite the evidence for the central role of EGF in wound healing and the maintenance of extracellular matrix (ECM) and keratocyte proliferation, little is known about which sub-population of cells produce EGF in the corneal stroma.

The effect of EGF is likely to be modified by other cytokines such as bFGF, platelet-derived growth factor (PDGF), and transforming growth factor-beta (TGF-β). These cytokines are present in the tear film and in combination can activate keratocytes and stimulate proliferation, differentiation, migration and collagen synthesis.[1, 9-15] Increased levels of bFGF, PDGF and TGF-β are all associated with a keratocyte wound healing response.[8, 16-18] These cytokines may also interact to modulate their effect as several studies have produced seemingly conflicting results for the same cytokines. For example, TGF-β in isolation decreases keratocyte proliferation and migration and promotes collagen synthesis, however, in combination with other cytokines such as bFGF and PDGF, keratocyte

proliferation is increased.[7, 15] This modulation of cytokine action is likely to also occur with EGF. In combination with TGF-β, EGF promotes cell differentiation into myofibroblasts, however EFG or TGF-β alone do not cause myofibroblastic transformation.[19]

The purpose of this study was to investigate the effect of varying EGF and FGF concentrations on the morphology of cultured human keratocyte spheres and to compare cytokine production in sub-populations of stromal cells.

4.2. Methods

4.2.1. Stromal cell culture morphology with varied EGF and FGF concentration

Stromal cells were isolated from two human corneal rims according to protocols as described in Chapter 3, section 3.1.1 and 3.2.1 (for details of the corneas see **Table 4.1**). Isolated cells were rinsed in PBS twice and re-suspended in Advanced DMEM (Life Technologies, Carlsbad, CA, USA) with 1x Anti anti and 1x L glutamine.

NZ Eye Bank reference	Donor age (years)	Gender	Experiment
09-089A	46	Male	EGF, FGF assay
09-089B	46	Male	EGF, FGF assay
10-001A	22	Female	Electron microscopy
10-002A	78	Female	Electron microscopy
10-006A	84	Male	Cytokine analysis
10-006B	84	Male	Cytokine analysis
10-107A	83	Male	Cytokine analysis
10-108B	66	Female	Cytokine analysis
10-121A	58	Male	Cytokine analysis

Table 4.1 Details of the human corneas used in this study.

Cells were divided equally into seven culture wells of a 12 well culture plate and supplemented with varying concentrations of EGF and FGF (for details of the concentrations used in each well see **Table 4.2**). Cells were cultured for 30 days with media changes every three days. Well 2 (20ng/ml EGF and 40ng/ml FGF) was cultured for 6 months and imaged using dark field microscopy and fluorescence microscopy following frozen sectioning and labelling with 4',6-diamidino-2-phenylindole (DAPI).

Well number	EGF (ng/ml)	FGF (ng/ml)
1	2	1
2	20	40
3	200	100
4	200	400
5	0	0
6	40	0
7	0	40

Table 4.2 Details of EGF and FGF concentrations used in each of the seven wells. Concentrations were selected based on the range of concentrations used in other studies.

4.2.2. Stromal cell cytokine expression

Stromal cells were isolated from five human corneal rims as described in Chapter 3, section 3.1.1 and 3.2.1 (for details of the corneas see **Table 4.1**). Isolated stromal cells were divided into four equal quantities following pooling of cells isolated from all five donor corneal rims. One quantity was immediately analysed for cytokine expression as outlined in Chapter 3, section 3.3.1; a second quantity was cultured in basal growth media (see section 3.2.4 for details) for 21 days at 37°C with 5% CO_2 prior to analysis for cytokine expression. The remaining two quantities were sorted into side population (SP) and non-SP cells using fluorescence activated cell sorting (FACS) following Hoechst 33342 incubation as described in Chapter 3, section 3.4.1. Sorted cells were then cultured in basal growth media with no supplemented EGF or bFGF (see section 3.2.4 for details) at 37°C with 5% CO_2. SP, non-SP and unsorted stromal cells were maintained in culture for 21 days with media changes every three days then analysed separately for cytokine expression as outlined in section 3.3. In accordance with the manufacturer stated cytokine array associated error for repeated

measurements on the same samples (i.e. <10%), changes in cytokine expression levels were considered significant if the 10% error bars did not overlap.

4.2.3 Scanning electron microscopy of stromal cell spheres cultured with and without EGF

Stromal cells were isolated from two human corneal rims as described in section 3.2.1 (for details of the corneas see **Table 4.1** Details of the human corneas used in this study.). Isolated cells were divided into two equal portions and cultured on glass coverslips in basal growth media, one portion with EGF and one portion without EGF (see section 3.2.4 for media details) at 37°C with 5% CO_2. Resulting spheres were imaged using scanning electron microscopy (SEM) as outlined in section 3.2.4.

4.3. Results

The two corneal rims used for culture with EGF and FGF yielded a total of 0.38gm (wet weight) of stromal tissue from which the stromal cells were isolated for culture. All of the seven treatment and control groups developed stromal cell spheres in culture by day 7. By day 21 in culture there were observable differences in sphere morphology between treatment groups with different concentrations of EGF but no difference was observed for different concentrations of bFGF. Culture wells that contained 20ng/ml EGF or above were observed to have qualitatively increased extracellular matrix (ECM) like deposits approximately proportional to EGF concentration around and between spheres which were highlighted when viewed using dark field microscopy (**Figure 4.1**). Well 2 (containing 20ng/ml EGF, 40ng/ml FGF) developed connecting bridges of ECM between adjacent spheres after 6 months in culture. Frozen sections demonstrated multiple nuclei visible in the connecting bridges when labelled with DAPI and imaged using fluorescence microscopy (**Figure 4.2**). The remaining primary cultures suffered contamination and did not persist in culture for 6 months.

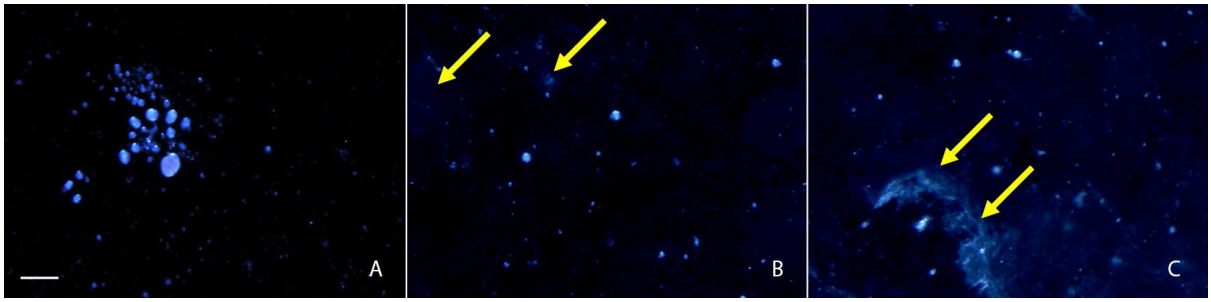

Figure 4.1 Higher concentrations of epidermal growth factor (EGF) were associated with increased extracellular matrix (ECM) like deposits around and between spheres (arrows) by day 21.Dark field microscopy images of spheres formed with various concentrations of EGF (2ng/ml (A), 20ng/ml (B), 200ng/ml (C)). Scale = 200µm.

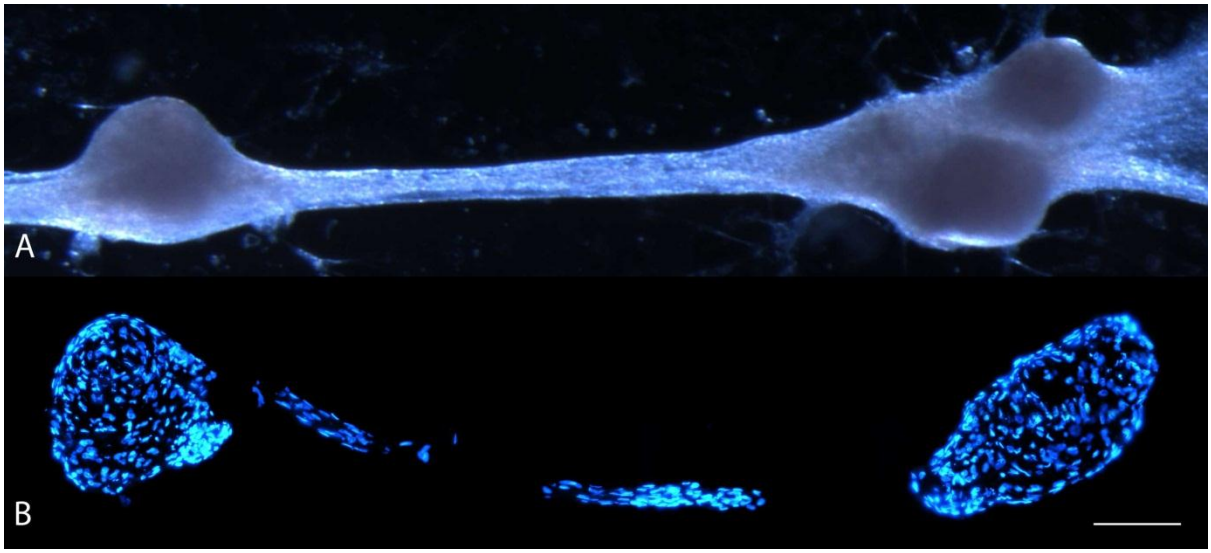

Figure 4.2 Dark field image of stromal cell spheres at 6 months in culture (A). Strand like deposits of cells with surrounding ECM-like material connect adjacent spheres. (B) DAPI labelling of cell nuclei in a frozen section of two connected spheres demonstrate cellularity of connecting strands. Scale bar = 100µm.

Stroma from two corneal rims with a total wet weight of 0.113gm was used for sphere culture and subsequent scanning electron microscopy (SEM) imaging. Cells cultured with and without EGF developed spheres at similar rates and the spheres appeared morphologically similar when viewed using bright field microscopy. When imaged using SEM, spheres cultured without EGF appeared to have less ECM deposition on and around the sphere compared to spheres cultured with EGF (**Figure 4.3**). Spheres cultured with EGF demonstrated a cap of ECM material and were anchored to the cover slip with ECM strands extending from the base of the sphere.

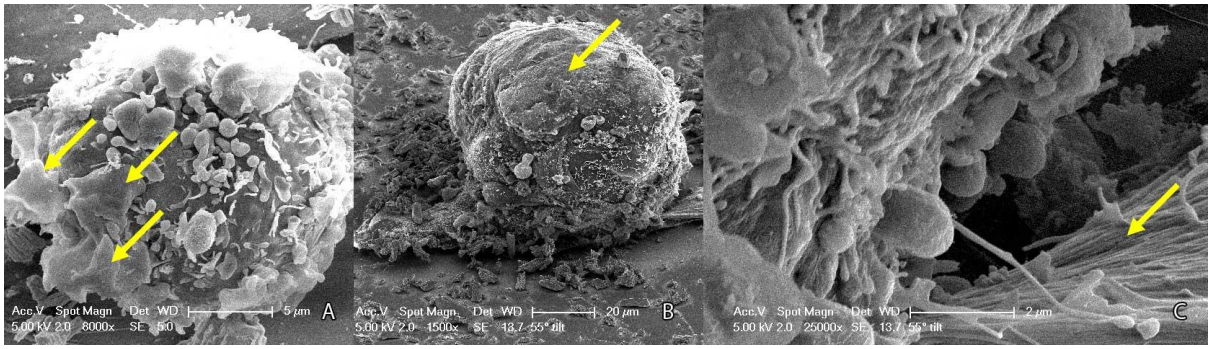

Figure 4.3 Scanning electron microscopy image of spheres cultured without EGF produce no ECM cap and single cells are clearly visible on the sphere surface (A, arrows). Spheres cultured with EGF demonstrate a cap like deposit on the surface of the sphere (B, arrow) and more extracellular matrix material adhering the sphere to the substrate (C, arrow).

For cytokine expression analysis, stromal tissue from five corneal rims was used. Half of the isolated cells were sorted using FACS and produced side population (SP) and non-SP cells for culture (**Figure 4.4**). Following 21 days in culture, cytokine expression in unsorted, SP, non-SP and uncultured-unsorted cells demonstrated significant differences in the expression levels of multiple cytokines (**Table 4.3**, **Figure 4.5**, **Figure 4.6**, **Figure 4.7**).

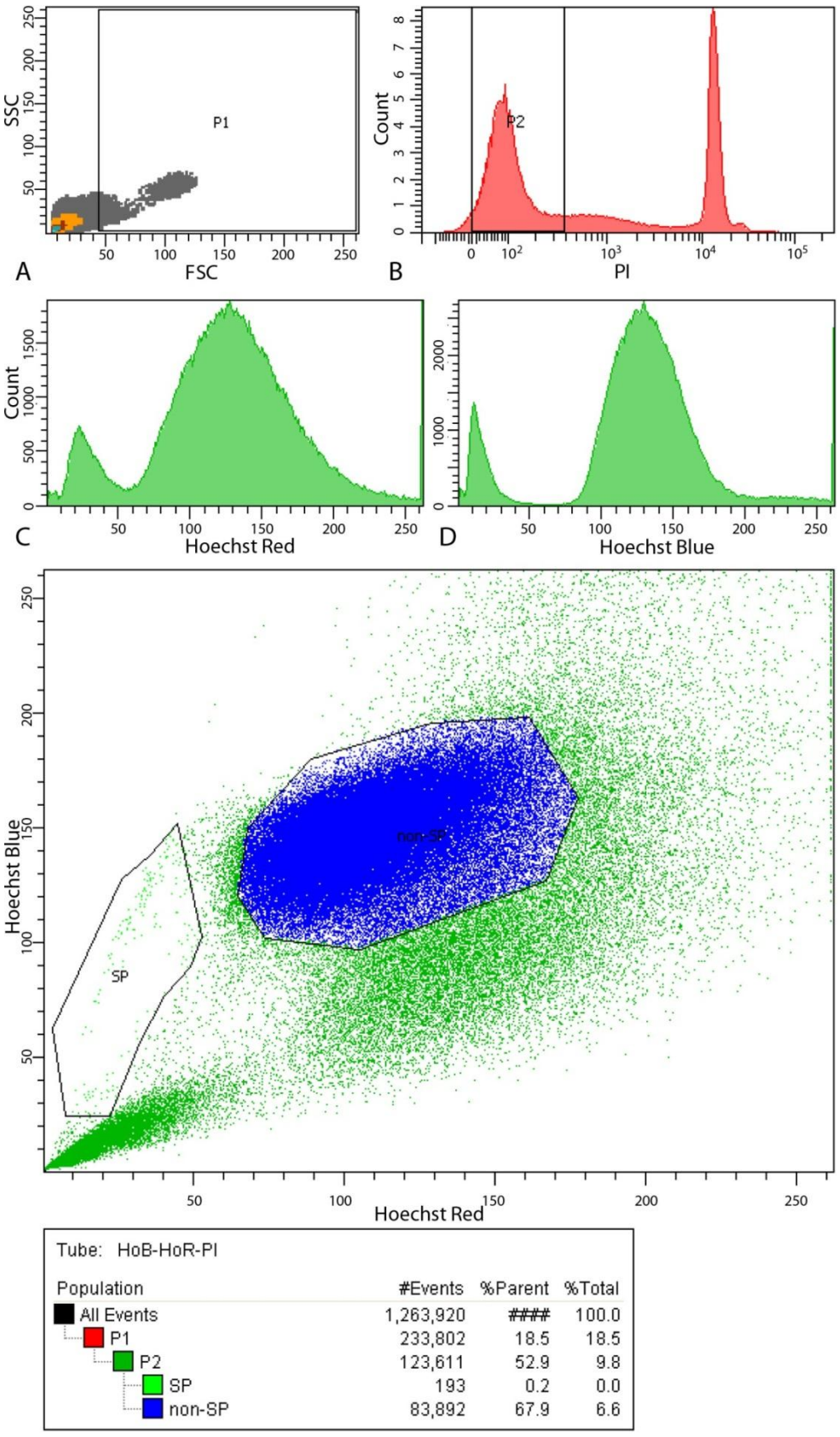

Figure 4.4 Fluorescence activated cell sorting (FACS) of isolated stromal cells. Cells were gated on forward scatter (FSC) and side scatter (SSC) to remove debris and cell doublets (top left). Cells were

also gated on propidium iodide uptake to exclude all non-viable cells (top right). SP (see label) and non-SP cells (coloured blue above) were isolated for subsequent culture and cytokine expression analysis.

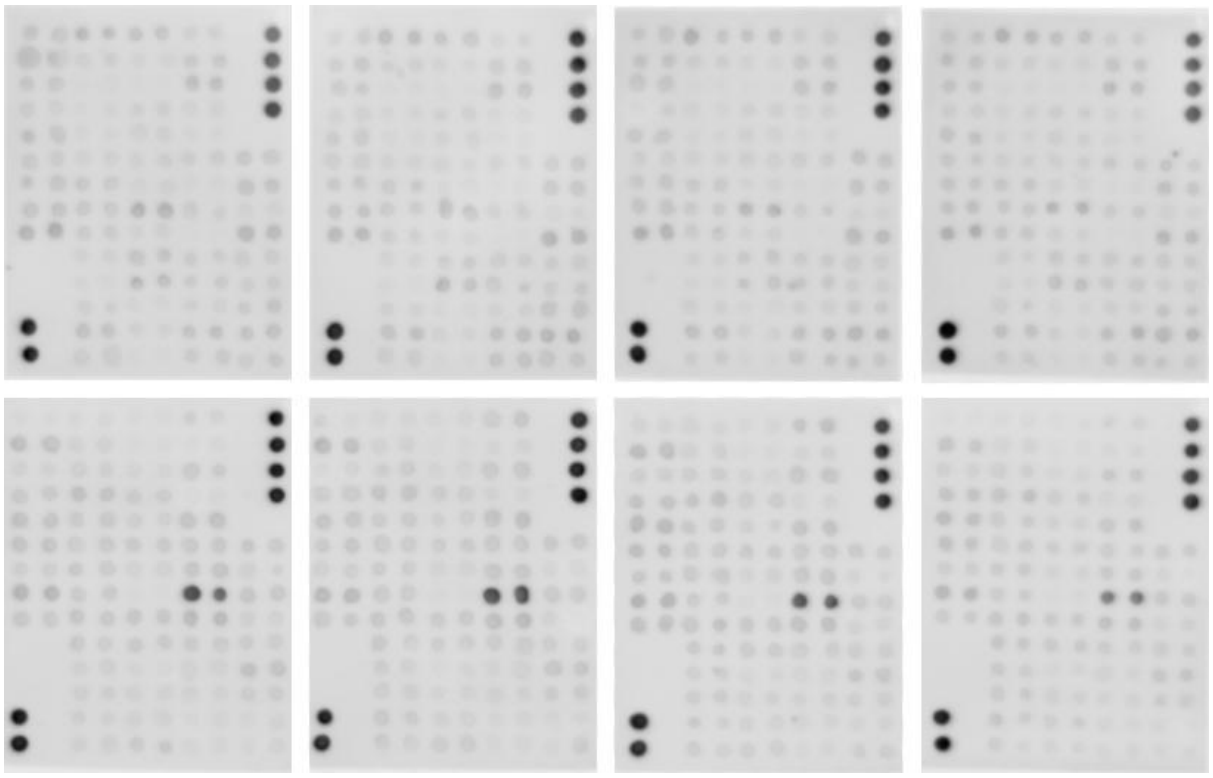

Figure 4.5 Cytokine arrays demonstrating varying spot intensities. The RayBio Human Cytokine Antibody Array C Series 1000 was used for analysis (top row is array VI and bottom row array VII). Each array corresponds to a different sample; from left to right SP cells, non-SP cells, unsorted cells, uncultured cells.

Cytokine	SP	Non-SP	Unsorted	Uncultured	max-10%	min+10%	significance
NEG	0	0	0	0			
POS	536845	536845	536845	536845			
Acrp30	38238	43792	47172	42338	42455	42062	*
AgRP	9695	15889	10842	20593	18534	10664	*
Amphiregulin	29341	26314	4218	24647	26407	4639	*
Angiogenin	50528	51252	42431	65286	58757	46675	*
Angiopoietin-2	56348	40281	44246	51137	50713	44310	*
axl	42890	37779	29600	36756	38601	32560	*
BDNF	75587	53877	52724	77964	70168	57996	*
Beta-NGF	43997	39967	44942	40475	40448	43963	
bFGF	57507	62448	58403	66275	59648	63258	
BLC	40960	13097	21618	36336	36864	14407	*
BMP-4	103341	76018	101322	120932	108838	83620	*
BMP-6	67406	32340	48571	54951	60666	35574	*
BTC	9416	22280	18621	16844	20052	10357	*
CCL28	11129	25898	23848	15854	23308	12242	*
CK beta 8-1	58152	27817	44485	53363	52337	30599	*
CNTF	76904	38883	72275	68911	69214	42772	*
CTACK	20783	68152	44268	11355	61336	12491	*
dtk	12892	31437	20641	4818	28293	5299	*
EGF	129054	84768	101909	83961	116148	92357	*
EGF-R	51318	63067	51251	43972	56760	48369	*
ENA-78	27733	23907	20964	6877	24960	7564	*
Eotaxin	69567	46812	73040	54429	65736	51493	*
Eotaxin-2	48281	33682	14852	25116	43453	16337	*
Eotaxin-3	66135	49308	34744	51195	59522	38218	*

Cytokine	SP	Non-SP	Unsorted	Uncultured	max-10%	min+10%	significance
Fas/TNFRSF6	57010	70729	74668	65605	67201	62710	*
FGF-4	37240	56976	47200	50500	51278	40964	*
FGF-6	85102	61320	58533	83959	76592	64386	*
FGF-7	32941	16988	12716	31331	29647	13987	*
FGF-9	50805	66713	57554	61918	60042	55886	*
Flt-3 Ligand	29252	2869	4725	21820	26327	3156	*
Fractalkine	56891	30775	19380	48355	51202	21318	*
GCP-2	29425	4100	3515	28210	26482	3866	*
G-CSF	273740	369204	402393	352325	362153	301113	*
GDNF	60771	26969	26970	44973	54694	29666	*
GITR	43100	39477	42843	43188	38869	43425	
GITR ligand	71147	86026	87458	87256	78712	78262	*
GM-CSF	28143	833	10223	20213	25328	916	*
GRO	28471	26807	25620	25366	25624	27903	
GRO-alpha	26609	33775	30807	26246	30397	28870	*
HCC-4	16954	26187	19245	15075	23568	16582	*
HGF	13261	16962	16603	13521	15265	14587	*
I-309	67255	33211	45294	48748	60529	36532	*
ICAM-1	1247	15130	11641	0	13617	0	*
ICAM-3	3814	14199	9086	4335	12779	4195	*
IFN-gamma	67626	48053	45750	52033	60863	50325	*
IGFBP-1	47813	23124	33678	39872	43031	25436	*
IGFBP-2	108151	57397	82979	69110	97336	63137	*
IGF-BP-3	17715	25975	19679	18022	23377	19486	*
IGFBP-4	78369	57131	71557	56633	70532	62297	*
IGF-BP-6	44838	42989	36801	40539	40354	40481	

Cytokine	SP	Non-SP	Unsorted	Uncultured	max-10%	min+10%	significance
IGF-I	90878	55403	48545	57160	81790	53399	*
IGF-I SR	26915	28674	27663	28585	25807	29607	
IL-1 R4/ST2	38217	51908	39609	43570	46717	42038	*
IL-1 RI	23167	29468	20394	22988	26521	22433	*
IL-10	41620	7539	16538	29837	37458	8293	*
IL11	10583	11085	7681	5182	9976	5700	*
IL12-p40	48274	59082	44137	50599	53174	48551	*
IL12-p70	48870	47562	33704	42504	43983	37074	*
IL-13	25799	0	9747	18959	23219	0	*
IL-15	52406	16032	27429	43043	47166	17635	*
IL-16	46067	16528	24133	45305	41461	18180	*
IL17	21485	17318	11960	13898	19337	13157	*
IL-1alpha	48621	22415	19721	44014	43759	21694	*
IL-1beta	41302	11072	13837	39067	37172	12179	*
IL-1ra	97650	78934	59470	131343	118208	65417	*
IL-2	43468	14402	15873	37712	39121	15843	*
IL-2 Ra	34225	29681	21900	25558	30803	24090	*
IL-3	68342	39856	37093	74448	67003	40802	*
IL-4	91386	41874	77806	89891	82247	46061	*
IL-5	34797	8340	19734	22022	31318	9175	*
IL-6	46020	14859	29988	35439	41418	16345	*
IL-6 R	32530	26336	24433	25778	29277	26877	*
IL-7	37126	7917	24924	21818	33413	8709	*
IL8	19150	33193	41376	38752	37239	21065	*
I-TAC	675	25300	12539	4619	22770	742	*
Leptin	131984	79323	62454	79370	118786	68700	*

Cytokine	SP	Non-SP	Unsorted	Uncultured	max-10%	min+10%	significance
LIGHT	50306	25214	29393	42152	45276	27736	*
Lymphotactin	24494	36845	26127	23283	33161	25611	*
MCP-1	31696	6200	16753	25729	28526	6820	*
MCP-2	42890	13620	21079	25661	38601	14982	*
MCP-3	39639	6737	20817	25594	35675	7410	*
MCP-4	50611	18502	29898	38979	45550	20352	*
M-CSF	73898	33870	47704	61028	66508	37257	*
MDC	64225	35160	40483	62858	57803	38676	*
MIF	37200	42464	34165	30312	38218	33343	*
MIG	75276	37407	33525	53360	67748	36878	*
MIP-1-alpha	75732	75649	58163	62802	68159	63979	*
MIP-1-beta	45630	51613	44018	47826	46452	48420	
MIP-1-delta	49656	13867	24295	34985	44691	15254	*
MIP-3-alpha	37961	10071	18657	22988	34165	11078	*
MIP-3-beta	46900	55889	42815	43575	50300	47097	*
MSP-a	45732	55739	33900	41369	50166	37290	*
NAP-2	52560	21454	34217	40646	47304	23599	*
NT-3	89285	74158	76580	81334	80357	81574	
NT-4	41957	41143	42120	34346	37908	37780	*
Oncostatin M	56004	45940	39185	41749	50403	43104	*
Osteoprotegerin	58109	70517	47939	49957	63465	52733	*
PARC	69765	21102	51512	58465	62789	23212	*
PDGF-BB	89386	59451	25401	76123	80448	27941	*
PlGF	48971	35701	30082	27732	44074	30506	*
RANTES	97962	80039	36927	98147	88332	40620	*
SCF	82456	57781	40595	69284	74211	44655	*

Cytokine	SP	Non-SP	Unsorted	Uncultured	max-10%	min+10%	significance
SDF-1	57530	6308	25453	47567	51777	6939	*
sgp130	52379	37468	34221	28175	47141	30993	*
sTNF RII	50833	31063	47071	27150	45750	29865	*
sTNF-RI	28802	35840	38203	28640	34383	31504	*
TARC	81616	50410	44285	73976	73455	48713	*
TECK	0	22681	13443	2771	20413	0	*
TGF-beta 1	68042	20291	41295	59129	61238	22320	*
TGF-beta 3	77608	46579	50445	70475	69847	51237	*
TIMP-1	63502	95210	82965	69325	85689	69852	*
TIMP-2	30029	39365	8979	23010	35428	9877	*
TNF-alpha	88861	48816	62789	80124	79975	53697	*
TNF-beta	137317	202815	92962	114277	182534	102258	*
TPO	72874	72828	36274	44570	65587	39902	*
TRAIL-R3	89873	111897	58553	65370	100708	64408	*
TRAIL-R4	74989	87595	49213	65040	78836	54134	*
uPAR	40313	57110	26616	31139	51399	29278	*
VEGF	101380	118080	93580	90846	106272	99931	*
VEGF-D	43593	87734	47898	48241	78961	47952	*

Table 4.3 Comparison of cytokine expression in cultured (21 days total) side population (SP), non-SP, unsorted, and uncultured stromal cells. Units are normalised quantified relative spot intensity for each cytokine tested in the RayBio Human Cytokine Antibody Array C Series 1000.

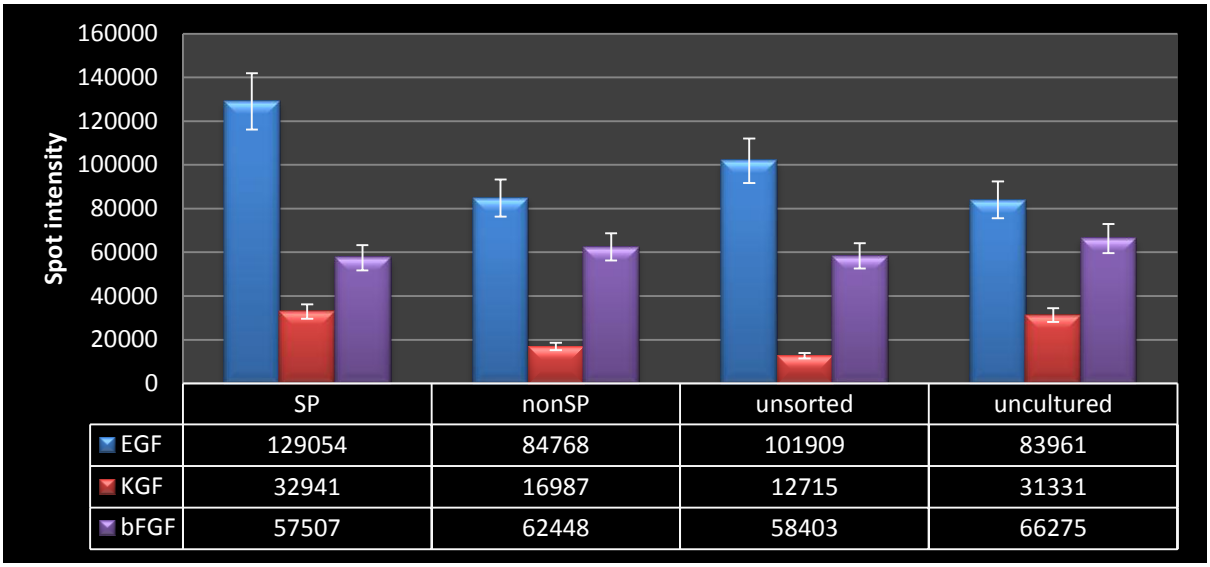

	SP	nonSP	unsorted	uncultured
EGF	129054	84768	101909	83961
KGF	32941	16987	12715	31331
bFGF	57507	62448	58403	66275

Figure 4.6 Relative expression of selected cytokines (arbitrary units corresponding to normalised spot intensity) as determined by spot intensity on the The RayBio Human Cytokine Antibody Array C Series 1000 in isolated cell populations. SP cells demonstrate relatively more growth factor expression including epidermal growth factor (EFG), keratinocyte growth factor (KGF), and less basic fibroblast growth factor (bFGF). Error bars demonstrate array manufacturer specified maximum error associated with repeated measurements on the same sample (±10%).

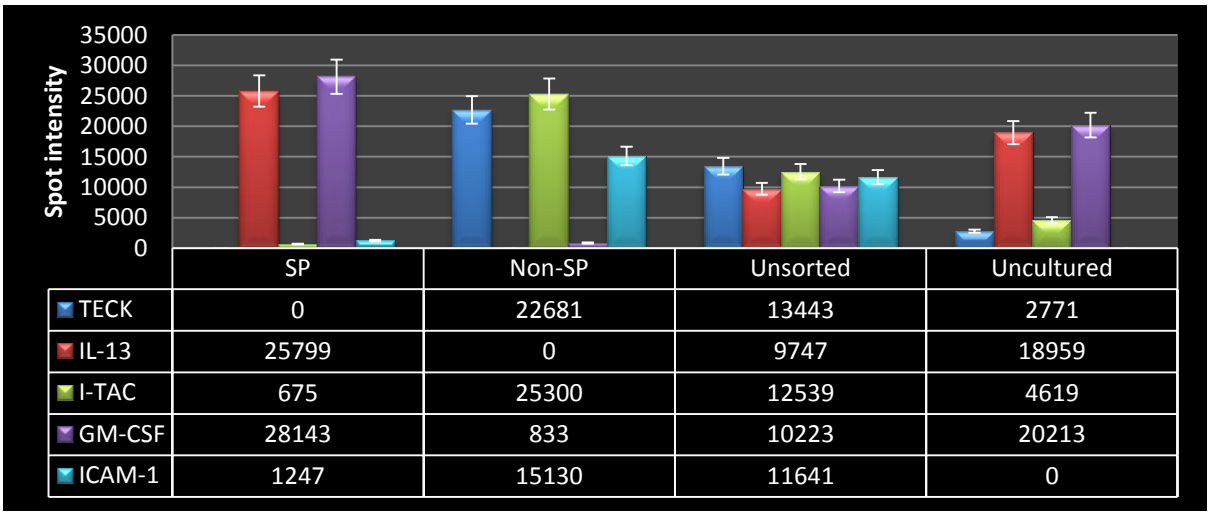

	SP	Non-SP	Unsorted	Uncultured
TECK	0	22681	13443	2771
IL-13	25799	0	9747	18959
I-TAC	675	25300	12539	4619
GM-CSF	28143	833	10223	20213
ICAM-1	1247	15130	11641	0

Figure 4.7 Relative expression of selected cytokines (arbitrary units corresponding to normalised spot intensity) as determined by spot intensity on the The RayBio Human Cytokine Antibody Array C Series 1000 in isolated cell populations. These five cytokines demonstrated the highest differential

expression between SP and nonSP cells (as a proportion of maximum expression). TECK = Thymus Expressed Chemokine; IL-13 = Interleukin 13; I-TAC = Interferon-inducible T-cell Alpha Chemoattractant, GM-CSF = Granulocyte Macrophage Colony Stimulating Factor; ICAM-1 = Inter-Cellular Adhesion Molecule 1.

4.4. Discussion

Exogenous EGF causes increased deposition of ECM like material around human stromal cell spheres in a dose dependant manner as observed with dark field and scanning electron microscopy. Similarly, a previous study using murine corneal stroma reported that cells form spheres and express ECM components when cultured with EGF in serum free media, however, the study did not investigate the effect of EGF concentration on ECM production.[20] EGF/EGF-receptor activation is known to cause cellular differentiation and proliferation in corneal stromal and other cell types as well as increased production of ECM components including collagen subtypes I, V and VI.[19, 21, 22] Interestingly, although EGF promotes ECM production, stromal cells fail to produce ECM when cultured as a monolayer and seem to require three-dimensional culture environments such as sphere or pellet culture in order to express ECM.[23] Despite the associations between stromal cell proliferation, wound healing and EGF, this is the first study to report a qualitative dose dependant response between stromal cell sphere ECM deposition and EGF concentration.

This study demonstrates that sphere based culture of human corneal stromal cells and expression of ECM is stable over long periods of time. Stromal spheres remain stable in culture for months and continue to express ECM that eventually develops as cellular bridges containing ECM connecting adjacent spheres. As a potential alternative to traditional corneal transplantation, the stable and maintained expression of ECM by transplanted stromal cell spheres is essential for continued ECM production and maintenance in host corneas. Additionally, the formation of cellular bridges in culture suggests that these cells may potentially migrate and repopulate host corneas while expressing ECM in the months following transplantation.

In contrast to EGF, bFGF did not appear to have any notable effects on keratocyte sphere morphology. It has been reported that bFGF may be involved in bovine keratocyte proliferation and simultaneously inhibits collagen synthesis.[24] Despite these observations in bovine cell cultures, human stromal cells appeared to produce ECM at increased rates as identified by dark field microscopy even at high concentrations of bFGF.

Previous studies have identified EGF expression in all layers of the cornea,[4, 5, 8] however, despite various sub-populations of cells existing in the corneal stroma there have been no previous reports of the differential expression of cytokines including EGF between these various cell types. The role of stromal SP cells was previously thought to be a quiescent pool of stem and progenitor cells that could act as a reservoir for maintenance of stromal keratocytes.[25, 26] Contrary to expectations, the current study noted that SP cells produce significantly more EGF, KGF (which is known to be produced by keratocytes and has a role in wound healing and proliferation[27-29]), and several other cytokines than non-SP cells as demonstrated using cytokine arrays to compare relative expression of cytokines in sub-populations of human stromal cells. These observations suggest that the SP-cell phenotype in the corneal stroma is not entirely quiescent and has an active role in maintaining the cytokine profile of the corneal stroma. These secreted cytokines and growth factors act on the stromal keratocytes to regulate the production and maintenance of the stromal ECM.

Interestingly several other cytokine molecules were also identified with a large differential expression between SP and nonSP cells including Thymus Expressed Chemokine (TECK), Interleukin 13 (IL-13), Interferon-inducible T-cell Alpha Chemoattractant (I-TAC), Granulocyte Macrophage Colony Stimulating Factor (GM-CSF), and Inter-Cellular Adhesion Molecule 1 (ICAM-1). Aside from ICAM-1 which has been reported to mediate keratocyte-neutrophil adhesion[30] and I-TAC which may be involved in keratocyte-mediated chemoattraction of lymphocyte and natural killer cells involved in cell-mediated immunity[31] little is known about the role of these molecules in the cornea. These differentially expressed cytokines certainly raise some questions about the role of the SP and nonSP

cells in the corneal stroma and further research is required to investigate this in more detail. Lastly not all of the cytokine expression values for the unsorted cells fall between the SP and nonSP values as might be expected. The likely reason for this observation is due to the 21 days of culture following cell sorting and changes in expression that may have either been induced by the process of sorting or by culturing as isolated populations in the absence of feedback loops that may be provided by a mixed population of cells as in the cornea.

There are several limitations to this study. Due to the availability of tissue and the amount required for each cytokine array, this study used tissue that was pooled from five donor corneal rims and only one replicate from each treatment group was analysed using the cytokine array. Although it would have been interesting to analyse each of the corneas individually to gain some insight into variation between corneas this would have required several intact human donor corneas which was simply not feasible due to the extremely limited availability of normal human corneal tissue for research. Pooling the corneas provided results that were essentially mean averages for the set of corneas used. Secondly, tissue availability aside, it is technically challenging to sort cells and maintain in culture for cytokine analysis as primary cell cultures due to contamination issues as the cell sorting is conducted in clean but not sterile conditions, unfortunately two attempts at repeating this experiment were aborted due to contamination. Finally, the cytokine array manufacturer states in the supplied user manual that repeated arrays using the same sample may demonstrate variations in spot intensity of up to 10%. The single replicates used in this study were a consequence of the limited supply of tissue available and the amount of tissue required for each array. This study design provided no estimate of the error term associated with repeated cytokine array measurements and therefore the manufacturer stated error was used for analysis to give the best possible estimate of likely stastical significance given the limited data available. Although there is some error associated with the cytokine array based assessment of cytokines, the error associated with an Enzyme-Linked Immunosorbent Assay (ELISA), an alternative strategy that could be used to obtain similar data, is typically 20% or more.[32]

4.5. Conclusions

SP cells may play an active role in the stroma, secreting increased EGF which stimulates surrounding keratocytes to secrete and maintain the ECM. It is possible that transplanting SP rich stromal cell spheres into keratoconic corneas may help prevent the ectasia and characteristic topographical changes observed in keratoconus.

4.6. References

1. Kim A, Lakshman N, Karamichos D, Petroll WM. Growth factor regulation of corneal keratocyte differentiation and migration in compressed collagen matrices. Investigative Ophthalmology and Visual Science 2010;51(2):864-75.

2. Schultz G, Khaw PT, Oxford K, et al. Growth factors and ocular wound healing. Eye 1994;8 (Pt 2):184-7.

3. Mohan RR, Wilson SE. Ex vivo human corneal epithelial cells express membrane-bound precursor and mature soluble epidermal growth factor (egf) and transforming growth factor (tgf) alpha proteins. Experimental Eye Research 1999;68(1):129-31.

4. Wilson SE, Lloyd SA. Epidermal growth factor and its receptor, basic fibroblast growth factor, transforming growth factor beta-1, and interleukin-1 alpha messenger rna production in human corneal endothelial cells. Investigative Ophthalmology and Visual Science 1991;32(10):2747-56.

5. Wilson SE, Schultz GS, Chegini N, et al. Epidermal growth factor, transforming growth factor alpha, transforming growth factor beta, acidic fibroblast growth factor, basic fibroblast growth factor, and interleukin-1 proteins in the cornea. Experimental Eye Research 1994;59(1):63-71.

6. Pancholi S, Tullo A, Khaliq A, et al. The effects of growth factors and conditioned media on the proliferation of human corneal epithelial cells and keratocytes. Graefe's Archive for Clinical and Experimental Ophthalmology 1998;236(1):1-8.

7. Haber M, Cao Z, Panjwani N, et al. Effects of growth factors (egf, pdgf-bb and tgf-beta 1) on cultured equine epithelial cells and keratocytes: Implications for wound healing. Veterinary Ophthalmology 2003;6(3):211-7.

8. Tuli SS, Liu R, Chen C, et al. Immunohistochemical localization of egf, tgf-alpha, tgf-beta, and their receptors in rat corneas during healing of excimer laser ablation. Current Eye Research 2006;31(9):709-19.

9. Garana RM, Petroll WM, Chen WT, et al. Radial keratotomy. Ii. Role of the myofibroblast in corneal wound contraction. Investigative Ophthalmology and Visual Science 1992;33(12):3271-82.

10. Hanna KD, Pouliquen Y, Waring GO, 3rd, et al. Corneal stromal wound healing in rabbits after 193-nm excimer laser surface ablation. Archives of Ophthalmology 1989;107(6):895-901.

11. Jester JV, Ho-Chang J. Modulation of cultured corneal keratocyte phenotype by growth factors/cytokines control in vitro contractility and extracellular matrix contraction. Experimental Eye Research 2003;77(5):581-92.

12. Long CJ, Roth MR, Tasheva ES, et al. Fibroblast growth factor-2 promotes keratan sulfate proteoglycan expression by keratocytes in vitro. Journal of Biological Chemistry 2000;275(18):13918-23.

13. Tuominen IS, Tervo TM, Teppo AM, et al. Human tear fluid pdgf-bb, tnf-alpha and tgf-beta1 vs corneal haze and regeneration of corneal epithelium and subbasal nerve plexus after prk. Experimental Eye Research 2001;72(6):631-41.

14. Zhou L, Beuerman RW, Huang L, et al. Proteomic analysis of rabbit tear fluid: Defensin levels after an experimental corneal wound are correlated to wound closure. Proteomics 2007;7(17):3194-206.

15. Blalock TD, Duncan MR, Varela JC, et al. Connective tissue growth factor expression and action in human corneal fibroblast cultures and rat corneas after photorefractive keratectomy. Investigative Ophthalmology and Visual Science 2003;44(5):1879-87.

16. Hassell JR, Birk DE. The molecular basis of corneal transparency. Experimental Eye Research 2010;91(3):326-35.

17. Hoppenreijs VP, Pels E, Vrensen GF, et al. Platelet-derived growth factor: Receptor expression in corneas and effects on corneal cells. Investigative Ophthalmology and Visual Science 1993;34(3):637-49.

18. Hoppenreijs VP, Pels E, Vrensen GF, Treffers WF. Basic fibroblast growth factor stimulates corneal endothelial cell growth and endothelial wound healing of human corneas. Investigative Ophthalmology and Visual Science 1994;35(3):931-44.

19. He J, Bazan HE. Epidermal growth factor synergism with tgf-beta1 via pi-3 kinase activity in corneal keratocyte differentiation. Investigative Ophthalmology and Visual Science 2008;49(7):2936-45.

20. Yoshida S, Shimmura S, Shimazaki J, et al. Serum-free spheroid culture of mouse corneal keratocytes. Investigative Ophthalmology and Visual Science 2005;46(5):1653-8.

21. Herbst RS. Review of epidermal growth factor receptor biology. International Journal of Radiation Oncology, Biology, Physics 2004;59(2 Suppl):21-6.

22. Santa-Olalla J, Covarrubias L. Epidermal growth factor (egf), transforming growth factor-alpha (tgf-alpha), and basic fibroblast growth factor (bfgf) differentially influence neural precursor cells of mouse embryonic mesencephalon. Journal of Neuroscience Research 1995;42(2):172-83.

23. Du Y, Sundarraj N, Funderburgh ML, et al. Secretion and organization of a cornea-like tissue in vitro by stem cells from human corneal stroma. Investigative Ophthalmology and Visual Science 2007;48(11):5038-45.

24. Etheredge L, Kane BP, Hassell JR. The effect of growth factor signaling on keratocytes in vitro and its relationship to the phases of stromal wound repair. Investigative Ophthalmology and Visual Science 2009;50(7):3128-36.

25. Challen GA, Little MH. A side order of stem cells: The sp phenotype. Stem Cells 2006;24(1):3-12.

26. Du Y, Roh DS, Funderburgh ML, et al. Adipose-derived stem cells differentiate to keratocytes in vitro. Molecular Vision 2010;16:2680-9.

27. Carrington LM, Boulton M. Hepatocyte growth factor and keratinocyte growth factor regulation of epithelial and stromal corneal wound healing. Journal of Cataract and Refractive Surgery 2005;31(2):412-23.

28. Wilson SE, Chen L, Mohan RR, et al. Expression of hgf, kgf, egf and receptor messenger rnas following corneal epithelial wounding. Experimental Eye Research 1999;68(4):377-97.

29. Wilson SE, Liang Q, Kim WJ. Lacrimal gland hgf, kgf, and egf mrna levels increase after corneal epithelial wounding. Investigative Ophthalmology and Visual Science 1999;40(10):2185-90.

30. Gagen D, Laubinger S, Li Z, et al. Icam-1 mediates surface contact between neutrophils and keratocytes following corneal epithelial abrasion in the mouse. Experimental Eye Research 2010;91(5):676-84.

31. McInnis KA, Britain A, Lausch RN, Oakes JE. Synthesis of alpha-chemokines ip-10, i-tac, and mig are differentially regulated in human corneal keratocytes. Investigative Ophthalmology and Visual Science 2005;46(5):1668-74.

32. RayBiotech I. Raybio human cytokine antibody array c series 1000 user manual. Package insert,2004.

Chapter 5. Fluorescence activated cell sorting analysis of isolated and cultured stromal cells

5.1. Introduction

Fluorescence activated cell sorting (FACS) facilitates the sorting of live cells based on physical parameters, metabolic state and cell surface characteristics including the presence and absence of certain cell surface proteins and transporters.[1] Forward scatter (FSC) and side scatter (SSC) are objective measures of refraction and reflection of laser light that can be measured during cell sorting and act as discriminatory markers or gates. FSC occurs when a cell redirects laser light at a shallow angle, typically less than 2 degrees, and is a relative measure of cell size.[2, 3] SSC occurs when cells reflect laser light, detected perpendicular to the incident light path, and is a relative measure of the complexity and extent of intracellular particles and cell organelles.[1] In addition to light scattering characteristics, cell viability can also be gated with the addition of propidium iodide (PI), a molecule that fluoresces when bound to DNA and selectively enters non-viable cells with compromised cell membranes.FSC and SSC can be used in combination with PI to gate sorted cells to enrich cell populations for small undifferentiated viable cells that are likely to harbour the resident stem cell population.

Size and differentiation alone are not enough to identify stem cells using FACS, however, the efflux of Hoechst 33342 provides an additional characteristic that can be used to isolate of a side population (SP) of cells. These SP cells have been characterised as putative stem cells in wide variety of tissues and organisms including the human cornea.[1, 4, 5] The SP phenotype was first identified in murine bone marrow where isolated SP cells were associated with haematopoietic stem cells that persistently maintained the ability to replicate and repopulate *in vivo*.[6] SP cells have subsequently been described in numerous tissues and organisms and share the same stem-like characteristics.

With the absence of any specific cell surface markers to identify stem cells, FACS on the basis of Hoechst 33342 efflux is the primary technique for identifying and isolating putative stem cells.[4, 5] Hoechst 33342 is a lipophilic molecule that is able to cross the cell membrane and binds the minor groove of DNA at regions with high adenine and thymine concentration.[7] On binding DNA, Hoechst

33342 fluorescence intensity is proportional to DNA content, condensation and conformation. [8] The specificity of Hoechst 33342 as a stem cell marker is due to its efflux by the ATP-binding cassette (ABC) transporter superfamily of membrane bound pumps such as ABCG2 found specifically on the SP cell population.[9] Hoechst 33342 efflux and ABCG2 mediated transport is inhibited by verapamil and correspondingly pre-incubation in the presence of verapamil prior to Hoechst labelling and FACS is associated with disappearance of the SP phenotype.[4]

Stem cells have been isolated from haematopoietic and neural lineages based on light scattering and Hoechst 33342 efflux alone and more recently studies have identified corneal stromal and epithelial stem cells using the same approach.[5, 10-12] Despite the attention that has been given to isolating stem cells in a number of tissues and organisms, there have been no studies to date that have compared the SP population in human corneal stroma and cultured stromal cells and the ability of SP and non-SP cells to form spheres and support a resident SP lineage in culture. The purpose of this study was to confirm the presence of SP cells in human stromal tissue and to investigate the regenerative and sphere forming capacity of SP and non-SP cells in culture.

5.2. Methods

Stromal cells were isolated from four human corneal rims according to protocols as described in sections 3.1.1 and 3.2.1. Isolated cells were prepared and sorted using fluorescence activated cell sorting (FACS) as described in section 3.4.1.

Following FACS, SP and non-SP cells were cultured at 37°C for 14 days, trypsin digested, mechanically dissociated and resorted using the same protocol with Hoechst 33342 incubation as initially used for stromal digest.

A second preparation of isolated stromal cells was prepared and sorted using FACS as described above. The sorted SP and non-SP cells were cultured in basal growth media (see section 3.2.4 for details) for 32 days at 37°C and 5% CO_2 and the resulting spheres were quantified by counting four

quadrants of each culture well using an inverted microscope and 4x objective. Culture media was replaced every 3 days in all cultures. Sphere formation in SP and non-SP cultures was analysed and compared using an unpaired independent sample students T-test for a difference between means. Data were analysed using the R statistical analysis package, version 2.13.1 (R Development Core Team, University of Auckland, New Zealand).

5.3. Results

Fluorescence activated cell sorting of isolated stromal cells demonstrated SP cells with reduced Hoechst 33342 fluorescence (see **Table 5.1**, **Figure 5.1**, **Figure 5.2**). When pre-treated with the ABCG2 inhibitor verapamil these SP cells disappeared (**Figure 5.1**). Both SP and non-SP cells were capable of forming spheres, however, non-SP cells formed spheres at higher rates (P-value = 0.0006,table 5.2). Spheres formed from non-SP cells demonstrated a reappearance of an SP population when disaggregated and re-sorted using fluorescence activated cell sorting. SP cell derived spheres also demonstrated SP and non-SP cell populations when disaggregated and re-sorted.

NZ Eye Bank cornea (pre-digest wet weight of stroma)	Total number of cells	Number of SP cells (% of total)	Number of non-SP cells (% of total)
10-20A,B 10-21A,B (0.14gm)	178,559	738 (0.4)	177,821 (99.6)
non-SP re-sort	61,615	8,929 (14.5)	52,686 (85.5)
SP re-sort	379	16 (4.2)	363 (95.8)

Table 5.1 Details of the corneal tissue, stroma wet weight prior to digestion and sub-population cell yield. SP re-sort and non-SP re-sort data following two weeks in culture and repeat FACS. The reduced cell numbers in the resorted cells represent some cell loss in digesting and processing cells as well as gating for cell doublets and debris during FACS.

Group	SP	Non-SP
Mean number of spheres/1000 cells plated/field	0.47	6.45
SD (SEM)	0.27 (0.09)	3.62 (1.81)
N	8	4
P-val (mean difference)	0.0006	0.0006

Table 5.2 Ability of SP and non-SP cells to form spheres in culture. Spheres were cultured from SP and non-SP cells cultured in standard media at 37 degrees C, 5% CO_2 with a plating density of 12,000 cells/ml for non-SP cells and 1,200 cells/ml for SP cells. Spheres were counted after 32 days in culture at four quadrants of each plate (top, bottom and two sides) and quantified using an inverted microscope and a 4x objective with results expressed as mean spheres per field of view per 1000 cells plated. A paired student T-test for a difference between means was conducted. P value and statistical significance: The two-tailed P value equals 0.0006, 95% confidence interval of this difference: From -8.7110191 to -3.2523609, t = 4.8833,df = 10, standard error of difference = 1.225. SD = standard deviation, SEM = standard error of the mean, N = number of fields (of view) counted.

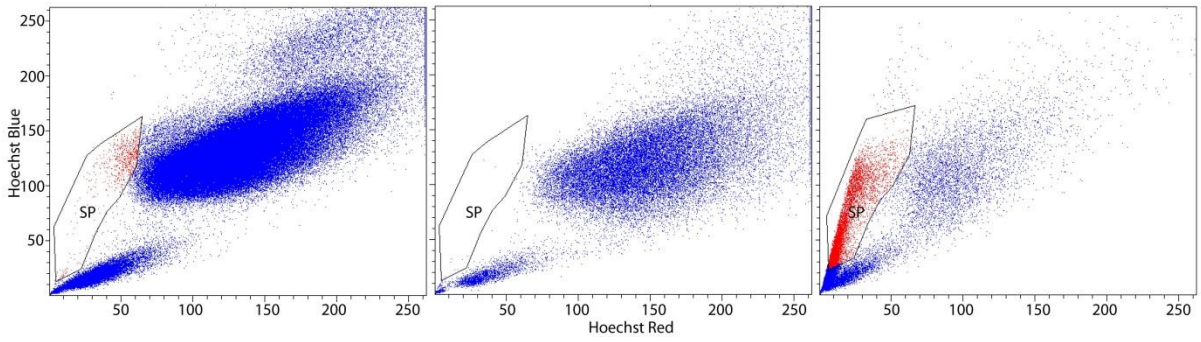

Figure 5.1 Fluorescence activated cell sorting using Hoechst red and blue fluorescence intensity of isolated stromal cells following Hoechst 33342 incubation. Side population (SP) cells were identified as a population of hypo fluorescent cells (SP cells are labelled red and comprise 0.4% of the total cells isolated from the corneal stroma (left)). When the cells were pre-treated with verapamil, an inhibitor of the ABCG2 membrane transporter that effluxes Hoechst 33342, the SP cells disappeared

(centre). Both SP and non-SP cells were capable of forming spheres in culture. Cells re-isolated from spheres formed from non-SP cells (blue cells isolated from top right of left plot) were resorted following Hoechst 33342 labelling after 14 days in culture and demonstrated the reappearance of SP cells (right) (labelled red, 14.5% of total cells isolated from spheres).

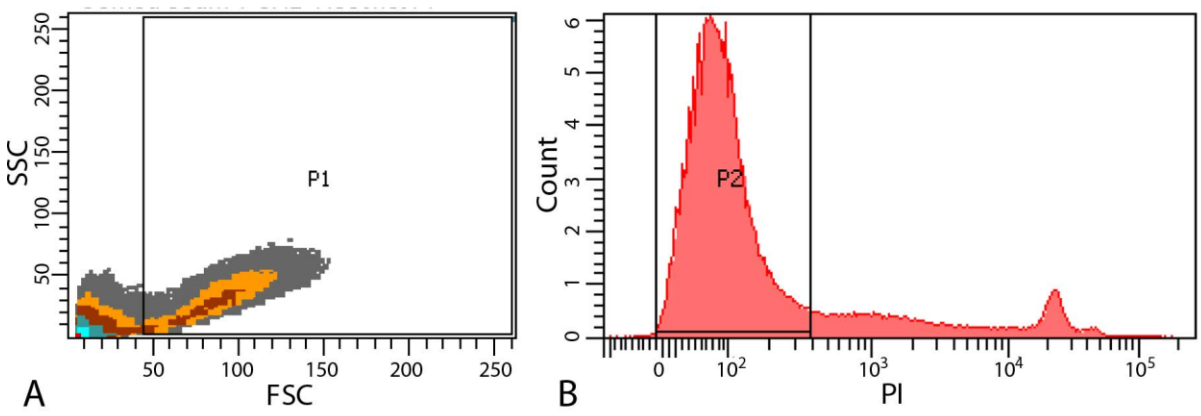

E

Tube: Hoechst PI

Population	#Events	%Parent	%Total
All Events	538,224	####	100.0
P1	218,441	40.6	40.6
P2	178,559	81.7	33.2
SP	738	0.4	0.1
NOT(SP)	177,821	99.6	33.0

Figure 5.2 Fluorescence activated cell sorting of isolated stromal cells pre-treated with Hoechst 33342. P1 population was gated to remove debris and cell doublets (A). P2 population was gated to remove non-viable cells that labelled with propidium iodide (B). Hoechst fluorescence was used to discriminate SP and non-SP cells (C, D). Final FACS plot is displayed in figure 5.1 (left). Cell sorting count of cell populations, NOT(SP)= non-SP (E).

5.4. Discussion

It is possible to sort isolated human corneal stromal cells based on FSC, SSC, PI and Hoechst 33342 efflux using FACS and identify a resident stem cell population. In the current study the SP cells comprised 0.4% of the total isolated stromal cells which agrees with the prevalence of SP cells (typically <1%) reported in other studies using a variety of primary tissue digests[4, 5, 9, 10] and confirms the results of a previous study using human stromal cells.[12] The SP population disappeared with pre-incubation with verapamil indicating that the SP cells were identified based on the presence of the ABC transporter – a specific marker of stem cells.[9]

Sorted cells remained viable in culture and interestingly both SP and non-SP cells were capable of forming spheres in culture. Studies documenting sphere formation from neural tissue in the presence of methylcellulose and 5-bromo-2'-deoxyuridine (BRDU) concluded that spheres form by proliferation of progenitor or stem cells[13, 14], and by association this method of culture has subsequently been proposed as a means of isolating stem or precursor cells from a variety of tissues including the cornea.[15-22] As non-SP cells are capable of forming spheres, and indeed at higher rates than the SP cells, corneal-stromal-cell sphere formation may occur by a different mechanism than neurosphere formation despite the same culture conditions (serum free media supplemented with epidermal growth factor and basic fibroblast growth factor).[13, 14]

Sphere formation is associated with the re-emergence of a SP phenotype in non-SP stromal cell cultures. It is unclear how sphere formation promotes the SP phenotype, however, one study that analysed cultured murine neurospheres also documented greatly increased SP cells in cultured spheres compared with primary cell digests although this study did not deplete the SP cells prior to culture.[10] The origin of these regenerated SP cells remains unclear. It may be possible that un-committed progenitor cells that have not yet fully differentiated are enticed back to a SP phenotype, however, the precise origin of these cells remains speculative at this time.

Due to the scarcity of SP cells it was not possible to plate the SP cells at the same density as the non-SP cells when analysing sphere forming potential of each of these sub populations. Although the data suggests that non-SP cells have higher sphere forming potential than SP cells, the effect of low plating density on SP cell sphere formation remains a confounding factor in the current study. Of note the FACS scatter plot of the re-sorted non-SP and SP cells appeared very similar and it may be that if consistent plating densities were maintained, both cell populations would form spheres at similar rates and re-sort with a similar distribution.

5.5. Conclusions

Side population (SP) cells efflux Hoechst 33342 using the ABC transporter proteins which are thought to be a marker of stem like properties.[6] Interestingly sphere formation still occurs with isolated non-SP cells in culture which is consistent with the observation that early sphere formation occurs predominantly as a result of cell migration/aggregation. These cultured non-SP cells exhibit ABCG2 expression and on repeat FACS demonstrate the reappearance of SP cells. It has been suggested that stromal SP cells represent corneal stem or progenitor cells that can be induced to differentiate into several cell lineages depending on the culture conditions.[23] The results of the current study suggest that spheroid culture of stromal cells has the potential to promote and maintain a progenitor cell population from differentiated-SP-depleted cells. The ability to maintain a viable SP cell and progenitor cell population is likely to be essential for therapeutic interventions including long-term repopulation of dystrophic corneal stroma with healthy donor cells.

5.6. References

1. Johnson KW, Dooner M, Quesenberry PJ. Fluorescence activated cell sorting: A window on the stem cell. Current Pharmaceutical Biotechnology 2007;8(3):133-9.
2. Mullaney PF, Dean PN. Cell sizing: A small-angle light-scattering method for sizing particles of low relative refractive index. Applied Optics 1969;8(11):2361-2.
3. Mullaney PF, Van Dilla MA, Coulter JR, Dean PN. Cell sizing: A light scattering photometer for rapid volume determination. Review of Scientific Instruments 1969;40(8):1029-32.
4. Challen GA, Little MH. A side order of stem cells: The sp phenotype. Stem Cells 2006;24(1):3-12.
5. Du Y, Roh DS, Funderburgh ML, et al. Adipose-derived stem cells differentiate to keratocytes in vitro. Molecular Vision 2010;16:2680-9.
6. Goodell MA, Brose K, Paradis G, et al. Isolation and functional properties of murine hematopoietic stem cells that are replicating in vivo. Journal of Experimental Medicine 1996;183(4):1797-806.
7. Lalande ME, Miller RG. Fluorescence flow analysis of lymphocyte activation using hoechst 33342 dye. Journal of Histochemistry and Cytochemistry 1979;27(1):394-7.
8. Arndt-Jovin DJ, Jovin TM. Analysis and sorting of living cells according to deoxyribonucleic acid content. Journal of Histochemistry and Cytochemistry 1977;25(7):585-9.
9. Zhou S, Schuetz JD, Bunting KD, et al. The abc transporter bcrp1/abcg2 is expressed in a wide variety of stem cells and is a molecular determinant of the side-population phenotype. Nature Medicine 2001;7(9):1028-34.
10. Hulspas R, Quesenberry PJ. Characterization of neurosphere cell phenotypes by flow cytometry. Cytometry 2000;40(3):245-50.
11. Zhang S, Uchida S, Inoue T, et al. Side population (sp) cells isolated from fetal rat calvaria are enriched for bone, cartilage, adipose tissue and neural progenitors. Bone 2006;38(5):662-70.

12. Du Y, Funderburgh ML, Mann MM, et al. Multipotent stem cells in human corneal stroma. Stem Cells 2005;23(9):1266-75.

13. Kawase Y, Yanagi Y, Takato T, et al. Characterization of multipotent adult stem cells from the skin: Transforming growth factor-beta (tgf-beta) facilitates cell growth. Experimental Cell Research 2004;295(1):194-203.

14. Gritti A, Frolichsthal-Schoeller P, Galli R, et al. Epidermal and fibroblast growth factors behave as mitogenic regulators for a single multipotent stem cell-like population from the subventricular region of the adult mouse forebrain. Journal of Neuroscience 1999;19(9):3287-97.

15. Yamagami S, Yokoo S, Mimura T, et al. Distribution of precursors in human corneal stromal cells and endothelial cells. Ophthalmology 2007;114(3):433-9.

16. Coles BL, Angenieux B, Inoue T, et al. Facile isolation and the characterization of human retinal stem cells. Proceedings of the National Academy of Sciences of the United States of America 2004;101(44):15772-7.

17. Krause DS, Theise ND, Collector MI, et al. Multi-organ, multi-lineage engraftment by a single bone marrow-derived stem cell. Cell 2001;105(3):369-77.

18. Li H, Liu H, Heller S. Pluripotent stem cells from the adult mouse inner ear. Nature Medicine 2003;9(10):1293-9.

19. Nunes MC, Roy NS, Keyoung HM, et al. Identification and isolation of multipotential neural progenitor cells from the subcortical white matter of the adult human brain. Nature Medicine 2003;9(4):439-47.

20. Reynolds BA, Weiss S. Generation of neurons and astrocytes from isolated cells of the adult mammalian central nervous system. Science 1992;255(5052):1707-10.

21. Toma JG, Akhavan M, Fernandes KJ, et al. Isolation of multipotent adult stem cells from the dermis of mammalian skin. Nature Cell Biology 2001;3(9):778-84.

22. Tropepe V, Coles BL, Chiasson BJ, et al. Retinal stem cells in the adult mammalian eye. Science 2000;287(5460):2032-6.

23. Funderburgh ML, Du Y, Mann MM, et al. Pax6 expression identifies progenitor cells for corneal keratocytes. FASEB Journal 2005;19(10):1371-3.

Chapter 6. Understanding the mechanism of early stromal cell sphere formation: the role of migration and aggregation versus cell division

6.1. Introduction

A sphere based culture system may be the most appropriate means of expanding human stromal cells without altering the phenotype of the cells, however, the mechanisms involved in sphere formation remain poorly understood. Culturing human keratocytes is challenging as typically these cells become fibroblastic in response to even small amounts of serum, unless cultured on amniotic membrane[1-3] and they tend to rapidly down-regulate expression of proteoglycans in culture. Several studies have demonstrated keratocyte spheroid culture using bovine[4, 5], rabbit[6], mouse[7], and human[8] corneal stromal cells. Spheroid culture is associated with a stable keratocyte phenotype including expression of keratocyte specific proteoglycans such as keratocan.[4-7] Using a sphere based culture system that maintains the phenotype of the isolated cells is therefore ideal for culturing and expanding stromal cells *in vitro.* Until now, however, the exact mechanism of corneal-stromal-cell sphere formation remains unclear.

Keratocyte sphere formation is thought to occur as a result of either cell migration/aggregation[4] or progenitor cell proliferation/propagation.[4, 6-10] Studies reporting sphere formation from neural tissue in the presence of methylcellulose and 5-bromo-2'-deoxyuridine (BRDU) concluded that spheres form by proliferation of progenitor or stem cells[11, 12], and by association this method of culture has subsequently been proposed as a means of isolating stem or precursor cells from a number of tissues including the cornea.[8, 13-19]

Quantum dot nanocrystals are small semiconductor particles that can be used as a live cell label to track migration of cells *in vitro*. These small fluorescent particles have unique optical properties including exceptionally bright fluorescence that remains largely resistant to photo-bleaching, and has broad excitation wavelengths and narrow emission spectra that can be tuned based on particle size.[20] In addition to the optical properties, quantum dots can be conjugated to signalling peptides to target cellular uptake by live cells and remain inert in endosomes without affecting cellular processes or cell viability, allowing tracking of live cells for several cell generations.[21-23] The physical

and optical properties of quantum dots make them ideal for labelling and tracking live cells including corneal stromal cells. The purpose of this study was to assess the relative contributions of cell migration and proliferation in early stromal cell sphere formation using time lapse fluorescence microscopy with quantum dot nanocrystals to track cell migration in combination with a cell proliferation assay.

6.2. Methods

6.2.1. Qtracker uptake by stromal cells

Stromal cells were isolated from two human corneal rims according to protocols as described in section 3.1.1 and 3.2.1 (for details of the corneas see table 6.1). Isolated cells were labelled with Qtracker 605 as described in Chapter 3, section 3.5.1. Cells were imaged at 24 hours and 5 days after counterstaining with DAPI to examine Qtracker uptake in single cells and early spheres.

6.2.2. Migration assay during early sphere formation

Stromal cells were isolated from three human corneal rims as described above (for details of the corneas see **Table 6.1**). Time lapse microscopy was conducted using the Biostation IM (Nikon corp. Tokyo, Japan). Isolated stromal cells from three corneas were divided into two equal aliquots and labelled with either Qtracker 525 or 605 for 60 minutes (as described in section 3.5.1). Labelled cells were then washed five times in phosphate buffered saline (PBS), and then recombined in basal culture media (see section 3.2.4 for details of media) and incubated at 37°C with 5% CO_2. Phase contrast and fluorescence images were captured using the Biostation IM software version 2.10 (Nikon corp.) over a 72 hour period. Spheres were imaged using a Leica DIL inverted microscope with a Nikon digital camera attachment and Nikon NIS Elements 3.0 software (Nikon corp.) for image acquisition.

NZ Eye Bank reference	Donor age (years)	Gender	Experiment
10-047B	15	Male	Qtracker uptake
10-050B	83	Male	Qtracker uptake
10-113A	76	Male	Migration assay
10-116A	62	Male	Migration assay
10-119A	61	Female	Migration assay

Table 6.1 Details of the human corneas used for Qtracker uptake experiments and migration assay.

6.3. Results

Stromal cells effectively endocytosed the Qtracker at high efficiency, with virtually all cells demonstrating fluorescent labelling of cytoplasmic endosomes at 24 hours (**Figure 6.1**). Q tracker-labelled live stromal cells formed morphologically identical spheres at the same rates and temporal sequence as unlabelled stromal cells. Qtracker labelled spheres demonstrated bright fluorescence when imaged using fluorescence and confocal microscopy (**Figure 6.2**).

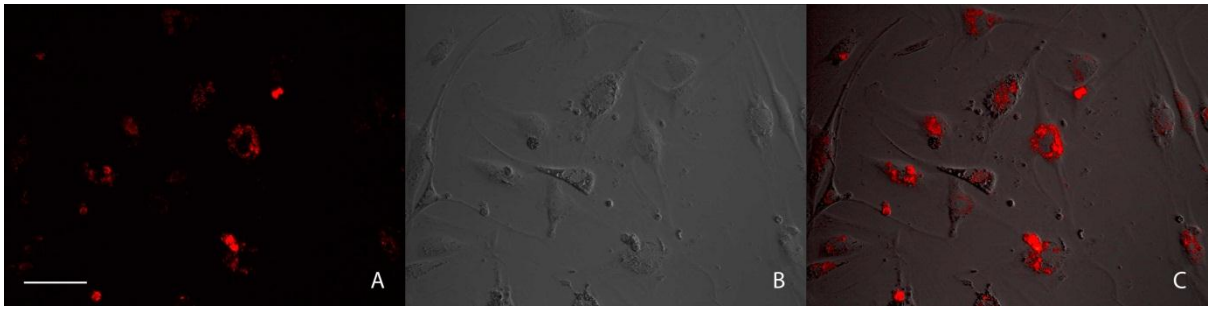

Figure 6.1 Stromal cells labelled with Qtracker 605 after 24 hours in culture. Qtracker demonstrates bright fluorescence in all cells. The Qtracker is located within cytoplasmic endosomes surrounding the nucleus (A), single cells are clearly visible with no sign of sphere formation at 24 hours in culture using differential interference contrast (DIC) microscopy (B), composite image with bright field (B) and fluorescence (A) images combined (C). Scale bar = 10µm.

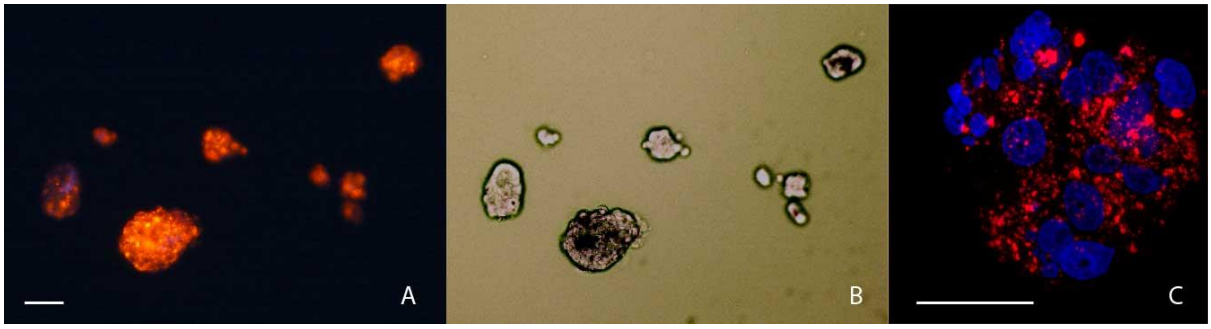

Figure 6.2 Fluorescence image of early stromal cell spheres labelled with Qtracker 605 at day 5 in culture. Qtracker demonstrates bright fluorescence in each sphere (A). Bright field microscopy demonstrates spheres during early sphere formation (B). Confocal maximum intensity projection of a sphere at day 5 in culture with Qtracker located within cytoplasmic endosomes (red) and DAPI counterstained nuclei (blue). Scale bar A & B = 25µm; C = 10µm.

Sphere morphology and the temporal pattern of sphere formation were unaltered in the Qtracker-labelled cells when compared with unlabelled controls. The Qtracker cells were clearly visible using fluorescence microscopy and the two different Qtracker labels (525 and 605) were easily distinguished in the two fluorescent channels of the Biostation (**Figure 6.3**, columns B-D).

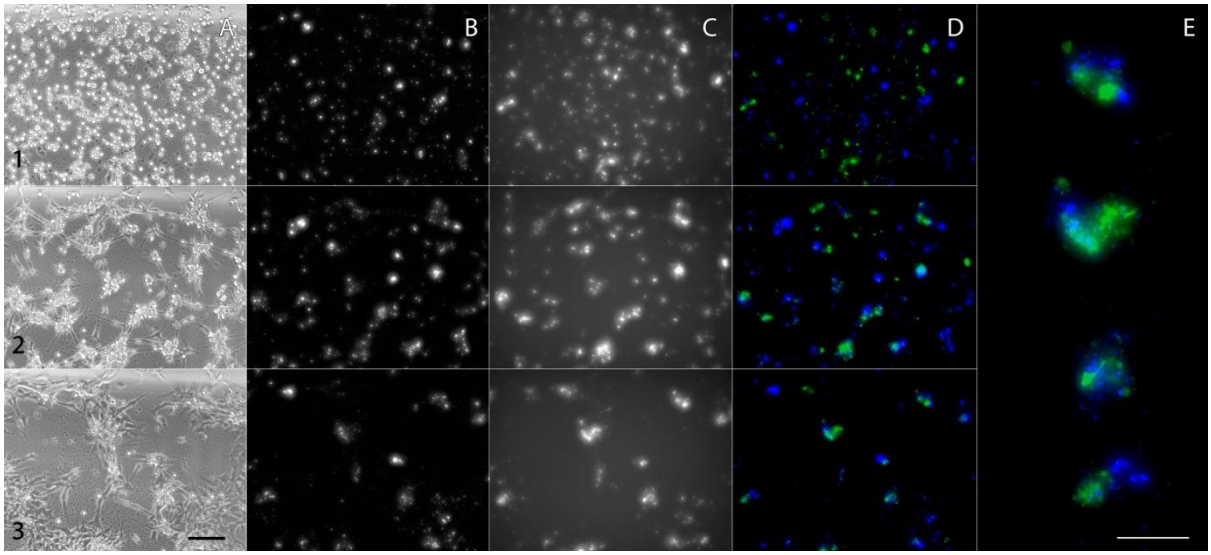

Figure 6.3 Time lapse bright field and fluorescent microscopy images of early sphere formation by stromal cells labelled with Qtracker 525 and 605. Row 1 (columns A-D) = 1 hour in culture, row 2 (columns A-D) = 27 hours in culture, row 3 (columns A-D) = 70 hours in culture. From left: column A= bright field image; column B= fluorescent channel 1 (Qtracker 525); column C= fluorescent channel 2 (Qtracker 605); column D= pseudo-coloured composite of both fluorescent channels; Column E= enlarged view of cell aggregates (early spheres) demonstrating that spheres contained cells labelled with Qtracker 525 and 605 as a result of cell migration. Scale bars (black, columns A-D) = 100µm, (white, column E) = 50µm.

Time lapse fluorescence microscopy over a 72hour period demonstrated that early sphere formation occurred predominantly via cell migration with formation of multi-coloured Qtracker-labelled cell aggregates (**Figure 6.3**, column E). EDU labelling over the same 72 hour period demonstrated relatively little cell division (**Figure 6.4**, C). Resulting early spheres contained both Qtracker 525 and 605 labels and relatively few cells remained outside of the formed spheres (**Figure 6.3**, column E).

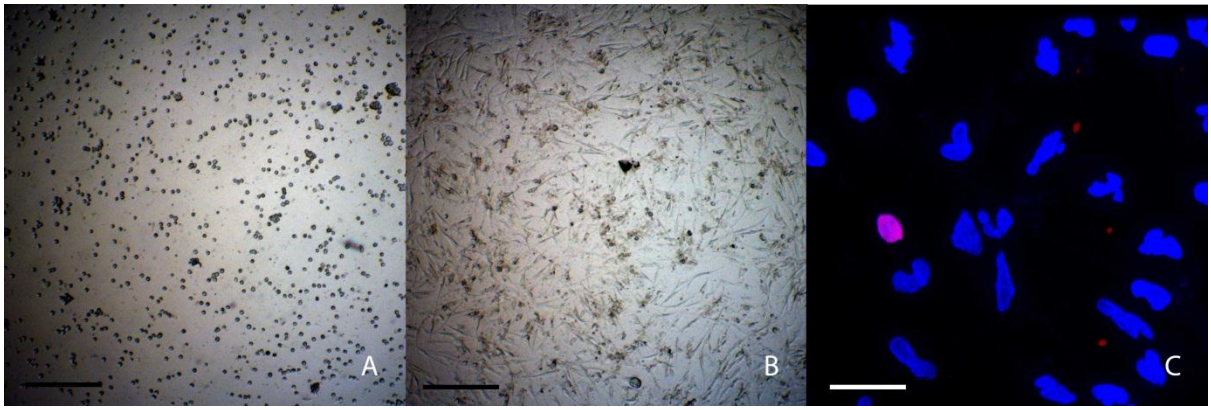

Figure 6.4 Sphere formation and cell proliferation from isolated human keratocytes. Isolated stromal cells during primary sphere formation imaged at 0 days – single cells were visible (A), and at 3 days – cell aggregates and early spheres were forming (B). Confocal microscopy image of stromal cell nuclei after 72 hours in culture (C). Nuclei that divided during the culture period were labelled red due to uptake of 5-ethynyl-2´-Deoxyuridine, all nuclei were counter-labelled blue with Hoechst 33342. Early sphere formation occurs with minimal cell division as demonstrated by the low ratio of red to blue nuclei by day 3. Scale bar black = 200µm, white = 20µm.

6.4. Discussion

Quantum dots for cell tracking have previously been used in a large array of cell types including stem cells.[24-26] The current study demonstrates that live human-stromal cells endocytose Quantum dots with high efficiency and subsequently can be tracked using time-lapse-fluorescence microscopy throughout early sphere formation. Live cell tracking in combination with a cell proliferation assay using EDU during early stromal cell sphere formation demonstrated that sphere formation occurs predominantly as a result of cell migration with minimal cell division over the same time period.

Despite claims that spheroid culture of neural and other cell types is a result of stem or progenitor cell expansion, there has been little evidence to support these claims. Support for sphere formation as a result of clonal expansion of progenitor cells comes largely from studies observing sphere formation in the presence of methylcellulose, a compound that demonstrated variable inhibition of cell aggregation during sphere formation of mouse neural and skin cells.[11, 12] Although this study did

not examine the effect of methylcellulose on stromal cell migration, the addition of methylcellulose may not inhibit migration in highly motile keratocytes by the same extent as neural cells during sphere formation and by no means conclusively excludes cell migration as a mechanism of sphere formation.[27] It cannot therefore be assumed that spheres form as a result of stem or progenitor proliferation or that their formation implies the existence of stem or progenitor cells *per se*. Indeed, it appears unlikely that even neurosphere formation is the result of purely cell proliferation as mathematical modelling suggests that spheres around 100µm in diameter are not possible purely as a result of proliferation of a single cell within 7 days.[27] Although early sphere formation occurs via cell migration/aggregation, cell division does appear to have a role in late sphere formation/development and the extent of the contribution is discussed in detail in Chapter 7.

In support of the results of this study and the observation that cell migration/aggregation plays the predominant role in early sphere formation is the further observation that stromal cell spheres still form from non-side population (non-SP, i.e. stem cell depleted) cells following fluorescence activated cell sorting as outlined in Chapter 5. Taken together these results suggest that sphere formation in human stromal cells either occurs via a different process to neural cell sphere formation, or that methylcellulose may not be an effective mechanism to inhibit cell migration during sphere formation.

6.5. Conclusions

Early human stromal cell sphere formation predominantly occurs as the result of cell migration and aggregation, with only a small contribution from cell division. Isolated stromal cells remain viable and highly motile in culture and can be tracked effectively using Quantum dot nanocrystals.

6.6. References

1. Espana EM, He H, Kawakita T, et al. Human keratocytes cultured on amniotic membrane stroma preserve morphology and express keratocan. Investigative Ophthalmology and Visual Science 2003;44(12):5136-41.
2. Kawakita T, Espana EM, He H, et al. Keratocan expression of murine keratocytes is maintained on amniotic membrane by down-regulating transforming growth factor-beta signaling. Journal of Biological Chemistry 2005;280(29):27085-92.
3. Choong PF, Mok PL, Cheong SK, Then KY. Mesenchymal stromal cell-like characteristics of corneal keratocytes. Cytotherapy 2007;9(3):252-8.
4. Funderburgh ML, Du Y, Mann MM, et al. Pax6 expression identifies progenitor cells for corneal keratocytes. FASEB Journal 2005;19(10):1371-3.
5. Chen YH, Wang IJ, Young TH. Formation of keratocyte spheroids on chitosan-coated surface can maintain keratocyte phenotypes. Tissue Engineering Part A 2009;15(8):2001-13.
6. Mimura T, Amano S, Yokoo S, et al. Isolation and distribution of rabbit keratocyte precursors. Molecular Vision 2008;14:197-203.
7. Yoshida S, Shimmura S, Shimazaki J, et al. Serum-free spheroid culture of mouse corneal keratocytes. Investigative Ophthalmology and Visual Science 2005;46(5):1653-8.
8. Yamagami S, Yokoo S, Mimura T, et al. Distribution of precursors in human corneal stromal cells and endothelial cells. Ophthalmology 2007;114(3):433-9.
9. Du Y, Sundarraj N, Funderburgh ML, et al. Secretion and organization of a cornea-like tissue in vitro by stem cells from human corneal stroma. Investigative Ophthalmology and Visual Science 2007;48(11):5038-45.
10. Uchida S, Yokoo S, Yanagi Y, et al. Sphere formation and expression of neural proteins by human corneal stromal cells in vitro. Investigative Ophthalmology and Visual Science 2005;46(5):1620-5.

11. Kawase Y, Yanagi Y, Takato T, et al. Characterization of multipotent adult stem cells from the skin: Transforming growth factor-beta (tgf-beta) facilitates cell growth. Experimental Cell Research 2004;295(1):194-203.

12. Gritti A, Frolichsthal-Schoeller P, Galli R, et al. Epidermal and fibroblast growth factors behave as mitogenic regulators for a single multipotent stem cell-like population from the subventricular region of the adult mouse forebrain. Journal of Neuroscience 1999;19(9):3287-97.

13. Coles BL, Angenieux B, Inoue T, et al. Facile isolation and the characterization of human retinal stem cells. Proceedings of the National Academy of Sciences of the United States of America 2004;101(44):15772-7.

14. Krause DS, Theise ND, Collector MI, et al. Multi-organ, multi-lineage engraftment by a single bone marrow-derived stem cell. Cell 2001;105(3):369-77.

15. Li H, Liu H, Heller S. Pluripotent stem cells from the adult mouse inner ear. Nature Medicine 2003;9(10):1293-9.

16. Nunes MC, Roy NS, Keyoung HM, et al. Identification and isolation of multipotential neural progenitor cells from the subcortical white matter of the adult human brain. Nature Medicine 2003;9(4):439-47.

17. Reynolds BA, Weiss S. Generation of neurons and astrocytes from isolated cells of the adult mammalian central nervous system. Science 1992;255(5052):1707-10.

18. Toma JG, Akhavan M, Fernandes KJ, et al. Isolation of multipotent adult stem cells from the dermis of mammalian skin. Nature Cell Biology 2001;3(9):778-84.

19. Tropepe V, Coles BL, Chiasson BJ, et al. Retinal stem cells in the adult mammalian eye. Science 2000;287(5460):2032-6.

20. Biju V, Itoh T, Ishikawa M. Delivering quantum dots to cells: Bioconjugated quantum dots for targeted and nonspecific extracellular and intracellular imaging. Chemical Society Reviews 2010;39(8):3031-56.

21. Chang CF, Chen CY, Chang FH, et al. Cell tracking and detection of molecular expression in live cells using lipid-enclosed cdse quantum dots as contrast agents for epi-third harmonic generation microscopy. Optics Express 2008;16(13):9534-48.

22. Delehanty JB, Mattoussi H, Medintz IL. Delivering quantum dots into cells: Strategies, progress and remaining issues. Analytical and Bioanalytical Chemistry 2009;393(4):1091-105.

23. Jaiswal JK, Goldman ER, Mattoussi H, Simon SM. Use of quantum dots for live cell imaging. Nature Methods 2004;1(1):73-8.

24. Lei Y, Tang H, Feng M, Zou B. Applications of fluorescent quantum dots to stem cell tracing in vivo. Journal of Nanoscience and Nanotechnology 2009;9(10):5726-30.

25. Lin S, Xie X, Patel MR, et al. Quantum dot imaging for embryonic stem cells. BMC Biotechnology 2007;7:67.

26. Walling MA, Novak JA, Shepard JR. Quantum dots for live cell and in vivo imaging. International Journal of Molecular Sciences 2009;10(2):441-91.

27. Singec I, Knoth R, Meyer RP, et al. Defining the actual sensitivity and specificity of the neurosphere assay in stem cell biology. Nature Methods 2006;3(10):801-6.

Chapter 7. Late sphere formation and the temporal sequence of cell division and glycoprotein production

7.1. Introduction

Several studies have reported that using a sphere forming culture system maintains the keratocyte phenotype in cultured stromal cells in a variety of animal models.[1-5] Spheroid culture has also been reported to maintain the expression of corneal specific proteoglycans such as keratocan.[1-3, 5] During the process of stromal-cell sphere formation, lobulated-cell clumps are visible by day three in culture, rounded spheres are first visible at approximately day 7, and by day 10 sphere formation appears complete with smooth rounded spheres. Based on the temporal pattern of morphological changes during sphere formation we have classified early sphere formation to be up to day 7 when rounded spheres are first detected in culture, and late sphere formation from day 7 until day 10 when sphere formation appears complete with the appearance of smooth rounded spheres. Within the first 72 hours spheres form predominantly as a result of cell migration and aggregation, however, the temporal sequence of late sphere formation and the extent of cell division and glycoprotein expression remain unclear.

Proteoglycans in the cornea are macromolecules composed of a central protein core with glycosaminoglycan side chains. In the cornea the glycosaminoglycan side chains are predominantly composed of keratan sulphate for the keratan sulphate proteoglycans (KSPGs), and dermatan sulphate for the dermatan sulphate proteoglycan decorin. KSPGs including keratocan, lumican, and mimecan contain keratin sulphate chains that are covalently linked to the protein backbone *via* an *N*-acetylglucosamine (*N*-linked) oligosaccharide residue.[6] The role of corneal proteoglycans remains poorly understood, however, experimental evidence suggests that *N*-linked KSPGs are involved in the regulation of collagen fibril diameter and decorin is involved in regulating interfibrillar spacing of collagen fibrils in the ECM.[6] Proteoglycans with sulphated keratin sulphate residues are only found in significant concentrations in the cornea and are likely to play a key role in corneal transparency.

Stromal cells in culture rapidly become fibroblastic and down regulate expression of proteoglycans even if only small amounts of serum are present in the culture media or if culture conditions are

suboptimal.[7, 8] The expression of proteoglycans in stromal cell cultures is therefore a useful and specific phenotypic marker to exclude trans-differentiation of cultured cells. As proteoglycans are composed of highly post-translationally modified proteins, gene or protein expression alone does not confirm their expression in a fully functional state. The incorporation of tetraacetylated N-azidoacetylgalactosamine (GalNAz) in the terminal azidosialic acid in the glycoprotein, however, is a specific marker of *de novo* glycoprotein (including KSPG) synthesis and can be monitored using a fluorescent reporter molecule and confocal microscopy to track proteoglycan synthesis *in vitro.*[9]

The purpose of this study was to evaluate the contribution of cell division to late stromal-cell sphere formation and the temporal sequence of glycoprotein expression using GalNAz uptake, in combination with a cell proliferation assay, to confirm the phenotype and expansion of spheroid-cultured stromal cells.

7.2. Methods

Stromal cells were isolated from two human corneal rims according to protocols as described in section 3.1.1 and 3.2.1 (for details of the corneas see **Table 7.1**). Isolated stromal cells were labelled with either 5-ethynyl-2´-Deoxyuridine (EDU, 3 samples total) or GalNAz (3 samples total) in basal culture media (as described in section 3.9.1) or unlabelled (control, 1 sample total). The media was changed every three days and cell division/glycoprotein production was detected using the Click-iT™ detection assay (Life Technologies) at days 3, 7, and 10. Labelled cells were imaged using an Andor Revolution spinning disc confocal microscope (Andor Technology Ltd, Belfast, U.K.) with an Andor Ixon DU-885 EM-CCD camera on a Nikon Ti-E inverted microscope (Nikon Corp., Kawasaki, Japan). Images were captured using Andor iQ v.2.3.1 software and analysed using Imaris v.7.3.0 (Bitplane AG, Zurich, Switzerland) and ImageJ v.1.45b (National Institutes of Health, Bethesda, Maryland, USA). Confocal image stacks were compiled to assess all EDU-labelled stromal cell nuclei in the forming spheres. For each z-axis image plane, data were collected in 3 channels for comparison. Channels were separated, thresholded and converted to binary in ImageJ and the nuclei were

counted using the ImageJ Three Dimensional Object Counter. The resulting object maps were inspected for accuracy and the labelled nuclei were quantified.

Keratocan expression was assessed using immunohistochemistry as outlined in section 3.7.1 with primary and secondary antibodies as outlined in

Table 3.1. Antibody labelled sections were analysed using the Andor Revolution spinning disc confocal microscope as outlined above.

NZ Eye Bank reference	Donor age (years)	Gender	Experiment
11-064A	80	Male	Glycoprotein expression/cell proliferation
11-064B	80	Male	Glycoprotein expression/cell proliferation

Table 7.1 Details of the human corneas used for cell proliferation and glycoprotein production assays.

7.3 Results

Stromal cells cultured in media supplemented with either EDU or GalNAz demonstrated no alteration in viability, morphology or sphere formation. The confocal image stacks of EDU labelled spheres covered an area measuring 173.3 x 172.7µm. Stack z-axis depth was 16µm in 33 image planes (day 3 sphere), 22µm in 45 image planes (day 7 sphere), and 37µm in 75 image planes (day 10 sphere). During early sphere formation cell proliferation was minimal with only 4% (1/25) of cell nuclei demonstrating positive labelling for EDU (**Figure 7.1**, F). By day 7 (onset of late sphere formation) cell proliferation has increased with 17.5% of nuclei (7/40) demonstrating positive EDU labelling. At day 10 43% of nuclei (29/68) demonstrated positive EDU labelling and were tightly clustered in spheres.

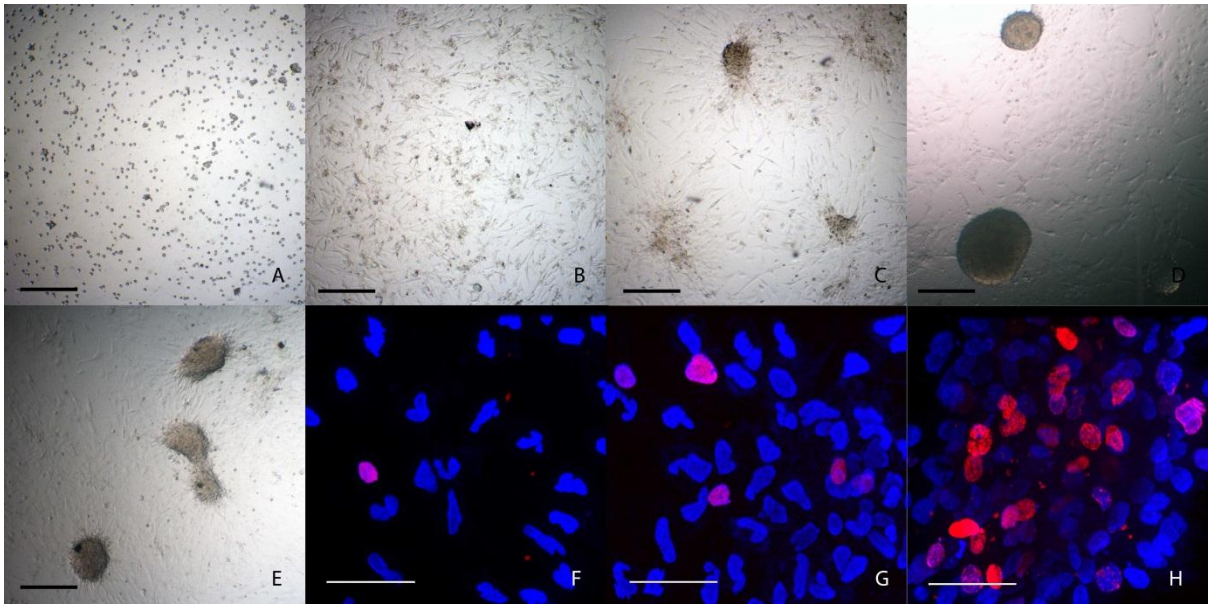

Figure 7.1 Sphere formation and cell proliferation from isolated human keratocytes. Isolated stromal cells during primary sphere formation pictured at 0 days - predominantly single cells were visible (A), 3 days – cell aggregates and early spheres were apparent (B), 7 days – regular smooth spheres had formed (C), 10 days – sphere formation appeared complete (D), 10 days - at half plating density (compared with cells pictured in A-D) produced uniformly smaller spheres (E). Confocal images of stromal cell nuclei during sphere formation. Nuclei that had divided in culture are labelled red due to uptake of 5-ethynyl-2´-deoxyuridine, all nuclei were counter-labelled blue with Hoechst 33342. Early sphere formation occurred with minimal cell division as demonstrated by the low ratio of red to blue nuclei by day 3 (F), most cell division occurred during and after late sphere formation as seen by the increasing proportion of red to blue nuclei on day 7 (G) and day 10 (H). Scale bar black = 200µm, white = 50µm.

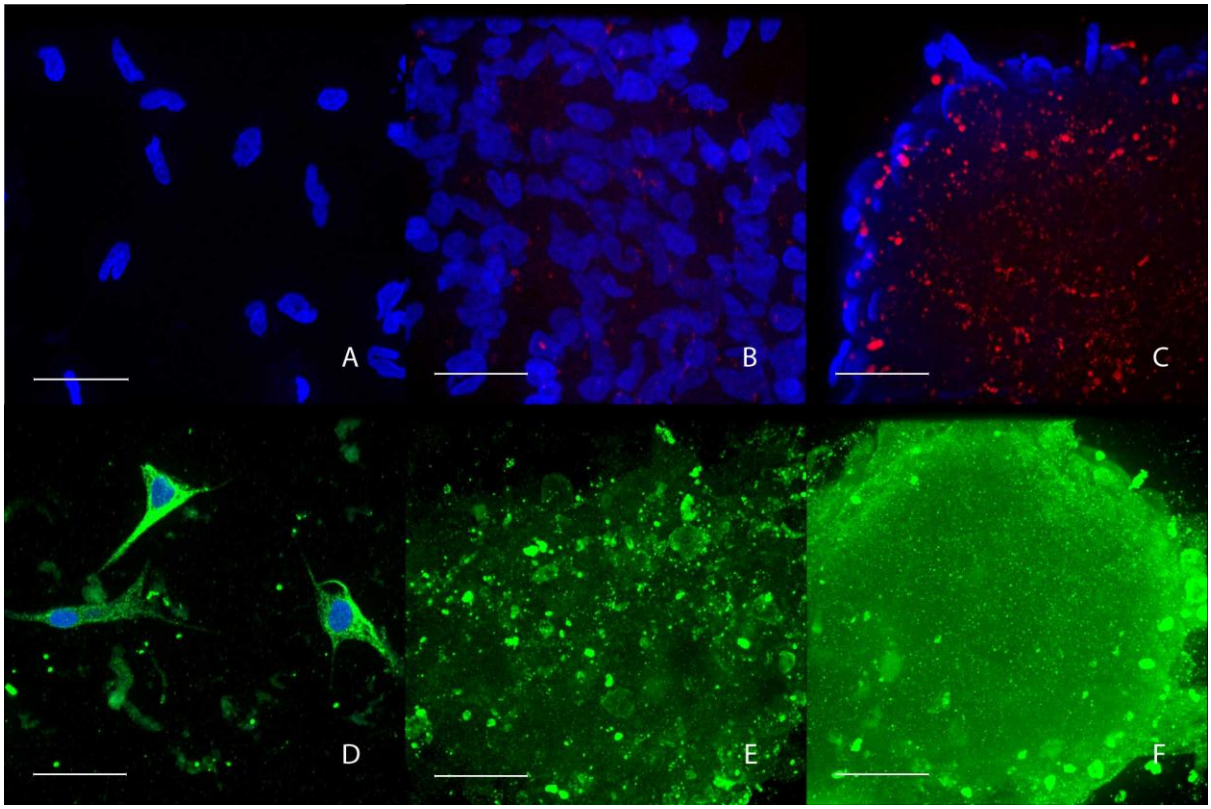

Figure 7.2 Cultured stromal cells demonstrated newly-synthesised glycoprotein deposition during cell culture and keratocan labelling during sphere formation. Stromal cells were cultured in the presence of tetraacetylated N-azidoacetylgalactosamine (red). At day 3 no newly synthesised glycoprotein was detectable (A). By day 7(B) there were traces of glycoprotein deposits detectable within and between cells (labelled red) which greatly increased in the center of the sphere by day 10 and late sphere formation (C). Nuclei are labelled blue with Hoechst 33342. Keratocan (labelled green) was detected at day 3 (D) and 7 (E) but greatly increased by day 10 (F) and late sphere formation. Hoechst 33342 channel was excluded on E, F as channel brightness obscures keratocan labelling. Scale bar = 40 µm

Glycoprotein synthesis and deposition was detected in early sphere formation using GalNAz (**Figure 7.2**). Dramatically increased deposition of glycoprotein was detected in late sphere formation by day 10 (**Figure 7.2**, C) compared with early sphere formation. A similar pattern for keratocan labelling was detected using immunocytochemistry, although keratocan was clearly visible at day 3

in culture, antibody labelling could not discriminate between newly synthesised and residual cytoplasmic keratocan.

7.3. Discussion

Early human-corneal-stromal-cell sphere formation is visible from 24 hours in culture with the formation of cell aggregates. These cell aggregates coalesce and enlarge over the following six days during early sphere formation. By day seven, the appearance of regular rounded spheres with smooth edges heralds the onset of late sphere formation. During late sphere formation the spheres enlarge in diameter and may be maintained in culture as stable spheres for several months.

Apart from the morphological changes that define the early and late phases of sphere formation, there appears to be corresponding changes in cell migration/aggregation, cell division/proliferation and glycoprotein expression within the spheres. During early sphere formation, by day 3, there is relatively little cell division with only 4% of nuclei labelling with EDU. By the onset of late sphere formation, at day 7, the number of nuclei that demonstrate positive EDU labelling has risen to 17.5%. Within the first three days of late sphere formation; there is an almost threefold rise in cell division with 43% of nuclei demonstrating EDU labelling. These data suggest that cell proliferation does play a significant role in sphere formation but this occurs predominantly in late sphere formation once a morphologically stable regular rounded sphere has formed.

Glycoprotein expression appears to follow a similar pattern to cell division during sphere formation. Early sphere formation is associated with minimal *de novo* glycoprotein production. With the onset of late sphere formation there is a large rise in glycoprotein deposition within the spheres. Immunohistochemistry demonstrates that intracellular keratocan protein is present within stromal cells during early sphere formation and intracellular and extracellular labelling greatly increases during late sphere formation. Although there is strong labelling of intracellular keratocan protein by day 3, it is possible that this labelling represents residual intracellular keratocan protein that may have been present prior to stromal cell isolation or newly produced keratocan that precedes the rise

in mature glycoprotein detected with GalNAz uptake. Interestingly, glycoprotein deposition is primarily observed in the centre of spheres where cells are predominantly dividing. It has been suggested that the three dimensional culture environment may play an important role in the differentiation and expression pattern of a keratocyte phenotype as pellet cultured adipose stem cells and cultured corneal SP cells also produce keratocan and collagen in response to three dimensional culture conditions.[2, 10, 11] In the current study the end of early sphere formation, and the subsequent development of a stable three dimensional culture environment, may act as a trigger to accelerate cell division and proliferation.

Keratocytes are easily activated by wounding or exposure to serum. The activated cells rapidly trans-differentiate to a fibroblastic or myofibroblastic phenotype which is associated with opaque scar formation in the cornea and the down regulation of KSPG expression.[7, 12, 13] Although the precise functions of the KSPGs remain poorly understood, it is likely that keratan sulphate in the KSPGs play a role in regulating corneal hydration and may also influence axonal growth during development and following wounding.[14] KSPG production and regulation is essential for maintaining the transparency and curvature of the cornea and may even play a role in coordinating immune cell responses to wounding.[12, 13, 15-18] Disruptions in the normal expression of stromal proteoglycans due to mutations in genes involved with glycoprotein production are associated with corneal dystrophies such as Cornea Plana (an inherited corneal dystrophy caused by a mutation in the KERA gene encoding the core protein for keratocan), and Macular dystrophy (caused by a mutation in a sulfotransferase enzyme that is responsible for sulphating keratan sulphate[13]). Given the integral nature of proteoglycans in the structure and function of the cornea, the stable expression of these molecules is pivotal in any culture system expanding stromal cells for transplant into dystrophic corneas.

Due to the limited amount of human stromal tissue available and the number of labelling experiments conducted in this study it was not possible to analyse multiple replicates (spheres) for each time point and labelling protocol investigated. Preliminary experiments investigating EDU

labelling of human-stromal-cell sphere nuclei, sphere glycoprotein deposition and keratocan expression demonstrated results that were consistent with the data presented in this study.

7.4. Conclusions

Late stromal-cell sphere formation is associated with a dramatic increase in cell division/proliferation and glycoprotein production. Glycoprotein synthesis functions as a phenotypic marker of stromal cells and confirms that the sphere forming culture system described in this study is able to maintain and promote the expansion of *ex vivo* human corneal stromal cells.

7.5. References

1. Chen YH, Wang IJ, Young TH. Formation of keratocyte spheroids on chitosan-coated surface can maintain keratocyte phenotypes. Tissue Engineering Part A 2009;15(8):2001-13.
2. Funderburgh ML, Du Y, Mann MM, et al. Pax6 expression identifies progenitor cells for corneal keratocytes. FASEB Journal 2005;19(10):1371-3.
3. Mimura T, Amano S, Yokoo S, et al. Isolation and distribution of rabbit keratocyte precursors. Molecular Vision 2008;14:197-203.
4. Yamagami S, Yokoo S, Mimura T, et al. Distribution of precursors in human corneal stromal cells and endothelial cells. Ophthalmology 2007;114(3):433-9.
5. Yoshida S, Shimmura S, Shimazaki J, et al. Serum-free spheroid culture of mouse corneal keratocytes. Investigative Ophthalmology and Visual Science 2005;46(5):1653-8.
6. Michelacci YM. Collagens and proteoglycans of the corneal extracellular matrix. Brazilian Journal of Medical and Biological Research 2003;36(8):1037-46.
7. Beales MP, Funderburgh JL, Jester JV, Hassell JR. Proteoglycan synthesis by bovine keratocytes and corneal fibroblasts: Maintenance of the keratocyte phenotype in culture. Investigative Ophthalmology and Visual Science 1999;40(8):1658-63.
8. Hassell JR, Schrecengost PK, Rada JA, et al. Biosynthesis of stromal matrix proteoglycans and basement membrane components by human corneal fibroblasts. Investigative Ophthalmology and Visual Science 1992;33(3):547-57.
9. Laughlin ST, Agard NJ, Baskin JM, et al. Metabolic labeling of glycans with azido sugars for visualization and glycoproteomics. Methods in Enzymology 2006;415:230-50.
10. Du Y, Roh DS, Funderburgh ML, et al. Adipose-derived stem cells differentiate to keratocytes in vitro. Molecular Vision 2010;16:2680-9.
11. Du Y, Sundarraj N, Funderburgh ML, et al. Secretion and organization of a cornea-like tissue in vitro by stem cells from human corneal stroma. Investigative Ophthalmology and Visual Science 2007;48(11):5038-45.

12. Long CJ, Roth MR, Tasheva ES, et al. Fibroblast growth factor-2 promotes keratan sulfate proteoglycan expression by keratocytes in vitro. Journal of Biological Chemistry 2000;275(18):13918-23.

13. Hassell JR, Birk DE. The molecular basis of corneal transparency. Experimental Eye Research 2010;91(3):326-35.

14. Funderburgh JL. Keratan sulfate: Structure, biosynthesis, and function. Glycobiology 2000;10(10):951-8.

15. Du Y, Carlson EC, Funderburgh ML, et al. Stem cell therapy restores transparency to defective murine corneas. Stem Cells 2009;27(7):1635-42.

16. Lee S, Bowrin K, Hamad AR, Chakravarti S. Extracellular matrix lumican deposited on the surface of neutrophils promotes migration by binding to beta2 integrin. Journal of Biological Chemistry 2009;284(35):23662-9.

17. Liu H, Zhang J, Liu CY, et al. Cell therapy of congenital corneal diseases with umbilical mesenchymal stem cells: Lumican null mice. PLoS ONE 2010;5(5):e10707.

18. Chakravarti S. Ocular and scleral alterations in gene-targeted lumican-fibromodulin double-null mice. Investigative Ophthalmology and Visual Science 2003;44(6):2422-32.

Chapter 8. Gene and protein expression in cultured stromal-cell spheres

8.1. Introduction

The corneal stromal matrix is primarily composed of proteins, the most abundant of which is collagen.[1, 2] The stromal extracellular matrix (ECM) scaffold including collagens and proteoglycans, are secreted by keratocytes located within the corneal stroma.[2-5] Although a range of collagen subtypes have been identified in the stromal ECM, the major constituents are subtypes I, V, and VI which are arranged in a very regular array of fibrils with a pattern that maintains the transparency and structural properties of the cornea.[2, 6] Collagen fibril growth and diameter play a key role in maintaining transparency and these properties are regulated by the stromal proteoglycans including decorin, lumican and keratocan which are also produced by the stromal keratocytes.[2]

Maintenance of the stroma involves ECM protein turnover and requires tightly regulated expression of the collagen-subtype proteins within the cornea. *In vitro* culture of keratocytes or altered growth conditions can cause radically altered ratios of collagen subtype expression and the arrangement of collagen fibrils. [7] This altered expression of collagen subtypes is observed during wound healing in the cornea and is associated with trans-differentiation of keratocytes to a fibroblastic/myofibroblastic phenotype and opaque scar tissue deposition.[2, 8, 9] A similar process of trans-differentiation occurs *in vitro* when keratocytes are cultured in the presence of serum or in suboptimal culture conditions.[8, 10, 11]

Quantitative gene expression analysis is a useful technique that can be used to monitor the relative abundance of ECM gene transcripts at a point in time compared with the expression of relatively stable 'housekeeping' genes that remain expressed at constant levels.[12] When these gene expression assays are conducted in parallel as an array format, it is possible to obtain an expression profile or 'snapshot' of how a cell or tissue transcriptome responds to certain culture conditions.

Although changes in gene expression provide insight into cellular responses to a variety of stimuli, it is important to validate changes in gene expression profiles with the relative changes in protein expression. The relationship between gene transcription and production of the corresponding

functional protein is often not linear as there are multiple levels of regulation that occur post transcription and post translation that can greatly affect the production of functional proteins. Despite these limitations, gene transcription can reveal patterns of expression that are characteristic to specific cell types and may be used to provide a molecular indicator of early cellular trans-differentiation.[13, 14]

The purpose of this study was to ensure that *in vitro* culture conditions used for keratocyte culture were conducive to sustained ECM and collagen subtype gene and protein expression at appropriate ratios as seen in the cornea. Secondly, this study aimed to monitor any induced trans-differentiation of cultured cells as defined at the transcript level and predict the potential of cultured cells to maintain and regenerate dystrophic stroma.

8.2. Methods

Stromal tissue was dissected from three human corneal rims (for details of the corneas see **Table 8.1**). Ribonucleic acid (RNA) was then extracted from the stroma of one quarter of each rim (as described in section 3.8.1) using the RNeasy kit (Qiagen Venlo, Netherlands) and quantified using the Nanodrop 2000 spectrophotometer (Thermo Fisher Scientific, Waltham). Extracted stromal RNA was then reverse transcribed to complementary deoxyribonucleic acid (cDNA) with the Vilo Superscript kit (Life technologies, Carlsbad, Ca, USA) as described in section 3.8.2. The remaining stromal tissue was enzymatically digested to isolate the stromal cells according to protocols as described in section 3.1.1 and 3.2.1. RNA was extracted and converted to cDNA from one third of the freshly isolated stromal cells as outlined above and the remaining two thirds (representing 50% of total tissue) were cultured in basal growth media to produce stromal-cell spheres (for details see section 3.2.4). After 14 days in culture, RNA was extracted from stromal-cell spheres and converted to cDNA as described above.

NZ Eye Bank reference	Donor age (years)	Gender	Experiment	Sample label (for gene expression analysis)
10-140	63	Male	Gene expression	A
10-141	71	Female	Gene expression	B
11-001	22	Female	Gene expression	C
11-064A	80	Male	Immunohistochemistry	na
11-064B	80	Male	Immunohistochemistry	na

Table 8.1 Details of the human corneas used for gene expression analysis.

A customised TaqMan® microfluidic array card (Life technologies) was designed for quantitative gene expression of key keratocyte genes using the manufacturer predesigned gene expression assays (see section 11.1 for a detailed description of the selected assays). Specific primers for detection of collagen-subtype expression, and other proteins including the housekeeping gene Beta-actin, on the Rotor-Gene (Qiagen) platform were synthesised (custom synthesis by GeneWorks, Hindmarsh, SA, Australia) using previously published sequences (for sequence details see **Table 8.2**). Newly synthesised cDNA from stroma, isolated cells and stromal cell spheres were then compared using quantitative Real-Time Polymerase Chain Reaction (RT-PCR) using the Rotor-gene and Taqman low density array and ABI 7900 (Applied Biosystems, Inc. Foster City, Ca, USA) platforms (for primer details see **Table 8.2**). Each assay was completed in duplicate (two replicates) for each of three donor corneas (for details of the corneas see **Table 8.1**).

For immunolabelling of collagen subtype proteins expressed in stromal-cell spheres, cultured spheres were removed from culture-plate wells using a pipette and inverted microscope at 10x magnification and placed in 0.5ml microfuge tubes. Optimal cutting temperature compound (OCT) was added, and the tubes were centrifuged. Tubes were then snap-frozen in liquid nitrogen, and their contents embedded in mounting wells containing OCT, and snap-frozen again. The embedded spheres were then sectioned at 16µm thickness using a Microm HM550 Cryostat (thermo-Scientific, Waltham, MA USA) and mounted on Superfrost Plus electrostatic slides (Menzel-Glenser, Braunscchweig, Germany).

Immunolabelling of collagen subtypes was conducted with cultured stromal cell spheres and undigested stromal tissue as described in section 3.7.1.

Gene target	Primer sequence	Published reference
ABCG2	Forward: TGCAACATGTACTGGCGAAGA Reverse: TCTTCCACAAGCCCCAGG	[15]
Beta-actin	Forward: AACTCCATCATGAAGTGTGACG Reverse: GATCCACATCTGCTGGAAGG	
Collagen I	Forward: ATGCCTGGTGAACGTGGT Reverse:AGGAGAGCCATCAGCACCT	[7]
Collagen II	Forward: CCGGGCAGAGGGCAATAGCAGGTT Reverse: CAATGATGGGGAGGCGTGAG	[15]
ColIVA1	Forward: ATGTCAATGCACCCATC Reverse: CTTCAAGGTGGACGGCGT	[16]
Col6A1	Forward: GACCTCGGACCTGTTGGGTAC Reverse: TACCCCATCTCCCCCTTCAC	[17]
Keratin 12	Forward: CTACCTGGATAAGGTGCGAGCT Reverse: TCTCGCATTGTCAATCTGCA	[15]
Keratocan	Forward: ATCTGCAGCACCTTCACCTT Reverse: CATTGGAATTGGTGGTTTGA	[15]
Neurofilament	Forward: GAGGAACACCAAGTGGGAGA Reverse: CTCCTCCTCTTTGGCCTCTT	[15]
Pax6	Forward: CAATCAAAACGTGTCCAACG Reverse: TAGCCAGGTTGCGAAGAACT	[15]

Table 8.2 Details of the primers used for gene expression analysis on the Rotor-gene platform. All Taqman gene expression assays were selected from the Life technologies pre-designed Real-time PCR assays (life technologies, Carlsbad, Ca, USA). For a full list of Taqman assays selected see section 11.1.

8.3. Results

Stromal tissue, isolated cells, and cultured spheres from all three donor samples (stroma from corneal rims) produced significant yields of RNA as measured by the Nanodrop spectrophotometer (**Table 8.3**). The cDNA synthesis reaction generated corresponding cDNA transcripts for all isolated RNA samples. cDNA demonstrated specific amplification for all of the TaqMan assays loaded on the microfluidic array cards (**Figure 8.1**, **Figure 8.2**, **Figure 8.3**, **Figure 8.8**).

The custom designed primers combined with the Rotor-Gene platform amplified the housekeeping gene (beta-actin) and demonstrated positive template-specific results following primer validation for ABCG2 (sample C only, **Figure 8.4**), Collagen VI (**Figure 8.5**) and Collagen I (**Figure 8.6**). Collagen II, Collagen IV, Keratin 12, keratocan, Neurofilament and Pax 6 either failed to amplify a product or demonstrated non-specific or genomic amplification.

RT-PCR analysis of corneal stromal proteoglycan genes using the TaqMan assays produced detectable results in all samples. Quantitative gene expression analysis of the three corneal donor stromal tissue samples and the corresponding isolated cells and cultured spheres demonstrated increased keratocan, lumican, decorin, and mimican proteoglycan transcript expression in day 14 cultured spheres compared with undigested stromal tissue (**Figure 8.3**).

Expression of stromal collagen subtypes collagen I (col1A1), Collagen V (col5A1) and collagen VI (col6A1) was increased in stromal-cell spheres compared with stromal tissue (**Figure 8.1**, **Figure 8.3**, **Figure 8.4**). Decreased expression or no significant change in expression was detected for collagen II (col2A1) and collagen IV (col4a1) transcripts (**Figure 8.1**).

Collagen subtype transcript expression was confirmed using sectioned spheres labelled with primary antibodies to collagen subtypes I, IV, V, and VI and compared with sections of adult corneal stroma for expression of these proteins. Sphere sections demonstrated similar ratios of labelling of the collagen subtypes to that seen in undigested stromal tissue using fluorescence microscopy (**Figure 8.7**). ABCG2 transcript expression was increased in spheres (in samples B and C using TaqMan assay and ABI 7900 thermocycler, and sample C alone using custom primers and the Rotor-gene thermocycler) compared with stromal tissue and demonstrated positive protein immunolabelling in spheres using confocal microscopy (**Figure 8.2**, **Figure 8.8**).

The expression of putative myofibroblast and fibroblast markers were compared in stromal tissue, isolated stromal cells and cultured stromal-cell spheres (**Figure 8.9**). Seven of the thirteen putative

phenotypic markers were decreased in stromal-cell spheres compared with stromal tissue. Four of the putative phenotypic marker transcripts that demonstrated up-regulation in stromal-cell spheres compared with stromal tissue were decreased relative to their expression in isolated stromal cells (**Figure 8.9**).

NZ Eye Bank reference	Sample	RNA yield (ng/µl)	Elution volume (µL)	Sample label
10-140	Stroma	12.9	30	At
10-140	Cells	16.6	30	Ac
10-140	Spheres	18.9	30	As
10-140	Migrating spheres	0.8	30	Acol
10-141	Stroma	5.3	30	Bt
10-141	Cells	12.3	30	Bc
10-141	Spheres	5.6	30	Bs
10-141	Migrating spheres	3.2	30	Bcol
11-001	Stroma	16.5	30	Ct
11-001	Cells	4.7	30	Cc
11-001	Spheres	16.5	30	Cs
11-001	Migrating spheres	18.9	30	Ccol

Table 8.3 Details of the RNA yields from each of the individual tissue, isolated stromal cell, and sphere samples.

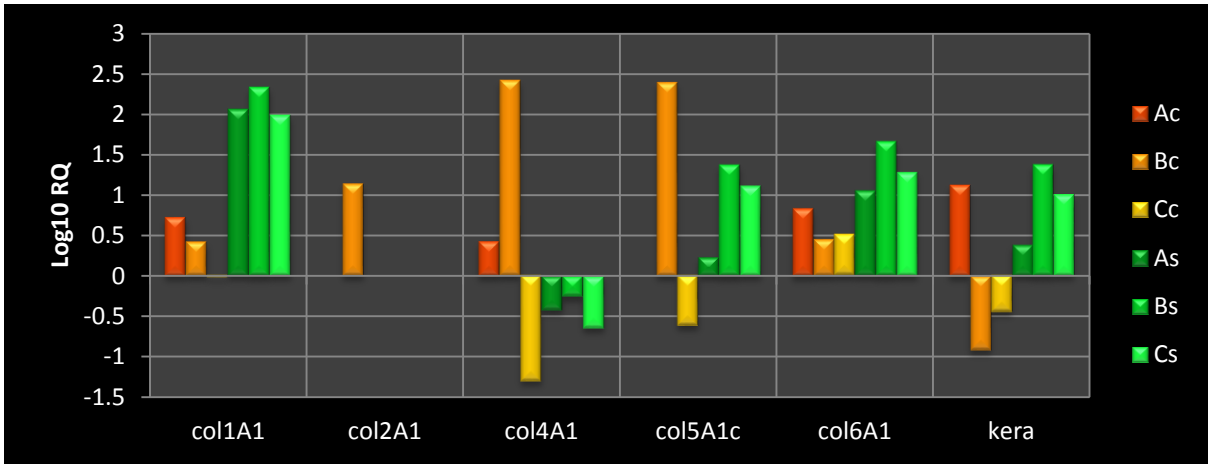

Figure 8.1 Quantitative gene expression of collagen subtypes and keratocan for individual tissue donor samples and associated cultured stromal-cell spheres measured using the TaqMan microfluidic arrays and ABI 7900 thermocycler. Expression of collagen subtype and proteoglycan gene transcripts in stromal tissue (baseline expression), digested cells from all three corneal samples (Ac, Bc, Cc) and day 14 cultured spheres from all three corneal samples (As, Bs, Cs). Three separate individual stromal tissue samples (A, B, C) were analysed and compared with their matched digested cells and cultured spheres. Increased expression of the collagen subtypes (I, V, VI), normally located within the cornea, were detected in cultured spheres. Samples from different donors demonstrate relatively consistent expression patterns. RQ = relative quantification.

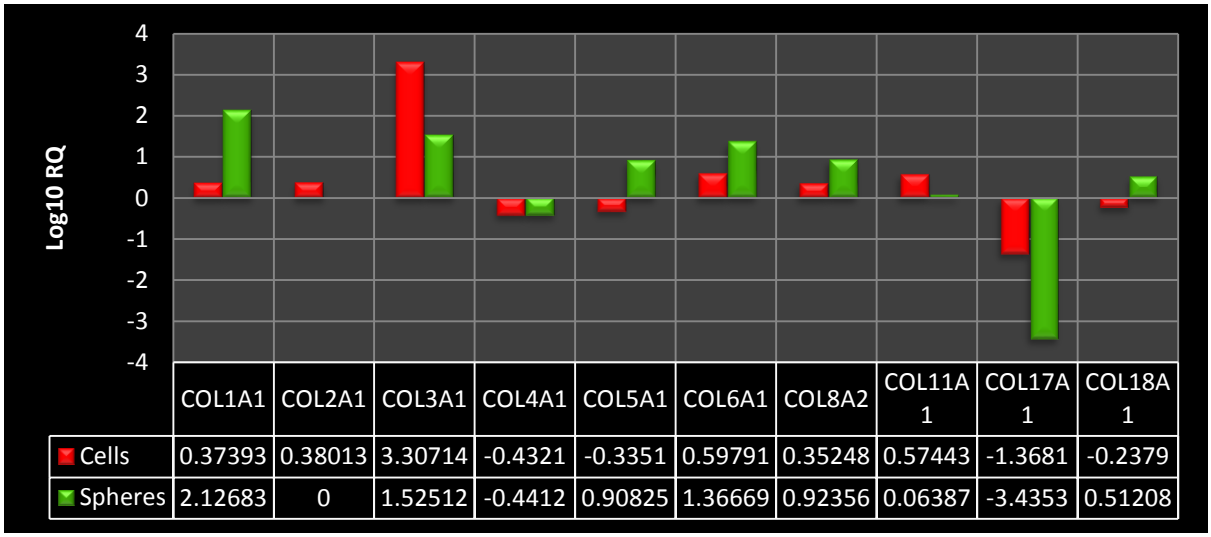

	COL1A1	COL2A1	COL3A1	COL4A1	COL5A1	COL6A1	COL8A2	COL11A1	COL17A1	COL18A1
Cells	0.37393	0.38013	3.30714	-0.4321	-0.3351	0.59791	0.35248	0.57443	-1.3681	-0.2379
Spheres	2.12683	0	1.52512	-0.4412	0.90825	1.36669	0.92356	0.06387	-3.4353	0.51208

Figure 8.2 Mean quantitative expression of a range of collagen subtypes measured using the TaqMan microfluidic arrays and ABI 7900 thermocycler. Collagen subtype gene transcript expression in stromal tissue (baseline expression) is compared with mean expression as measured in digested cells and day 14 stromal cell spheres. Collagen subtypes found in the corneal stroma including I, V and VI are all elevated in stromal-cell spheres as well as collagen III. RQ = relative quantification.

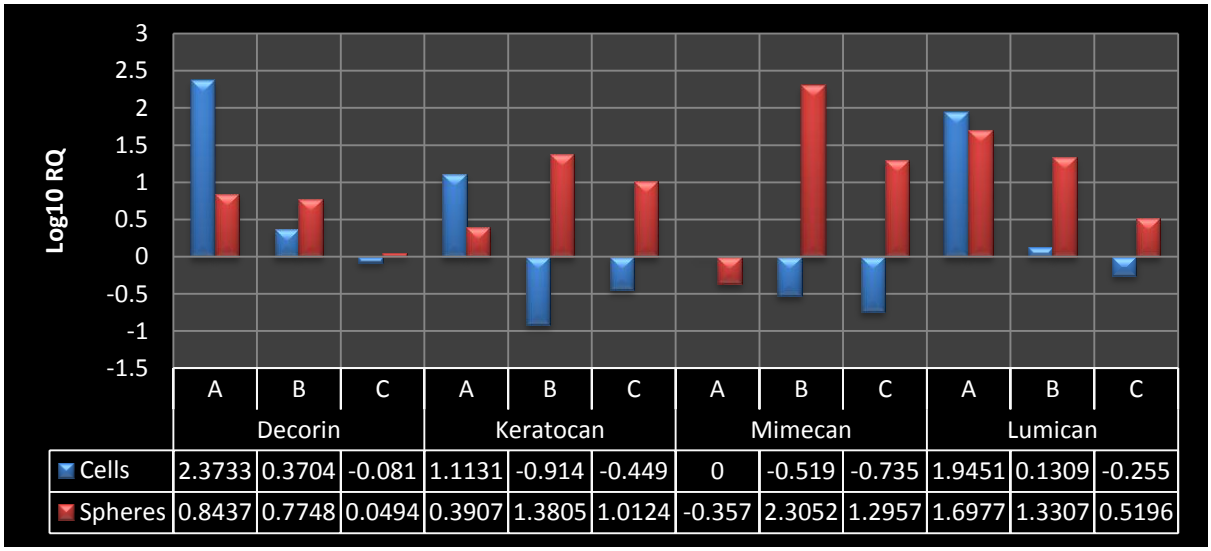

	A	B	C	A	B	C	A	B	C	A	B	C
	Decorin			Keratocan			Mimecan			Lumican		
Cells	2.3733	0.3704	-0.081	1.1131	-0.914	-0.449	0	-0.519	-0.735	1.9451	0.1309	-0.255
Spheres	0.8437	0.7748	0.0494	0.3907	1.3805	1.0124	-0.357	2.3052	1.2957	1.6977	1.3307	0.5196

Figure 8.3 Quantitative proteoglycan gene expression measured using the TaqMan microfluidic arrays and ABI 7900 thermocycler. Expression of proteoglycan gene transcripts in stromal tissue (baseline expression) compared with digested cells from all three corneal samples (A, B, C) and day

14 cultured spheres from all three corneal samples (A, B, C). Cultured spheres demonstrated increased relative expression (of up to over 100 fold above baseline expression in stromal tissue) of all of the main corneal proteoglycan transcripts including decorin, keratocan, mimecan and lumican. RQ = relative quantification.

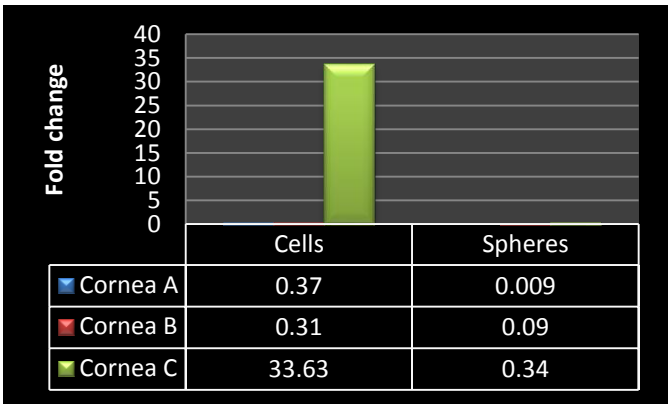

	Cells	Spheres
Cornea A	0.37	0.009
Cornea B	0.31	0.09
Cornea C	33.63	0.34

Figure 8.4 Quantitative expression of ABCG2 gene transcript measured using the Rotor-Gene thermocycler and custom synthesised primers. ABCG2 gene expression from the three corneal samples (A, B, C) is compared between stromal tissue (baseline), freshly isolated stromal cells (Cells), day 14 cultured spheres (Spheres) and cultured spheres placed on collagen coated coverslips (Collagen). Results are normalised using beta-actin expression.

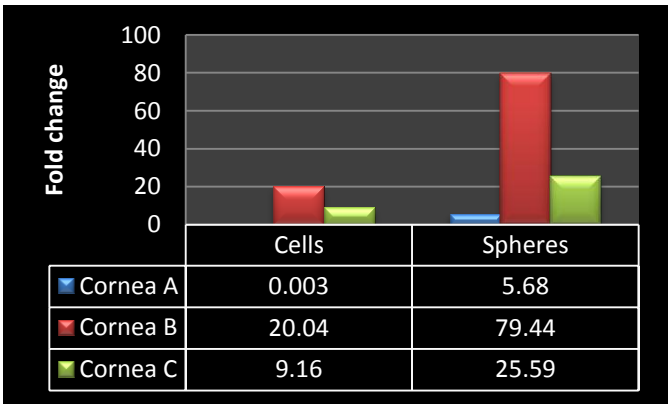

	Cells	Spheres
Cornea A	0.003	5.68
Cornea B	20.04	79.44
Cornea C	9.16	25.59

Figure 8.5 Quantitative gene expression of Collagen VI (col6A1) transcript expression measured using the Rotor-Gene thermocycler and custom synthesised primers. Col6AI gene expression from

the three corneal samples (A, B, C) is compared between stromal tissue (baseline), freshly isolated stromal cells (Cells), day 14 cultured spheres (Spheres) and cultured spheres placed on collagen coated coverslips (Collagen). Results are normalised using beta-actin expression.

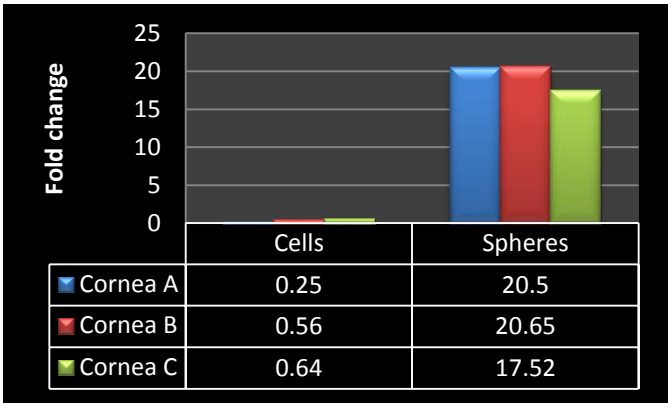

Figure 8.6 Quantitative gene expression of Collagen I transcript expression measured using the Rotor-Gene thermocycler and custom synthesised primers. Collagen I gene expression from the three corneal samples (A, B, C) is compared between stromal tissue (baseline), freshly isolated stromal cells (Cells), day 14 cultured spheres (Spheres) and cultured spheres placed on collagen coated coverslips (Collagen). Results are normalised using beta actin (housekeeping gene) expression.

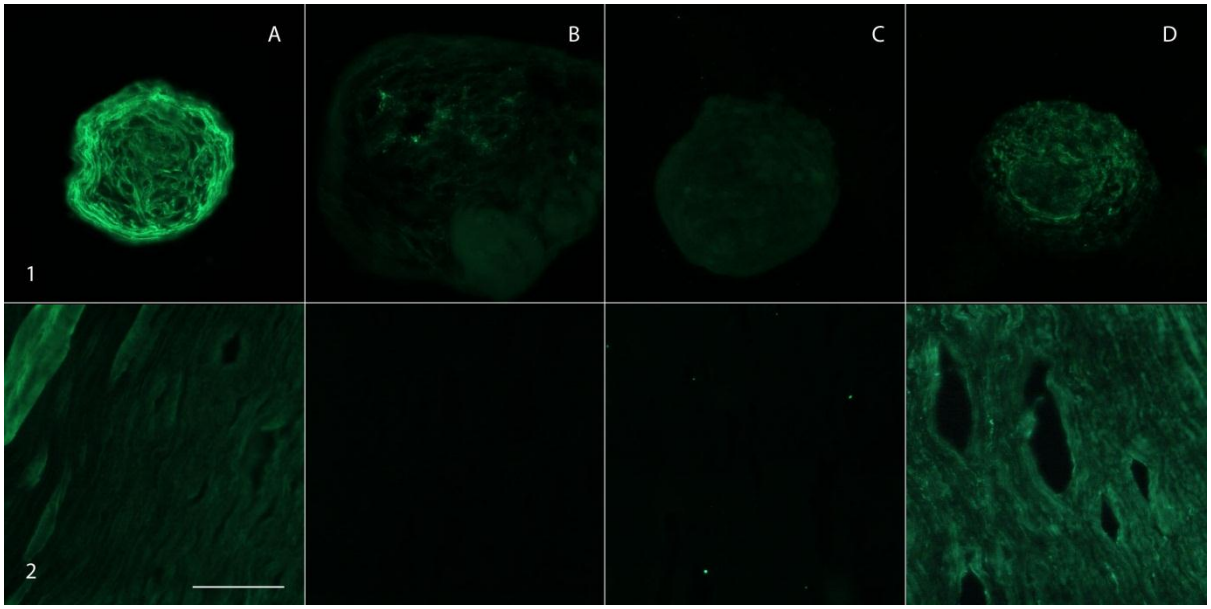

Figure 8.7 Stromal-cell spheres express collagen subtypes in the same ratios as those detected in human stromal tissue and appear to deposit the collagen in a lamellar arrangement particularly in the peripheral regions of the spheres (A). Antibody labelling of stromal-cell sphere (row 1) and corneal stroma sections (row 2) demonstrated collagen subtype expression of collagen I (A), Collagen IV (B), Collagen V (C), Collagen VI (D). Scale bar = 100 µm.

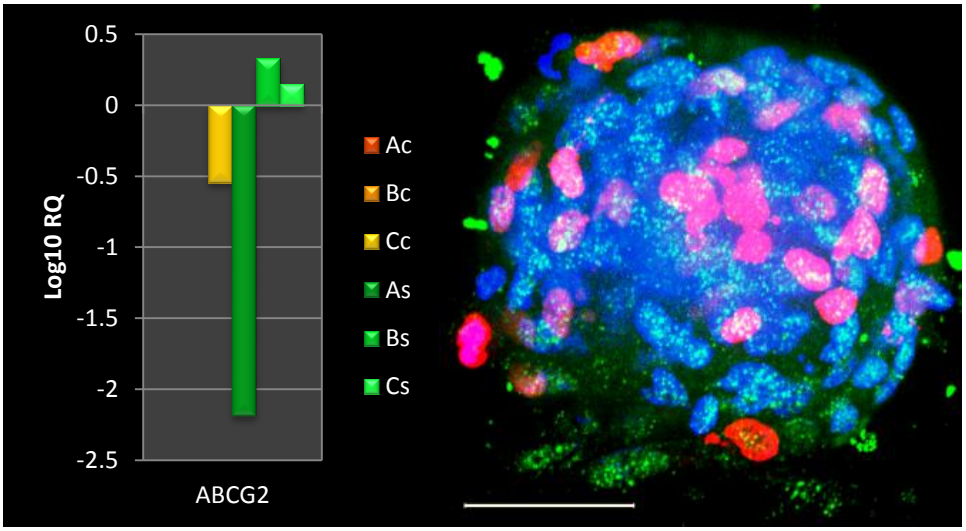

Figure 8.8 Quantitative ABCG2 transcript expression measured using the TaqMan microfluidic arrays and ABI 7900 thermocycler (Left). Expression of three donor corneal samples (A, B, C) is compared

between undigested stromal tissue (baseline), isolated cells (c) and d14 cultured spheres (s). Increased expression of ABCG2 transcripts were identified in two out of three of the sphere samples (Bs, Cs) when compared with ABCG2 expression in stromal tissue of matched samples. (Right) Confocal microscopy of a single image slice of a cultured sphere at day 10 demonstrates ABCG2 labelling (green) in many cells including some that have divided (red nuclei). Nuclei are labelled with Hoescht 33342 (blue) and 5-ethynyl-2′-deoxyuridine labelled nuclei (red) for cells that have divided in culture. Scale bar = 40µm.

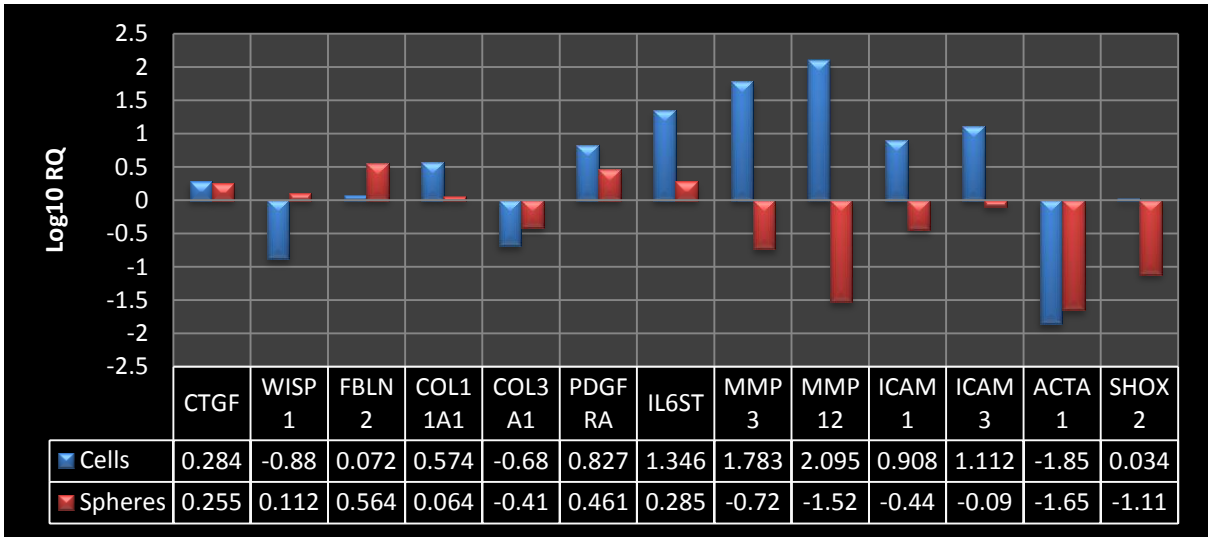

	CTGF	WISP 1	FBLN 2	COL1 1A1	COL3 A1	PDGF RA	IL6ST	MMP 3	MMP 12	ICAM 1	ICAM 3	ACTA 1	SHOX 2
Cells	0.284	-0.88	0.072	0.574	-0.68	0.827	1.346	1.783	2.095	0.908	1.112	-1.85	0.034
Spheres	0.255	0.112	0.564	0.064	-0.41	0.461	0.285	-0.72	-1.52	-0.44	-0.09	-1.65	-1.11

Figure 8.9 Quantitative gene expression of putative phenotypic markers of keratocyte trans-differentiation measured using the TaqMan microfluidic arrays and ABI 7900 thermocycler. Expression of candidate markers for myofibroblastic and fibroblastic trans-differentiation measured in isolated stromal cells and day 14 stromal-cell spheres. Spheres demonstrate downregulation of transcripts that are putative markers of myofibroblast and fibroblast phenotypes. RQ = relative quantification.

8.4. Discussion

Quantitative gene expression of collagen subtypes demonstrated that stromal-cell spheres maintain expression of the collagen subtypes found in the corneal stroma. The ratio and orientation of collagen subtypes that comprise the stromal collagen fibrils is likely to play an important role in the

transparency and structural integrity of the cornea.[18-25] Interestingly collagen type III transcripts were increased in isolated stromal cells and to a lesser extent in the stromal-cell spheres. Expression of type III collagen protein was not assessed in this study and therefore it is unclear if the increased transcript level is correlated with increased protein production in spheres. Collagen type III expression is associated with inflammation in the cornea and interestingly the ratio of type III to type I collagen in the conjunctiva increases with ageing and diabetes.[26-28] Collagen type III has not been identified as a significant constituent of the normal corneal stroma, however, there are reports of increased expression of type III collagen in cultured keratocytes.[29] In the current study, expression levels of collagen type III were almost 100 fold greater in isolated stromal cells than in cultured spheres and may indicate an inflammatory response associated with the enzymatic digestion of the stroma used to isolate the stromal cells which settles once the cells form spheres in culture.

Stromal cell spheres demonstrate increased expression of corneal proteoglycan transcripts including keratocan, lumican, mimecan and decorin. As part of the wound healing response, keratocytes typically down-regulate expression of proteoglycans *in vitro* and *in vivo*.[2, 8, 9, 30] Until now only one other study has reported sustained keratocan transcript expression in human stromal cells and this study used pellet cultured purified stromal stem cells and did not report maintained expression of any of the other stromal proteoglycans.[31] Indeed, multiple studies have reported that in vitro culture of stromal cells is associated with trans-differentiation and loss of proteoglycan expression. [2, 8, 9, 32]

Results using the Rotor-gene and TaqMan platforms were consistent despite differential amplification-probe binding sites. All TaqMan assays were carefully selected and assays that included exon-exon junctions were preferentially included when possible to minimise the chance of non-specific or genomic sequence amplification. This careful selection of the most appropriate assays may have contributed to the large number of positive results obtained using the TaqMan assays. Primer sequences for amplification using the Rotor-Gene platform were based on previously published sequences; however, despite some differences in design, the amplification data

demonstrated a similar trend across platforms for the assays that produced positive amplification results.

Protein expression of collagen subtypes in stromal-cell spheres, as detected using immunohistochemistry, are consistent with the detected alterations in gene expression. Observed up-regulation of specific collagen subtype gene transcripts are consistent with stromal ECM regeneration. Collagen I, V and VI all demonstrated brighter immunofluorescence in spheres when compared with the corresponding labelling in corneal stroma and interestingly sphere immunolabelling demonstrated a lamellar pattern of collagen deposition similar to that of the corneal stroma. These three collagen subtypes are the major collagen constituents of the corneal stroma comprising approximately 94% of total corneal collagens.

Observed increases in collagen types I, V, VI gene expression are consistent with regeneration of new corneal stroma. Collagen type I demonstrated the largest increase in expression (over 100 fold increase) which is not unexpected as this subtype comprises 75% of total corneal collagen and has one of the longest protein half-lives as determined using radiolabelled prolene incorporation in bovine corneas (approximately 36 hours).[26] A dramatic increase in expression would be required to regenerate new stroma and reach steady state expression. The second most abundant corneal collagen subtype, collagen VI (17% of corneal collagen with a short half-life of 6 hours[26]) demonstrated the second largest increase in expression with an approximately 20 fold increase in expression. Finally collagen V, which is the least abundant of the major three corneal collagen subtypes, at just 1.8% of total collagen and a half-life of 10 hours,[26] demonstrated a smaller rise in expression with an approximately 8 fold increase in expression in cultured spheres. Taken together these data suggest collagen gene expression ratios rise in accordance with expected levels required to regenerate corneal stromal tissue.

The molecular phenotype of cells in stromal-cell-spheres does not suggest any trans-differentiation into myofibroblasts or fibroblasts. Microarray gene expression studies using Murine stromal

keratocytes induced to form myofibroblasts or fibroblasts have identified a number of putative transcripts whose altered expression patterns characterise the molecular phenotype of these cell types.[13] The expression pattern of human homologs in stromal sphere cells did not match either of these expression patterns in this study. When viewed in the context of maintained keratocyte associated expression of proteoglycans and collagen subtypes in stromal cells spheres, it is highly unlikely that the culture system used in this study induces any trans-differentiation of the cultured cells.

Although trans-differentiation is not observed in cultured stromal-cell spheres, it is possible that some de-differentiation to maintain a resident population of progenitor and stem cells may occur in cultured spheres. Stromal-cell spheres demonstrate increased expression of the ABCG2 transcript and the ABCG2 protein as seen with RT-PCR and immunolabelling of the ABCG2 protein.

The ability to form spheres in culture and the presence of the ABCG2 protein are both thought to be markers of stem or progenitor cells.[15, 33-36] As discussed in Chapter 5, it is likely that cells other than stem cells are able to form spheres in certain conditions, however, there is something unique about the sphere micro-environment that retains keratocyte specific gene and protein expression and also cultivates and maintains a resident stem cell population that express the ABCG2 protein and sort using fluorescence-activated cell sorting as side-population cells following Hoechst 33342 incubation (as outlined in Chapter 5). This is the first study to culture human corneal stromal cells as spheres and demonstrate increased expression of stem cell markers at the gene and protein level within the sphere microenvironment.

ABCG2 expression was not uniformly elevated in spheres formed from all donor tissue samples. Indeed, one of the three tissue donor samples demonstrated down-regulation of ABCG2 transcript expression. The donor tissue demonstrating diminished ABCG2 expression originated from a 63 year old male, whereas the donors demonstrating increased ABCG2 expression were both females aged 22 and 71 years old. With such small samples sizes it is difficult to reach any firm conclusions

regarding possible explanations for this observation, however, further studies in this area may reveal more details.

The results of the current study suggest that spheroid culture of stromal cells not only maintains the keratocyte phenotype but also has the potential to promote and maintain a progenitor cell population from these differentiated cells. These progenitor characteristics in combination with healthy stromal ECM expression are likely to be essential for therapeutic interventions including long-term repopulation of dystrophic corneal stroma.

8.5. Conclusions

Cultured stromal-cell spheres demonstrate increased collagen-subtype gene expression for the collagen subtypes normally observed in the corneal stroma compared with gene expression in stromal tissue. The ratios of collagen-subtype proteins expressed in cultured spheres remain consistent with expression ratios of collagen subtypes observed in stromal tissue and the collagen appears to be deposited in layers as seen in the adult corneal stroma. Corneal-specific proteoglycan-gene expression is also up-regulated in stromal-cell spheres compared with stromal tissue. Stromal-cell spheres demonstrate up-regulation of ABCG2 transcripts and ABCG2 protein expression indicating that this sphere based culture system maintains and expands the resident stem and progenitor cell populations and maintains the keratocyte phenotype in culture.

8.6. References

1. Birk DE, Fitch JM, Linsenmayer TF. Organization of collagen types i and v in the embryonic chicken cornea. Investigative Ophthalmology and Visual Science 1986;27(10):1470-7.
2. Hassell JR, Birk DE. The molecular basis of corneal transparency. Experimental Eye Research 2010;91(3):326-35.
3. Cintron C, Covington H, Kublin CL. Morphogenesis of rabbit corneal stroma. Investigative Ophthalmology and Visual Science 1983;24(5):543-56.
4. Cornuet PK, Blochberger TC, Hassell JR. Molecular polymorphism of lumican during corneal development. Investigative Ophthalmology and Visual Science 1994;35(3):870-7.
5. Funderburgh JL, Caterson B, Conrad GW. Keratan sulfate proteoglycan during embryonic development of the chicken cornea. Developmental Biology 1986;116(2):267-77.
6. Michelacci YM. Collagens and proteoglycans of the corneal extracellular matrix. Brazilian Journal of Medical and Biological Research 2003;36(8):1037-46.
7. Marlovits S, Hombauer M, Truppe M, et al. Changes in the ratio of type-i and type-ii collagen expression during monolayer culture of human chondrocytes. Journal of Bone and Joint Surgery 2004;86(2):286-95.
8. Beales MP, Funderburgh JL, Jester JV, Hassell JR. Proteoglycan synthesis by bovine keratocytes and corneal fibroblasts: Maintenance of the keratocyte phenotype in culture. Investigative Ophthalmology and Visual Science 1999;40(8):1658-63.
9. Long CJ, Roth MR, Tasheva ES, et al. Fibroblast growth factor-2 promotes keratan sulfate proteoglycan expression by keratocytes in vitro. Journal of Biological Chemistry 2000;275(18):13918-23.
10. Espana EM, He H, Kawakita T, et al. Human keratocytes cultured on amniotic membrane stroma preserve morphology and express keratocan. Investigative Ophthalmology and Visual Science 2003;44(12):5136-41.

11. Yoshida S, Shimmura S, Shimazaki J, et al. Serum-free spheroid culture of mouse corneal keratocytes. Investigative Ophthalmology and Visual Science 2005;46(5):1653-8.

12. Jung R, Soondrum K, Neumaier M. Quantitative pcr. Clinical chemistry and laboratory medicine : CCLM / FESCC 2000;38(9):833-6.

13. Chakravarti S, Wu F, Vij N, et al. Microarray studies reveal macrophage-like function of stromal keratocytes in the cornea. Investigative Ophthalmology and Visual Science 2004;45(10):3475-84.

14. Funderburgh JL, Mann MM, Funderburgh ML. Keratocyte phenotype mediates proteoglycan structure: A role for fibroblasts in corneal fibrosis. Journal of Biological Chemistry 2003;278(46):45629-37.

15. Du Y, Funderburgh ML, Mann MM, et al. Multipotent stem cells in human corneal stroma. Stem Cells 2005;23(9):1266-75.

16. Lam S, van der Geest RN, Verhagen NA, et al. Secretion of collagen type iv by human renal fibroblasts is increased by high glucose via a tgf-beta-independent pathway. Nephrology, Dialysis, Transplantation 2004;19(7):1694-701.

17. Schnoor M, Cullen P, Lorkowski J, et al. Production of type vi collagen by human macrophages: A new dimension in macrophage functional heterogeneity. Journal of Immunology 2008;180(8):5707-19.

18. Abahussin M, Hayes S, Knox Cartwright NE, et al. 3d collagen orientation study of the human cornea using x-ray diffraction and femtosecond laser technology. Investigative Ophthalmology and Visual Science 2009;50(11):5159-64.

19. Almubrad T, Akhtar S. Structure of corneal layers, collagen fibrils, and proteoglycans of tree shrew cornea. Molecular Vision 2011;17:2283-91.

20. Boote C, Hayes S, Abahussin M, Meek KM. Mapping collagen organization in the human cornea: Left and right eyes are structurally distinct. Investigative Ophthalmology and Visual Science 2006;47(3):901-8.

21. Boote C, Hayes S, Jones S, et al. Collagen organization in the chicken cornea and structural alterations in the retinopathy, globe enlarged (rge) phenotype--an x-ray diffraction study. Journal of Structural Biology 2008;161(1):1-8.

22. Boote C, Kamma-Lorger CS, Hayes S, et al. Quantification of collagen organization in the peripheral human cornea at micron-scale resolution. Biophysical Journal 2011;101(1):33-42.

23. Kamma-Lorger CS, Boote C, Hayes S, et al. Collagen and mature elastic fibre organisation as a function of depth in the human cornea and limbus. Journal of Structural Biology 2010;169(3):424-30.

24. Morishige N, Takagi Y, Chikama T, et al. Three-dimensional analysis of collagen lamellae in the anterior stroma of the human cornea visualized by second harmonic generation imaging microscopy. Investigative Ophthalmology and Visual Science 2011;52(2):911-5.

25. Segev F, Heon E, Cole WG, et al. Structural abnormalities of the cornea and lid resulting from collagen v mutations. Investigative Ophthalmology and Visual Science 2006;47(2):565-73.

26. Robert L, Legeais JM, Robert AM, Renard G. Corneal collagens. Pathologie-Biologie 2001;49(4):353-63.

27. Kern P, Sebert B, Robert L. Increased type-iii/type-i collagen ratios in diabetic human conjunctival biopsies. Clinical Physiology and Biochemistry 1986;4(2):113-9.

28. Labat-Robert J, Kern P, Robert L. Biomarkers of connective tissue aging: Biosynthesis of fibronectin, collagen type iii, and elastase. Annals of the New York Academy of Sciences 1992;673:16-22.

29. BenEzra D, Foidart JM. Collagens and non collagenous proteins in the human eye. I. Corneal stroma in vivo and keratocyte production in vitro. Current Eye Research 1981;1(2):101-10.

30. Carlson EC, Wang IJ, Liu CY, et al. Altered kspg expression by keratocytes following corneal injury. Molecular Vision 2003;9:615-23.

31. Du Y, Sundarraj N, Funderburgh ML, et al. Secretion and organization of a cornea-like tissue in vitro by stem cells from human corneal stroma. Investigative Ophthalmology and Visual Science 2007;48(11):5038-45.

32. Fini ME. Keratocyte and fibroblast phenotypes in the repairing cornea. Progress in Retinal and Eye Research 1999;18(4):529-51.

33. Du Y, Roh DS, Funderburgh ML, et al. Adipose-derived stem cells differentiate to keratocytes in vitro. Molecular Vision 2010;16:2680-9.

34. Hulspas R, Quesenberry PJ. Characterization of neurosphere cell phenotypes by flow cytometry. Cytometry 2000;40(3):245-50.

35. Zhang S, Uchida S, Inoue T, et al. Side population (sp) cells isolated from fetal rat calvaria are enriched for bone, cartilage, adipose tissue and neural progenitors. Bone 2006;38(5):662-70.

36. Zhou S, Schuetz JD, Bunting KD, et al. The abc transporter bcrp1/abcg2 is expressed in a wide variety of stem cells and is a molecular determinant of the side-population phenotype. Nature Medicine 2001;7(9):1028-34.

Chapter 9. Cell migration from cultured stromal cell spheres in two and three dimensional collagen matrices and the effect of cell migration on gene expression

9.1. Introduction

Keratocytes within the corneal stroma trans-differentiate and migrate in response to wounding and cytokine stimulation.[1] Cell migration is an essential process for maintenance and repair of the corneal stroma, however, little is known about the processes that initiate cell migration or the effect migration has on gene expression and keratocyte trans-differentiation.

Although the mechanism of keratocyte migration remains poorly understood, keratocytes are known to migrate rapidly under specific conditions and may act to regulate migration of other cell types within the stroma including neutrophils.[2-4] The mechanism of control of migration remains unclear, however, several growth factors may influence keratocyte migration including epidermal growth factor (EGF), basic fibroblast growth factor (bFGF) and platelet derived growth factor (PDGF).[1, 5, 6]

Keratocytes are capable of active migration through collagen gels. Interestingly, keratocytes in collagen gels assume a stellate morphology and form an interconnecting network in a similar arrangement to that seen in the corneal stroma.[7] Cell migration also occurs within the corneal stroma in response to corneal transplantation. Keratocytes migrate into the transplanted tissue from the surrounding host tissue and it is likely that they also migrate in the opposite direction. [8]Although keratocytes can migrate through collagen gels and the corneal stroma, the precise triggers that initiate migration are unknown and it remains unclear if migration causes keratocyte trans-differentiation.

Successful repopulation of dystrophic corneal stroma with healthy keratocytes requires cell migration throughout the host stroma, maintenance of the keratocyte phenotype, and normal expression of stromal extracellular matrix (ECM). The purpose of this study was to characterise the ability of spheroid cultured stromal cells to migrate on collagen matrices and stromal tissue, and to evaluate the subsequent gene expression and cell trans-differentiation.

9.2. Methods

Stromal cells were isolated from donor corneal rims and cultured into spheres as described in sections 3.1.1, 3.2.1, 3.2.2 (for details of the corneas used see **Table 9.1**). Some of the cells were labelled with Qtracker prior to sphere formation to facilitate tracking individual cells as outlined in section 3.5.1.

Following sphere formation, stromal-cell spheres were placed on collagen-coated coverslips in basal culture media (for details of collagen coating see section 3.7.2). Time lapse fluorescence and bright field microscopy was conducted using the Biostation IM (Nikon corp. Tokyo) to observe cell migration.

To assess migration within stromal tissue, Qtracker labelled spheres were implanted into human stromal tissue at a depth of approximately 100µm, and observed using confocal microscopy over a period of 72 hours while maintained at 37°C and 5% CO_2 in basal culture media.

To evaluate gene expression in migrating stromal-cell spheres, cultured stromal-cell spheres were stimulated to migrate on type I collagen-gel-coated coverslips. Several spheres from each of three separate tissue donors were placed on both collagen-coated and uncoated coverslips, maintained in culture with basal culture media (section 3.2.4) for 72 hours and then total RNA was extracted (for details see section 8.2, for details of the donor corneas see **Table 9.1**). Following RNA extraction, cDNA was produced for quantitative gene expression analysis using the TaqMan microfluidic array cards exactly as outlined in section 8.2. Gene expression analysis was conducted in duplicate using three individual sources of donor tissue. Gene expression data were then compared with expression data from stromal tissue (baseline), isolated cells, and stromal cell spheres as outlined in section 3.8.6.

NZ Eye Bank reference	Donor age (years)	Gender	Experiment	Sample label (for gene expression analysis)
10-140	63	Male	Gene expression	A
10-141	71	Female	Gene expression	B
11-001	22	Female	Gene expression	C
11-015	66	Male	Sphere migration	Na
11-017A,B	66	Male	Sphere migration	Na

Table 9.1 Details of the human corneas used for gene expression analysis and cell migration.

9.3. Results

Isolated stromal cells formed spheres in culture over a 14 day period as outlined in previous chapters. Spheres placed on uncoated glass coverslips (control) remained as spheres and no migration was observed. Spheres placed on type I collagen coated coverslips demonstrated radial migration of cells out of the spheres within several minutes and continued over the 18 hour period when the spheres were directly observed using time lapse microscopy (**Figure 9.1**). Migration away from the spheres continued and was confirmed after three days in culture with confocal microscopy (**Figure 9.2**).

Qtracker labelled stromal-cell spheres implanted into stromal tissue also demonstrated migration of labelled cells away from the sphere over the 72hour period (**Figure 9.3**).

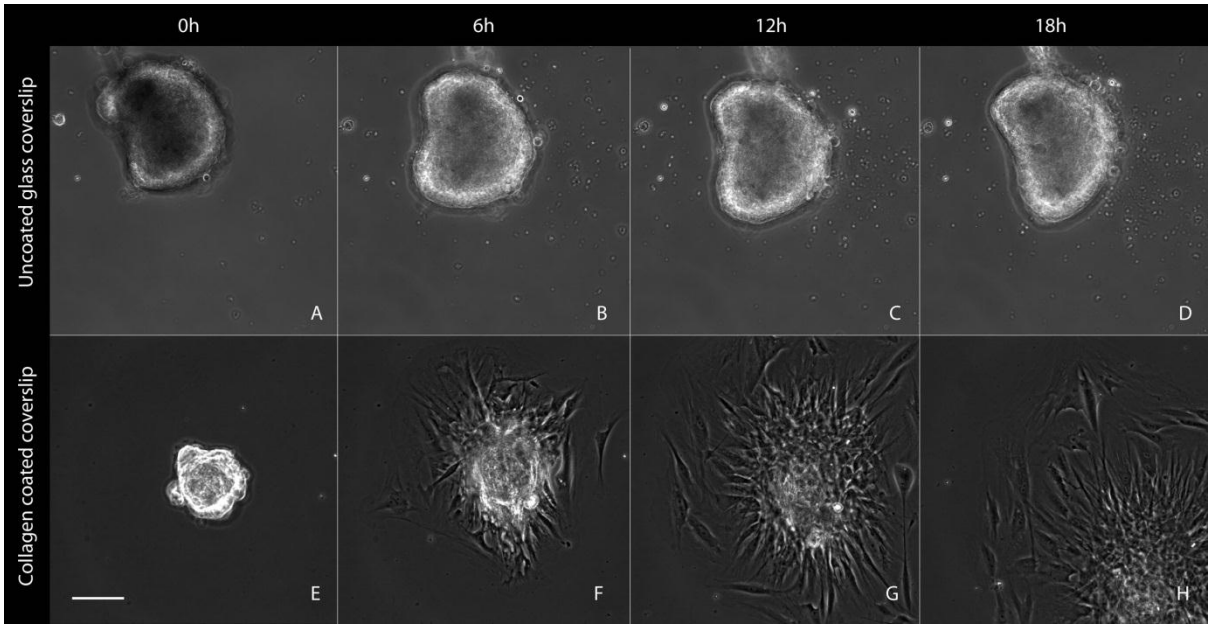

Figure 9.1 Type I collagen gel induced migration of stromal-cell sphere cells over an 18 hour period (E-H) compared with control samples with no collagen present (A-D). A stromal-cell sphere was placed on an uncoated glass coverslip with no exogenous collagen present (control sample) and imaged using bright field microscopy at 6 hour intervals (A-D). The control sphere with no exogenous collagen present remained inactive with no migration observed (A=0h, B=6h, C=12h, D=18h). The stromal-cell sphere placed on a type I collagen coated cover slip demonstrated rapid migration of single cells out of the sphere in a radial direction away from the sphere (E-H). Migration was detected within minutes of placing the stromal-cell sphere on the collagen coated coverslip (E=0h, F=6h, G=12h, H=18h). Scale bar 100µm.

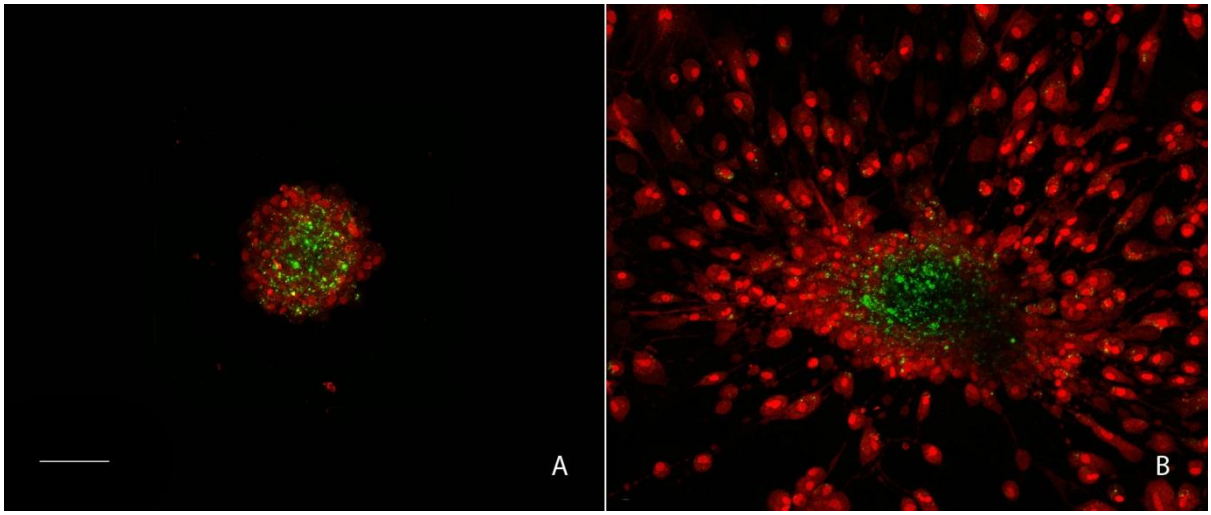

Figure 9.2 Type I collagen gel induced migration of cells from a stromal-cell sphere. Stromal-cell spheres were placed on an uncoated glass coverslip (control, A) and a type I collagen coated coverslip (B) and imaged after 3 days using confocal microscopy. The sphere on the collagen coated coverslip demonstrated extensive migration of cells out of the sphere (B). Cells were labelled with syto63 (red) and Qtracker (green). Scale bar 100µm.

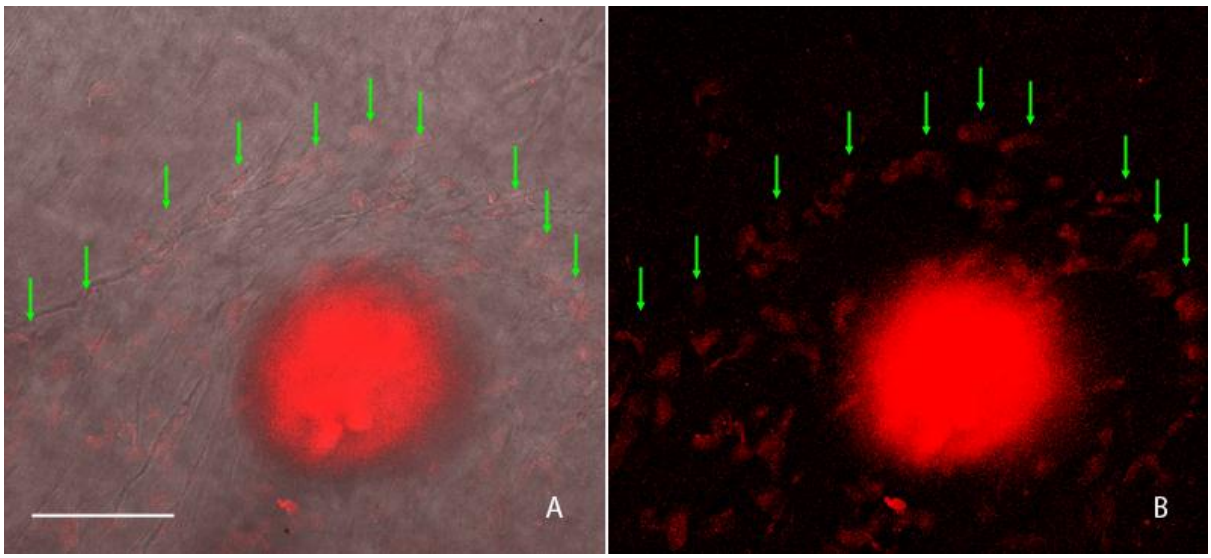

Figure 9.3 Migration of Qtracker labelled cells from stromal-cell spheres. Stromal-cell spheres were implanted within stromal tissue at an approximate depth of 100µm and imaged at 72hours (bright field and confocal composite A, confocal fluorescent channel alone B). A wave of migrating cells was

detected moving away from the implanted sphere in a radial direction (green arrows). Scale bar = 100μm.

Stromal-cell spheres used for gene expression analysis demonstrated migration when placed on type I collagen coated coverslips whereas control spheres on coverslips with no exogenous collagen present did not (**Figure 9.4**). Migrating stromal-cell spheres and non-migrating spheres produced significant yields of RNA as measured by the Nanodrop spectrophotometer and outlined in more detail in section 8.2. The cDNA synthesis reaction generated the corresponding cDNA transcripts for all isolated RNA samples. cDNA demonstrated specific amplification for all of the TaqMan assays loaded on the microfluidic array cards (**Figure 9.5**, **Figure 9.6**, **Figure 9.7**). Gene expression of keratocan, decorin, lumican and mimecan proteoglycan transcripts in migrating stromal-cell spheres were maintained at similar levels to those observed in non-migrating (control) stromal-cell sphere samples (**Figure 9.5**). Collagen subtype expression in migrating cells also remained relatively unchanged from expression detected in non-migrating control samples (**Figure 9.6**). Expression of putative phenotypic marker gene expression also remained consistent with that observed in non-migrating control samples with the exception of the ICAM1 and ICAM3 which both demonstrated reduced expression in migrating cell samples compared with non-migrating control samples (**Figure 9.7**).

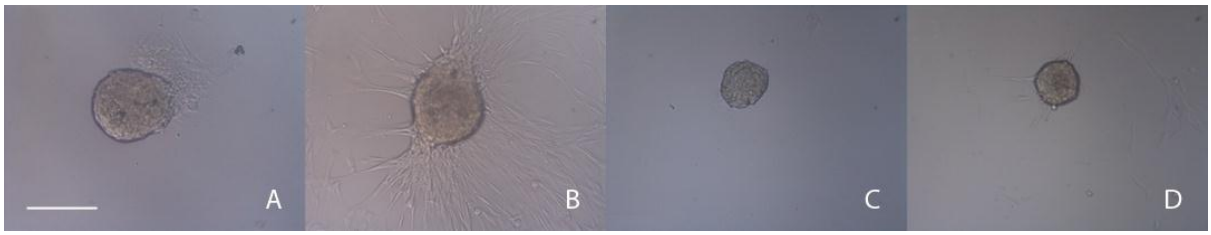

Figure 9.4 Bright field images of corneal stromal keratocyte spheres demonstrating migration when placed on type I collagen coated coverslips and subsequently used for gene expression studies. (A) Sphere immediately after transfer onto a type I collagen coated coverslip. (B) Identical Sphere

depicted in (A) after 72 hours demonstrated extensive cell migration out of sphere and across cover slip. (C) Sphere immediately after transfer onto an uncoated coverslip (control). (D) Sphere depicted in (C, control) after 72 hours demonstrated adhesion onto the coverslip but no migration as seen in B.

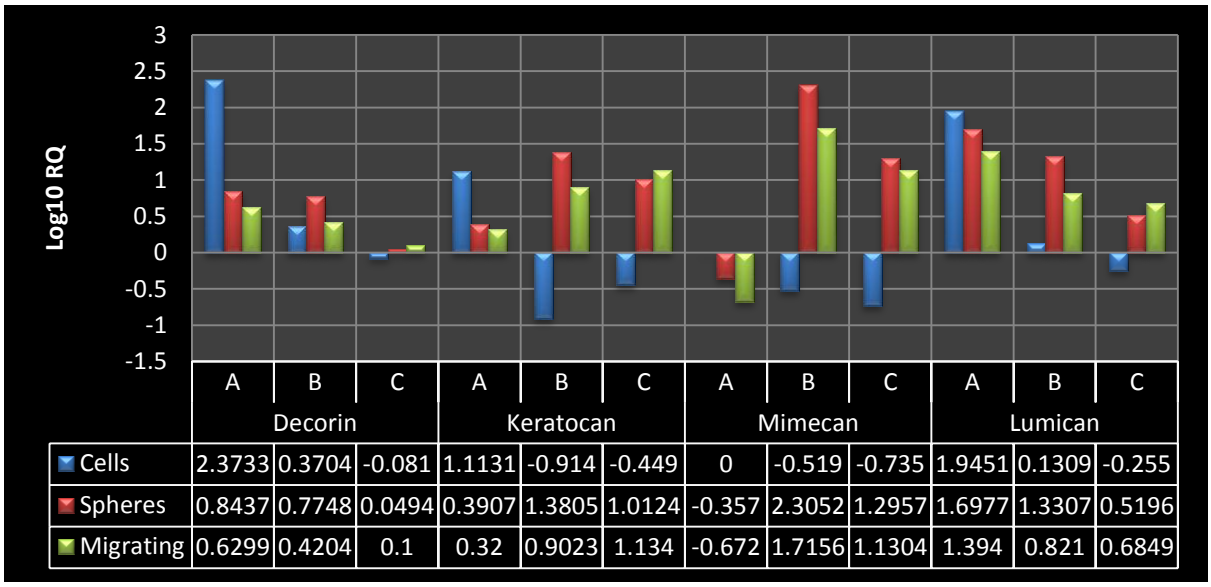

	A	B	C	A	B	C	A	B	C	A	B	C
	Decorin			Keratocan			Mimecan			Lumican		
Cells	2.3733	0.3704	-0.081	1.1131	-0.914	-0.449	0	-0.519	-0.735	1.9451	0.1309	-0.255
Spheres	0.8437	0.7748	0.0494	0.3907	1.3805	1.0124	-0.357	2.3052	1.2957	1.6977	1.3307	0.5196
Migrating	0.6299	0.4204	0.1	0.32	0.9023	1.134	-0.672	1.7156	1.1304	1.394	0.821	0.6849

Figure 9.5 Quantitative proteoglycan gene expression measured using the TaqMan microfluidic arrays and ABI 7900 thermocycler. Expression of proteoglycan gene transcripts in stromal tissue (baseline expression) compared with digested cells from all three corneal samples (A, B, C), non-migrating stromal-cell spheres and migrating cells from all three corneal samples (A, B, C). Cultured spheres and migrating cells demonstrated increased relative expression (of up to over 100 fold above baseline expression in stromal tissue) of all of the main corneal proteoglycan transcripts including decorin, keratocan, mimecan and lumican. RQ = relative quantification.

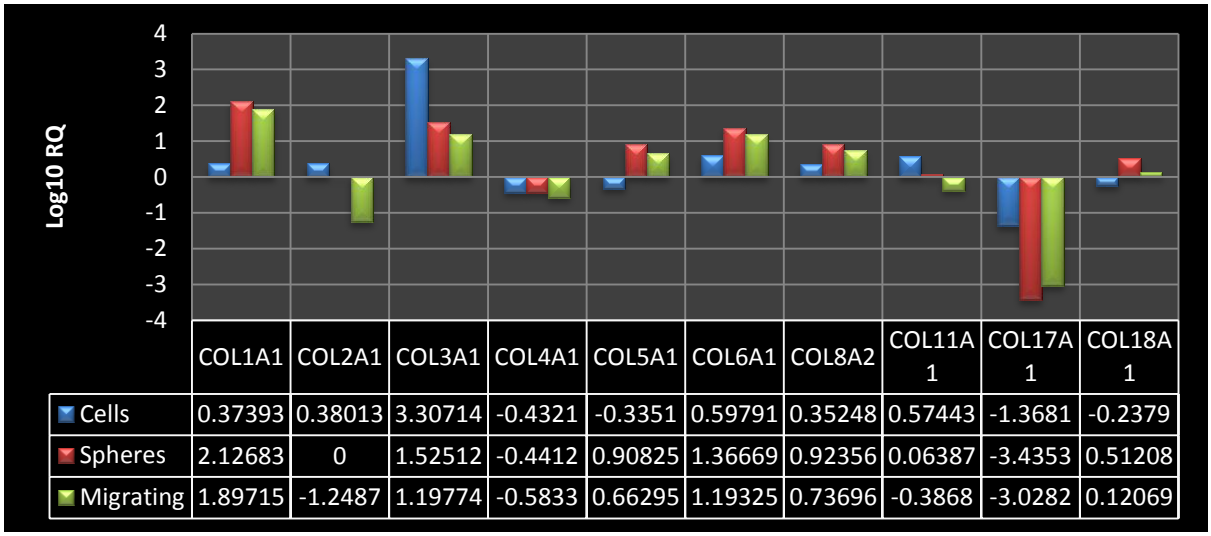

	COL1A1	COL2A1	COL3A1	COL4A1	COL5A1	COL6A1	COL8A2	COL11A1	COL17A1	COL18A1
Cells	0.37393	0.38013	3.30714	-0.4321	-0.3351	0.59791	0.35248	0.57443	-1.3681	-0.2379
Spheres	2.12683	0	1.52512	-0.4412	0.90825	1.36669	0.92356	0.06387	-3.4353	0.51208
Migrating	1.89715	-1.2487	1.19774	-0.5833	0.66295	1.19325	0.73696	-0.3868	-3.0282	0.12069

Figure 9.6 Mean quantitative expression of a range of collagen subtypes in migrating cells compared to non-migrating spheres, isolated cells and stromal tissue (baseline) measured using the TaqMan microfluidic arrays and ABI 7900 thermocycler. Collagen subtypes found in the corneal stroma including I, V and VI were all elevated in stromal-cell spheres and migrating cells. RQ = relative quantification.

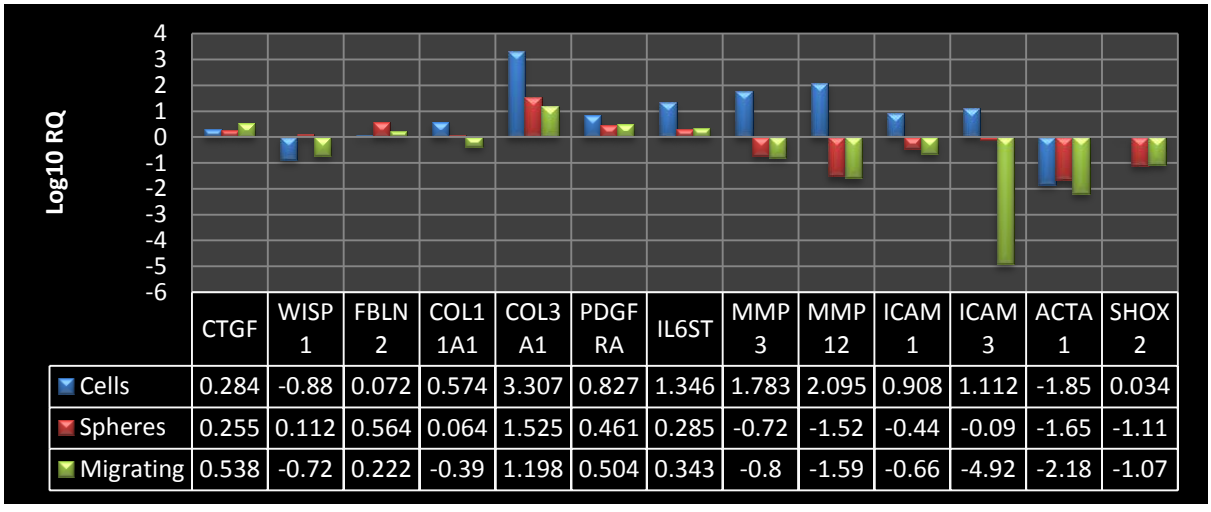

	CTGF	WISP1	FBLN2	COL11A1	COL3A1	PDGFRA	IL6ST	MMP3	MMP12	ICAM1	ICAM3	ACTA1	SHOX2
Cells	0.284	-0.88	0.072	0.574	3.307	0.827	1.346	1.783	2.095	0.908	1.112	-1.85	0.034
Spheres	0.255	0.112	0.564	0.064	1.525	0.461	0.285	-0.72	-1.52	-0.44	-0.09	-1.65	-1.11
Migrating	0.538	-0.72	0.222	-0.39	1.198	0.504	0.343	-0.8	-1.59	-0.66	-4.92	-2.18	-1.07

Figure 9.7 Quantitative gene expression of putative phenotypic markers of keratocyte trans-differentiation measured using the TaqMan microfluidic arrays and ABI 7900 thermocycler. Expression of candidate markers for myofibroblastic and fibroblastic trans-differentiation measured

in isolated stromal cells, non-migrating stromal-cell spheres and migrating cells. Spheres and migrating cells demonstrate downregulation of transcripts that are putative markers of myofibroblast and fibroblast phenotypes. Migrating cells demonstrated decreased ICAM1 and ICAM3, cell adhesion molecule expression. RQ = relative quantification.

9.4. Discussion

The addition of exogenous type I collagen gel or human stroma appears to act as a stimulus to initiate the migration of cells from stromal-cell spheres. Interestingly these spheres remain essentially inert in culture in the absence of exogenous collagen despite actively producing collagen, including type I collagen, as part of sphere formation. The endogenously produced collagen within and around stromal-cell spheres does not appear to provide the same stimulus for migration that exogenous collagen does. Migration of stromal cells in collagen gels has previously been observed;[5-7] however, until now the role of exogenous collagen in initiating migration in stromal cells independent of growth factors has not been reported. Although the basal growth media that migrating stromal-cell sphere cells were placed in contained EGF and bFGF that are known to promote stromal cell migration in the absence of exogenous collagen,[5] these growth factors alone were not sufficient to induce migration.

Gene expression in migrating stromal-cell sphere cells remains relatively consistent with expression patterns observed in cultured stromal-cell spheres. Proteoglycan transcript levels in migrating stromal cells remain constant with a small decrease in expression when compared with non-migrating-stromal-cell spheres. Collagen subtype expression in migrating cells also remained consistent with non-migrating stromal-cell spheres. The only observed changes of note in the putative markers of cellular phenotype in the migrating cells were a decrease in the cell adhesion molecules ICAM1 and ICAM3 as might be expected with migrating cells.

Interestingly, ICAM1 has been implicated in cell-to-cell signalling between keratocytes and neutrophils and is involved in a keratocyte mediated stromal inflammatory response to wounding. [9]

The observation that ICAM1 is down-regulated in migrating stromal-cell spheres suggests that the migratory activity initiated by exogenous type I collagen is not associated with the typical inflammatory response seen with migrating keratocytes in the cornea in the context of wounding. In addition, keratocyte migration in the cornea that is related to wounding is typically associated with myofibroblastic trans-differentiation and loss of proteoglycan expression – events that were not observed in collagen-induced migration of stromal-cell spheres in this study.[10-12] Taken together these data suggest that migration of stromal cells can be initiated by at least two separate pathways, an inflammatory response leading to trans-differentiation and scar tissue formation, or a response to exogenous ECM where the keratocyte phenotype is maintained along with keratocyte appropriate ratios of ECM transcripts. Further to this observation, it may be that transforming growth factor beta (TGFβ) is responsible for keratocyte migration associated with inflammation as this cytokine is known to stimulate keratocyte migration in the zebrafish cornea[13] and is also known to cause keratocyte to myofibroblast trans-differentiation[14] and ECM remodelling associated with myofibroblastic trans-differentiation in rabbit keratocytes. [6]

Despite the evidence of collagen induced migration of stromal-cell spheres with the absence of inflammation, the underlying cause of the increased expression of type III collagen noted in stromal cell spheres and migrating spheres remains unclear. Type III collagen is a fibril forming collagen normally expressed at low levels and that has been associated with a wound healing/inflammatory response in the cornea[11, 15] It is unclear if this increased transcript level is associated with increased type III collagen protein expression in migrating stromal-cell spheres, however, the abundance of the collagen type III transcript in migrating stromal-cell spheres is over 130 times lower than in freshly isolated stromal cells and approximately half of that seen in stromal-cell spheres and may therefore represent a slowly reducing response to the enzymatic digestion and isolation of stromal cells from the stromal tissue.

The potential to use stromal-cell spheres as a vector for repopulating dystrophic stromal tissue with healthy ECM expressing stromal cells is reliant on migration of the transplanted cells. The results of this study indicate that migration is likely to occur *in vivo* following transplantation of stromal-cell spheres, however, further work will be required to assess the pattern and extent of migration in dystrophic tissue. There are no publications specifically assessing the migration of stromal cells *in vivo* following corneal transplantation in humans however one study has demonstrated migration of transplanted endothelial cells *in vivo* in the context of dystrophic host tissue.[16] There are two studies that have used human cells labelled with carbocyanine dyes injected into lumican null mouse corneas.[17, 18] The first of these studies injected human stromal stem cells into mouse corneas but did not specifically assess migration.[17] The second study reported migration of human umbilical mesenchymal stem cells in mouse corneas although this was not quantified.[18] Although cell migration was not a primary endpoint for either of these studies, carbocyanine dyes may not be ideal for long term migration assays as they are prone to transfer to unlabelled cells where cell fusion or adhesion is present.[19-23] As keratocytes form an interconnecting network within the stroma, it is possible that the carbocyanine dye may transfer to unlabelled cells over time and control experiments would be required to validate this method before firm conclusions regarding keratocyte migration could be made. With the combination of high resolution *in vivo* imaging combined with live-cell labelling with fluorescent nanocrystals and other non-toxic cell tracking probes, the extent and pattern of stromal-cell migration following corneal transplantation is likely to be an area of interest in the future. Using these modalities it may be possible to further our understanding of the long-term topographic changes and events at the graft-host-junction that can occur in the years following corneal transplantation.

9.5. Conclusions

Migration of cells from cultured stromal-cell spheres is stimulated by the addition of exogenous type I collagen or transplantation into human stromal tissue. These results imply that transplantation of human stromal cell spheres into the stroma of dystrophic host patient corneas is likely to result in migration of the transplanted cells to repopulate the host cornea. This cellular migration is not associated with any detectable trans-differentiation in cellular phenotype of the migrating cells as detected at the gene expression level. Migrating cells demonstrate persistent and stable expression of keratocyte specific marker transcripts such as the collagen subtypes and proteoglycans without any indication of an inflammatory response.

9.6. References

1. Sandeman SR, Allen MC, Liu C, et al. Human keratocyte migration into collagen gels declines with in vitro ageing. Mechanisms of Ageing and Development 2000;119(3):149-57.
2. Anderson KI, Cross R. Contact dynamics during keratocyte motility. Current Biology 2000;10(5):253-60.
3. Burns AR, Li Z, Smith CW. Neutrophil migration in the wounded cornea: The role of the keratocyte. Ocular Surface 2005;3(4 Suppl):S173-6.
4. Gurelik G, Bilgihan K, Sezer C, et al. Effect of mechanical vs dilute ethanol epithelial removal on keratocyte apoptosis and polymorphonuclear leukocyte migration. Eye 2002;16(2):136-9.
5. Andresen JL, Ledet T, Ehlers N. Keratocyte migration and peptide growth factors: The effect of pdgf, bfgf, egf, igf-i, afgf and tgf-beta on human keratocyte migration in a collagen gel. Current Eye Research 1997;16(6):605-13.
6. Kim A, Lakshman N, Karamichos D, Petroll WM. Growth factor regulation of corneal keratocyte differentiation and migration in compressed collagen matrices. Investigative Ophthalmology and Visual Science 2010;51(2):864-75.
7. Lakshman N, Kim A, Petroll WM. Characterization of corneal keratocyte morphology and mechanical activity within 3-d collagen matrices. Experimental Eye Research 2010;90(2):350-9.
8. Kratz-Owens KL, Hageman GS, Schanzlin DJ. An in-vivo technique for monitoring keratocyte migration following lamellar keratoplasty. Refractive and Corneal Surgery 1992;8(3):230-4.
9. Gagen D, Laubinger S, Li Z, et al. Icam-1 mediates surface contact between neutrophils and keratocytes following corneal epithelial abrasion in the mouse. Experimental Eye Research 2010;91(5):676-84.
10. Beales MP, Funderburgh JL, Jester JV, Hassell JR. Proteoglycan synthesis by bovine keratocytes and corneal fibroblasts: Maintenance of the keratocyte phenotype in culture. Investigative Ophthalmology and Visual Science 1999;40(8):1658-63.

11. Hassell JR, Birk DE. The molecular basis of corneal transparency. Experimental Eye Research 2010;91(3):326-35.

12. Long CJ, Roth MR, Tasheva ES, et al. Fibroblast growth factor-2 promotes keratan sulfate proteoglycan expression by keratocytes in vitro. Journal of Biological Chemistry 2000;275(18):13918-23.

13. Tan B, Pascual A, de Beus A, et al. Transforming growth factor-beta (tgf-beta) & keratocyte motility in 24-hour zebrafish explant cultures. Cell Biology International 2011.

14. He J, Bazan HE. Epidermal growth factor synergism with tgf-beta1 via pi-3 kinase activity in corneal keratocyte differentiation. Investigative Ophthalmology and Visual Science 2008;49(7):2936-45.

15. Robert L, Legeais JM, Robert AM, Renard G. Corneal collagens. Pathologie-Biologie 2001;49(4):353-63.

16. Jacobi C, Zhivov A, Korbmacher J, et al. Evidence of endothelial cell migration after descemet membrane endothelial keratoplasty. American Journal of Ophthalmology 2011;152(4):537-42 e2.

17. Du Y, Carlson EC, Funderburgh ML, et al. Stem cell therapy restores transparency to defective murine corneas. Stem Cells 2009;27(7):1635-42.

18. Liu H, Zhang J, Liu CY, et al. Cell therapy of congenital corneal diseases with umbilical mesenchymal stem cells: Lumican null mice. PLoS ONE 2010;5(5):e10707.

19. Blumenthal R, Sarkar DP, Durell S, et al. Dilation of the influenza hemagglutinin fusion pore revealed by the kinetics of individual cell-cell fusion events. Journal of Cell Biology 1996;135(1):63-71.

20. Spotl L, Sarti A, Dierich MP, Most J. Cell membrane labeling with fluorescent dyes for the demonstration of cytokine-induced fusion between monocytes and tumor cells. Cytometry 1995;21(2):160-9.

21. Malhotra JD, Tsiotra P, Karagogeos D, Hortsch M. Cis-activation of l1-mediated ankyrin recruitment by tag-1 homophilic cell adhesion. Journal of Biological Chemistry 1998;273(50):33354-9.

22. Kreft B, Berndorff D, Bottinger A, et al. Li-cadherin-mediated cell-cell adhesion does not require cytoplasmic interactions. Journal of Cell Biology 1997;136(5):1109-21.

23. Kuriyama S, Yamazaki M, Mitoro A, et al. Analysis of intrahepatic invasion of hepatocellular carcinoma using fluorescent dye-labeled cells in mice. Anticancer Research 1998;18(6A):4181-8.

Chapter 10. The potential for cell based transplants as an alternative to traditional corneal transplantation: summary and conclusions

10.1. Introduction

Over recent years there has been significant progress in corneal transplantation techniques and the diagnosis and treatment of keratoconus. Despite this forward momentum, we still do not fully understand the underlying mechanisms of the disease and many patients still face difficulty living with the disability and reduced quality of life that typically affects those with visual impairment and blindness.

The relatively recent introduction of corneal cross linking is generating some promising results for treating a subset of keratoconic patients; however, we have yet to see how this strategy will fare in the longer term. Certainly, as stromal collagen has a relatively short half-life it may be expected that the effect of cross linking on the keratometric progression of keratoconus may not last indefinitely.

Cell based corneal transplants are likely to offer yet another therapeutic tool that can be used to proactively treat and prevent or slow further deterioration in early keratoconus. This thesis has evaluated the cellular and molecular biology and the *in vitro* methodology and culture system required to commence *ex vivo* and subsequent *in vivo* trials of cell based implants as a novel therapeutic intervention for keratoconus.

The chapters in this thesis have addressed the plausibility and cellular and molecular biological changes induced with isolation, culture and expansion of *ex vivo* human stromal cells and ultimately their suitability as a therapeutic cell-based corneal transplant. What follows is a summary of the conclusions reached in each of the individual chapters of this thesis and challenges that remain for the future.

10.2. The production and effect of growth factors and cytokines on corneal stromal cells (chapter 4)

The purpose of this study was to investigate the effect of varying growth factor concentrations on the morphology of cultured human keratocyte spheres and to compare cytokine production in subpopulations of stromal cells.

Conclusions:

1. Epidermal growth factor (EGF) promotes increased deposition of extracellular matrix (ECM) like material around human stromal cell spheres.
2. Side population (SP) cells produce EGF, and other cytokines at higher levels than non-SP cells which may act to regulate expression of ECM by keratocytes in the corneal stroma.
3. It is possible that transplanting SP-rich stromal-cell spheres into keratoconic corneas may prevent the ectasia and characteristic topographical changes observed in keratoconus by altering the expression and maintenance of ECM in the host corneal stroma

10.3. Fluorescence activated cell sorting analysis of isolated and cultured stromal cells (chapter 5)

The purpose of this study was to confirm the presence of SP cells in human stromal tissue and to investigate the regenerative and sphere forming capacity of SP and non-SP cells in culture.

Conclusions:

1. It is possible to sort isolated human corneal stromal cells using fluorescence activated cell sorting in combination with Hoechst 33342 efflux to identify a resident stem cell population.
2. The SP-cells disappeared with pre-incubation with verapamil indicating that the SP cells were identified based on the presence of the ABC transporter – a putative marker of stem cells.
3. SP and non-SP cells were capable of forming spheres in culture.
4. Sphere formation is associated with the re-emergence of the SP phenotype in non-SP stromal cell cultures.

5. Spheroid culture of stromal cells not only maintains the keratocyte phenotype but also has the potential to promote and maintain a progenitor cell population from differentiated-SP-depleted cells.
6. The ability to maintain a viable SP cell and progenitor cell population is likely to be essential for therapeutic interventions including long-term repopulation of dystrophic corneal stroma.

10.4. Understanding the mechanism of early stromal cell sphere formation: the role of migration and aggregation versus proliferation and cell division (chapter 6)

The purpose of this study was to assess the relative contributions of cell migration and proliferation in early stromal cell sphere formation using time lapse fluorescence microscopy with quantum dot nanocrystals to track cell migration in combination with a cell proliferation assay.

Conclusions:

1. Early stromal-cell sphere formation is predominantly a result of cell migration with only a small contribution from cell division.
2. Isolated stromal cells remain viable and highly motile in culture and can be tracked using Quantum Dot nanocrystals.

10.5. Late sphere formation and the temporal sequence of cell division and glycoprotein production (chapter 7)

The purpose of this study was to evaluate the contribution of cell division to late stromal-cell sphere formation and the temporal sequence of glycoprotein expression using tetra-acetylated N-azidoacetylgalactosamine (GalNAz) uptake, in combination with a cell proliferation assay, to confirm the phenotype and expansion of spheroid-cultured stromal cells.

Conclusions:

1. Late stromal-cell sphere formation is associated with a dramatic increase in cell division/proliferation with concomitant glycoprotein production.
2. Glycoprotein synthesis functions as a phenotypic marker of stromal cells and confirms that the sphere forming culture system described in this study is able to maintain and promote the expansion of ex vivo human corneal stromal cells without fibroblastic or myofibroblastic transformation which is associated with loss of glycoprotein expression.
3. Given the integral nature of proteoglycans in the structure and function of the cornea, the stable expression of these molecules as demonstrated in this study is pivotal in any culture system expanding stromal cells for transplant into dystrophic corneas.

10.6. Gene and protein expression in cultured stromal-cell spheres (chapter 8)

The purpose of this study was to ensure that *in vitro* culture conditions used for keratocyte culture were conducive to sustained ECM and collagen subtype gene and protein expression at appropriate ratios as seen in the cornea. Secondly, this study aimed to monitor any induced trans-differentiation of cultured cells as defined at the gene transcript level and predict the potential of cultured cells to maintain and regenerate dystrophic stroma.

Conclusions:

1. Cultured stromal-cell spheres demonstrate increased collagen-subtype gene expression for the collagen subtypes normally observed in the corneal stroma compared with gene expression in stromal tissue.
2. The ratios of collagen-subtype proteins expressed in cultured spheres remain consistent with expression ratios of collagen subtypes observed in stromal tissue and the collagen appears to be deposited in layers as seen in the adult corneal stroma.

3. Corneal-specific proteoglycan-gene expression is also up-regulated in stromal-cell spheres compared with stromal tissue.
4. Stromal-cell spheres demonstrate up-regulation of ABCG2 transcripts and ABCG2 protein expression indicating that this sphere based culture system maintains and expands the resident stem and progenitor cell populations and maintains the keratocyte phenotype in culture. These results confirm the findings from the cell sorting study outlined in chapter 5.

10.7. Cell migration from cultured stromal cell spheres in two and three dimensional collagen matrices and the effect of cell migration on gene expression (chapter 8)

The purpose of this study was to characterise the ability of spheroid cultured stromal cells to migrate and to evaluate the subsequent gene expression and trans-differentiation on collagen matrices and stromal tissue.

Conclusions:

1. Migration of cultured stromal-cell sphere cells is stimulated by the addition of exogenous type I collagen or transplantation into human stromal tissue.
2. These results imply that transplantation of human stromal cell spheres into the stroma of dystrophic host patient corneas is likely to result in migration of the transplanted cells to repopulate the host cornea.
3. This cellular migration is not associated with any detectable trans-differentiation in cellular phenotype of the migrating cells as detected at the gene expression level.
4. Migrating cells demonstrate persistent and stable expression of keratocyte specific marker transcripts such as the collagen subtypes and proteoglycans.

10.8. Final conclusions and future directions

The studies outlined in this thesis represent a significant inroad into the development of a new paradigm in corneal transplantation and potentially a novel therapeutic strategy for early keratoconus with the transplantation of spheroid cultured stromal cells. The application of stromal cell transplants, if effective in keratoconus, will assist in addressing the increasing demand for donor corneal tissue by potentially utilising the peripheral donor corneal tissue that is now discarded following transplantation. Because stromal cell transplantation would be used for treating early keratoconus, it has the potential to reduce the morbidity associated with severe keratoconus.

There are still challenges that remain before stromal cell transplants can be trialled in keratoconic patients. It is likely that the manual transplantation of individual spheres will be impractical due to their small size, potential mechanical damage to the stromal cells due to sphere manipulation, and the time required for transplantation of individual spheres. A more practical alternative would be to use a carrier medium that enables injection of cultured spheres into precut-intrastromal channels. The selection of an appropriate vector/carrier medium for transfer of cells into the host cornea will required to enable this injection transplantation protocol. To facilitate the transplantation of stromal cell spheres, avoid damage to the individual sphere cells, and reduce shear stress on the spheres during injection, it is likely that some form of viscous gel would be the most ideal carrier medium. There are several options for gel carrier media including sodium chondroitin sulphate/sodium hyaluronate, methylcellulose, or partially-polymerised fibrin or collagen gels. Although several of these compounds are used routinely during corneal and other ophthalmic surgical procedures, generally these compounds are carefully removed before the conclusion of the surgical procedure. The effects of residual intrastromal carrier media within the host cornea and on the transplanted spheres will require further assessment.

The number of spheres required for repopulation of a host cornea and halting disease progression remains unknown. Little is known about the movement of stromal cells following corneal

transplantation and the success of stromal cell implants is reliant on transplanted cell migration and repopulation of the host cornea. Live cell labelling of stromal cell spheres with a combination of a fluorescent Quantum Dot nanocrystal labels and a suitable non-toxic membrane label should allow the tracking of individual migrating live cells within the intact host corneal stroma. The intensity of fluorescence, minimal toxicity, and resistance to photobleaching of the Quantum Dot nanocrystals in combination with a far red fluorescence to minimise light scatter and allow deep tissue imaging, make this an ideal live-cell label for transplanted cell migration assays. The only limitation of Quantum Dot labelling is that it does not label the cell membrane or nucleus, and therefore, it is difficult to identify and track individual live cells as they migrate. For this reason using a second membrane-bound live cell label would assist in discriminating between cells and would potentially demonstrate fluorescence transfer when cell-to-cell contact occurs. The results of these studies will determine the number and distribution of transplanted spheres required for successful host repopulation.

Finally, as with any clinical therapy it is essential that therapeutic efficacy is confirmed. The data collected in this thesis suggests that stromal-cell based corneal transplantation is likely to be successful, however, these results will require clinical data to support the *in vivo* evidence presented in this thesis. In the case of stromal cell transplants in keratoconus, efficacy would almost certainly be demonstrated by maintenance of corneal clarity, and stability of repeated keratometric, pachymetric and visual assessments over time.

The refinement of corneal transplantation, with the associated increase in popularity of lamellar transplant techniques, has continued to provide ever increasing benefits for patients and continues to challenge the technical skills of the corneal surgeon. This progress in corneal surgery has required an on-going process of innovation and development that has led us from the operating theatre and clinic into the laboratory. With the possibility of stromal-cell transplants on the horizon, there is now the potential for more efficient use of the limited supply of donor corneal tissue that is available,

and a therapeutic paradigm shift from treatment to prevention. To this end, the potential of stromal cell transplants for treatment of early keratoconus represents an exciting new step in the evolution of corneal transplant surgery.

Chapter 11. Appendices

11.1. Taqman assays for microfluidic array cards

Sample		001-01		001-02		140-01		140-02		141-01		141-02	
Sample	Detector	delta delta Ct	RQ	delta delta Ct	RQ	delta delta Ct	RQ	delta delta Ct	RQ	delta delta Ct	RQ	delta delta Ct	RQ
tissue	18S-Hs99999901_s1												
cells	18S-Hs99999901_s1												
spheres	18S-Hs99999901_s1												
migrating spheres	18S-Hs99999901_s1												
tissue	ABCG2-Hs01053787_m1					0	1						
cells	ABCG2-Hs01053787_m1					0.98542976	0.5	-2.0720463	4.205			0.80911636	0.5707
spheres	ABCG2-Hs01053787_m1	9.392773	0.0015	6.371176	0.01	1.8659267	0.3	-1.9955502	3.988			-1.4972134	2.823
migrating spheres	ABCG2-Hs01053787_m1	8.3381195	0.0031	6.6669197	0.01	5.1745815	0	-2.0869446	4.248	-0.10767174	1.08	0.9284401	0.5254
tissue	ACTA1-Hs00559403_m1							0	1			0	1
cells	ACTA1-Hs00559403_m1							7.2059727	0.007			9.20359	0.0017
spheres	ACTA1-Hs00559403_m1	3.7839165	0.0726	10.669092	###	3.1587238	0.1	9.280432	0.002			6.4910526	0.0111
migrating spheres	ACTA1-Hs00559403_m1			5.05735	0.03			5.014366	0.031			8.70306	0.0024
tissue	AIM1-Hs00413464_m1					0	1	0	1	0	1	0	1
cells	AIM1-Hs00413464_m1					4.180664	0.1	3.6191158	0.081	-1.5208931	2.87	1.3552856	0.3909
spheres	AIM1-Hs00413464_m1	5.4486504	0.0229	3.5562649	0.09	4.0701447	0.1	3.816887	0.071	-1.136013	2.2	2.444067	0.1838
migrating spheres	AIM1-Hs00413464_m1	4.300411	0.0508	2.6291218	0.16	6.088524	0	5.028324	0.031	-1.7606125	3.39	1.905468	0.2669
tissue	ALDH1A3-Hs00167476_m1	0	1			0	1	0	1	0	1	0	1
cells	ALDH1A3-Hs00167476_m1	2.7334385	0.1504			3.654686	0.1	3.3353558	0.099	1.3281059	0.4	1.8550682	0.2764
spheres	ALDH1A3-Hs00167476_m1	0.6200743	0.6506	1.6048717	0.33	4.0448875	0.1	3.6433086	0.08	1.7767639	0.29	2.171564	0.222
migrating spheres	ALDH1A3-Hs00167476_m1	1.982913	0.253	1.6497421	0.32	4.0656967	0.1	3.7331352	0.075	1.1930962	0.44	1.7715683	0.2929
tissue	ASS1-Hs00540723_m1					0	1	0	1	0	1	0	1
cells	ASS1-Hs00540723_m1			-4.3755665	20.8	0.6968622	0.6	0.8498306	0.555	0.4959154	0.71	-0.12405872	1.0898
spheres	ASS1-Hs00540723_m1	2.4483757	0.1832	-0.25440788	1.19	1.4661436	0.4	1.3976822	0.38	0.32066727	0.8	0.40019035	0.7578

migrating spheres	ASS1-Hs00540723_m1	1.3398371	0.3951	-1.243021	2.37	1.9762068	0.3	1.9249716	0.263	-0.17767334	1.13	-0.21100521	1.1575
tissue	ATP1A1-Hs00167556_m1					0	1	0	1	0	1	0	1
cells	ATP1A1-Hs00167556_m1	-3.070654	8.4015	-4.413233	21.3	-0.76266384	1.7	-0.91438484	1.885	0.6836519	0.62	-0.13153934	1.0955
spheres	ATP1A1-Hs00167556_m1	0.99714375	0.501	-0.73649216	1.67	0.80613613	0.6	0.75065994	0.594	1.4568825	0.36	0.96310234	0.513
migrating spheres	ATP1A1-Hs00167556_m1	0.82615566	0.564	-0.30503654	1.24	1.8517818	0.3	1.5094643	0.351	0.85087585	0.55	0.8665304	0.5485
tissue	BGN-Hs00156076_m1					0	1	0	1	0	1	0	1
cells	BGN-Hs00156076_m1			-3.2075672	9.24	0.56264687	0.7	-0.007341385	1.005	1.3098793	0.4	1.0819817	0.4724
spheres	BGN-Hs00156076_m1	-3.3155794	9.9561	-5.8919315	59.4	-5.4398146	43	-5.7781334	54.88	-4.916025	30.2	-4.5614834	23.613
migrating spheres	BGN-Hs00156076_m1	-1.9405527	3.8385	-4.3068256	19.8	-4.688693	26	-4.705165	26.09	-4.1672287	18	-3.8961668	14.889
tissue	BMP4-Hs00370078_m1					0	1	0	1	0	1	0	1
cells	BMP4-Hs00370078_m1					0.6334286	0.6	0.7348347	0.601	3.606533	0.08	3.2601357	0.1044
spheres	BMP4-Hs00370078_m1	6.2291145	0.0133	3.596117	0.08	-0.45648766	1.4	-0.7382393	1.668	2.1611824	0.22	3.9096966	0.0665
migrating spheres	BMP4-Hs00370078_m1	5.3306313	0.0248	2.9066334	0.13	0.006872177	1	-0.08807373	1.063	1.5187969	0.35	1.2313042	0.4259
tissue	C1QA-Hs00381122_m1					0	1					0	1
cells	C1QA-Hs00381122_m1			-3.1050282	8.6	3.843851	0.1	1.1374989	0.455	2.002098	0.25	7.5341415	0.0054
spheres	C1QA-Hs00381122_m1	3.2851715	0.1026	-0.95989037	1.95	6.498892	0	-0.22470665	1.169			4.821604	0.0354
migrating spheres	C1QA-Hs00381122_m1			0.36736298	0.78	1.4814854	0.4					7.0336113	0.0076
tissue	CA12-Hs01080909_m1					0	1	0	1	0	1	0	1
cells	CA12-Hs01080909_m1	-2.7778263	6.8582	-5.455702	43.9	-3.681325	13	-3.8566437	14.49	-0.22685528	1.17	-1.25348	2.3842
spheres	CA12-Hs01080909_m1	2.152916	0.2249	2.114254	0.23	-0.80254936	1.7	-1.1427288	2.208	3.116867	0.12	1.880167	0.2717
migrating spheres	CA12-Hs01080909_m1	2.0471687	0.242	1.7450676	0.3	0.01067543	1	-0.2063713	1.154	2.6326199	0.16	3.007286	0.1244
tissue	CCL2-Hs00234140_m1					0	1	0	1	0	1	0	1
cells	CCL2-Hs00234140_m1	-7.5069675	181.9	-9.390213	671	-2.5144873	5.7	-2.4478931	5.456	-1.048358	2.07	-1.4546862	2.741
spheres	CCL2-Hs00234140_m1	3.640854	0.0802	1.0487957	0.48	1.013072	0.5	1.181963	0.441	3.3670578	0.1	3.5881805	0.0831
migrating spheres	CCL2-Hs00234140_m1	2.2638512	0.2082	0.03180313	0.98	1.8326683	0.3	1.8931313	0.269	3.325985	0.1	3.6818256	0.0779
tissue	CCL7-Hs00171147_m1					0	1	0	1	0	1	0	1
cells	CCL7-Hs00171147_m1			-2.4442005	5.44	-5.6548243	50	-4.3080235	19.81	-1.7958298	3.47	-3.0930738	8.5331
spheres	CCL7-Hs00171147_m1	7.576515	0.0052	3.9177094	0.07	-3.128992	8.7	-1.7492085	3.362	1.193737	0.44	-0.13763237	1.1001

migrating spheres	CCL7-Hs00171147_m1	6.3392143	0.0124	3.1904697	0.11	-2.460497	5.5	-1.1745987	2.257	0.6568661	0.63	-0.6004143	1.5162
tissue	CD68-Hs00154355_m1					0	1	0	1	0	1	0	1
cells	CD68-Hs00154355_m1	-3.0769253	8.4381	-6.771755	109	-2.5688372	5.9	-1.9563751	3.881	-0.48675823	1.4	-0.80865574	1.7516
spheres	CD68-Hs00154355_m1	1.8071127	0.2858	0.21343422	0.86	-1.8393888	3.6	-1.5905685	3.012	0.15316391	0.9	0.53469276	0.6903
migrating spheres	CD68-Hs00154355_m1	1.0778971	0.4737	-0.327034	1.25	-0.52731514	1.4	-0.45633698	1.372	-0.28744316	1.22	-0.2872305	1.2203
tissue	CDC42-Hs00741586_mH												
cells	CDC42-Hs00741586_mH					0.71795464	0.6	-0.1558094	1.114	2.0318832	0.24	-3.5499763	11.712
spheres	CDC42-Hs00741586_mH	9.67738	0.0012	7.486044	0.01	-0.9479122	1.9	-1.6239376	3.082			-1.2039013	2.3036
migrating spheres	CDC42-Hs00741586_mH	9.328442	0.0016	6.646328	0.01			-1.0283089	2.04	0.37379265	0.77	-0.27832413	1.2128
tissue	CDH5-Hs00901463_m1					0	1	0	1	0	1	0	1
cells	CDH5-Hs00901463_m1			-1.3986874	2.64	2.8016987	0.1	4.716139	0.038	1.7142563	0.3	0.12754059	0.9154
spheres	CDH5-Hs00901463_m1	8.670795	0.0025	5.210146	0.03	-0.45067024	1.4	-1.0338879	2.048	6.159149	0.01	-1.1849957	2.2736
migrating spheres	CDH5-Hs00901463_m1	10.090782	#####	6.267166	0.01	0.49892616	0.7	-0.5469475	1.461	1.5658703	0.34	0.23637009	0.8489
tissue	COL11A1-Hs00266273_m1												
cells	COL11A1-Hs00266273_m1					0.68793297	0.6	-3.2069454	9.234			-4.42387	21.464
spheres	COL11A1-Hs00266273_m1	5.554657	0.0213	3.2723255	0.1	-2.2146015	4.6	-5.4980507	45.19				
migrating spheres	COL11A1-Hs00266273_m1	6.892254	0.0084	4.6310463	0.04	-1.920618	3.8	-0.91319275	1.883				
tissue	COL17A1-Hs00166711_m1					0	1	0	1	0	1	0	1
cells	COL17A1-Hs00166711_m1			-2.4163227	5.34	8.263506	0	8.168219	0.003	8.310945	0	6.1215754	0.0144
spheres	COL17A1-Hs00166711_m1	9.824127	0.0011	8.6974125	0	17.230421	###	17.29064	####	8.876074	0	7.2192535	0.0067
migrating spheres	COL17A1-Hs00166711_m1	11.39352	#####	9.655746	0	13.165792	###	13.024574	####	5.8164825	0.02	13.189653	#####
tissue	COL18A1-Hs00181017_m1					0	1	0	1				
cells	COL18A1-Hs00181017_m1			-1.3243084	2.5	3.7901325	0.1	1.5918102	0.332	0.68371964	0.62	0.1422844	0.9061
spheres	COL18A1-Hs00181017_m1	4.02861	0.0613	-2.389223	5.24	0.38345528	0.8	-1.1936493	2.287	-2.925312	7.6	-3.23176	9.3941
migrating spheres	COL18A1-Hs00181017_m1	6.3748436	0.012	-0.27583694	1.21	-0.03627968	1	-0.79362106	1.733	-2.08045	4.23	-0.29774094	1.2292
tissue	COL1A1-Hs01076777_m1					0	1	0	1	0	1	0	1
cells	COL1A1-Hs01076777_m1	-2.972723	7.8502	-1.4088154	2.66	-2.2743778	4.8	1.1174202	0.461	-0.49765396	1.41	1.0278816	0.4904
spheres	COL1A1-Hs01076777_m1	-6.332078	80.565	-7.241699	151	-8.553231	376	-5.819109	56.46	-7.311571	159	-5.0386753	32.869
migrating	COL1A1-Hs01076777_m1	-5.617879	49.108	-5.949089	61.8	-8.319165	319	-5.388543	41.89	-6.417471	85.5	-3.661397	12.653

spheres													
tissue	COL2A1-Hs01064869_m1												
cells	COL2A1-Hs01064869_m1					-4.7883015	28						
spheres	COL2A1-Hs01064869_m1												
migrating spheres	COL2A1-Hs01064869_m1	11.443905	#####										
tissue	COL3A1-Hs00943809_m1					0	1	0	1	0	1	0	1
cells	COL3A1-Hs00943809_m1	-34.779984	#####	-2.4757442	5.56	-0.8229389	1.8	-0.7750473	1.711	2.015995	0.25	1.3110924	0.403
spheres	COL3A1-Hs00943809_m1	-7.7260466	211.72	-5.422209	42.9	-4.9594183	31	-5.0158424	32.35	-3.1712189	9.01	-3.265297	9.6151
migrating spheres	COL3A1-Hs00943809_m1	-6.1403227	70.538	-3.75708	13.5	-3.771039	14	-3.8227339	14.15	-2.275095	4.84	-3.1004133	8.5766
tissue	COL4A1-Hs01007469_m1					0	1	0	1	0	1	0	1
cells	COL4A1-Hs01007469_m1			-2.425829	5.37	0.94724846	0.5	2.1241207	0.229	3.6901588	0.08	5.4350433	0.0231
spheres	COL4A1-Hs01007469_m1	3.6233253	0.0811	0.566803	0.68	0.87607384	0.5	0.81552315	0.568	2.0748215	0.24	2.2256107	0.2138
migrating spheres	COL4A1-Hs01007469_m1	4.845669	0.0348	1.9413853	0.26	0.14239311	0.9	0.8983078	0.537	2.219473	0.21	3.064495	0.1195
tissue	COL5A1-Hs00609088_m1					0	1	0	1	0	1	0	1
cells	COL5A1-Hs00609088_m1					1.0327549	0.5	1.5809727	0.334	1.9151878	0.27	2.2168694	0.2151
spheres	COL5A1-Hs00609088_m1	0.6609297	0.6325	-1.4783516	2.79	-4.0920305	17	-4.9329853	30.55	-3.8788204	14.7	-3.5074062	11.372
migrating spheres	COL5A1-Hs00609088_m1	1.5803785	0.3344	-0.30892563	1.24	-4.1221323	17	-4.5988083	24.23	-3.0039806	8.02	-1.9557314	3.8791
tissue	COL6A1-Hs00242448_m1					0	1	0	1	0	1	0	1
cells	COL6A1-Hs00242448_m1	-3.0454464	8.256	-2.389162	5.24	-0.9491329	1.9	-1.9131012	3.766	-1.9889326	3.97	-1.3231688	2.5022
spheres	COL6A1-Hs00242448_m1	-4.0444193	16.5	-3.582241	12	-4.7035036	26	-6.0538063	66.43	-4.690834	25.8	-3.6341953	12.417
migrating spheres	COL6A1-Hs00242448_m1	-3.4709368	11.088	-2.62426	6.17	-4.888278	30	-5.60464	48.66	-3.920557	15.1	-2.8806696	7.3649
tissue	COL8A2-Hs00697025_m1							0	1			0	1
cells	COL8A2-Hs00697025_m1			-1.4094296	2.66	-3.7090893	13	-1.6038055	3.039	-0.46268463	1.38	0.4060173	0.7547
spheres	COL8A2-Hs00697025_m1	3.7075958	0.0765	1.2013588	0.43	-6.6097813	98	-4.7758274	27.39	-5.9642677	62.4	-3.5030785	11.338
migrating spheres	COL8A2-Hs00697025_m1	4.3460884	0.0492	1.6595669	0.32	-6.897146	119	-5.1407156	35.28	-4.0942917	17.1	-2.5687494	5.9329
tissue	CRABP2-Hs00275636_m1					0	1	0	1	0	1	0	1
cells	CRABP2-Hs00275636_m1	-3.1072903	8.6176	-4.033285	16.4	0.38152218	0.8	-0.014432907	1.01	-0.29038906	1.22	0.58843136	0.6651
spheres	CRABP2-Hs00275636_m1	-1.7026472	3.255	-3.4538193	11	-4.2700834	19	-4.6426296	24.98	-5.1053085	34.4	-3.8745747	14.668
migrating	CRABP2-Hs00275636_m1	-1.8741732	3.6659	-3.4501553	10.9	-2.8497248	7.2	-3.4368715	10.83	-5.313637	39.8	-3.9157782	15.093

spheres													
tissue	CRYAA-Hs00166138_m1												
cells	CRYAA-Hs00166138_m1												
spheres	CRYAA-Hs00166138_m1												
migrating spheres	CRYAA-Hs00166138_m1												
tissue	CRYBA1-Hs00193230_m1					0	1						
cells	CRYBA1-Hs00193230_m1					5.5522537	0			-4.999031	32		
spheres	CRYBA1-Hs00193230_m1					4.2988396	0.1	2.1803188	0.221	-3.2149048	9.29	-3.60034	12.129
migrating spheres	CRYBA1-Hs00193230_m1			9.661743	0	10.293041	###						
tissue	CRYBA4-Hs00608089_m1												
cells	CRYBA4-Hs00608089_m1			-5.2649784	38.5								
spheres	CRYBA4-Hs00608089_m1			4.5480423	0.04	2.1340694	0.2	2.182623	0.22			-8.918341	483.82
migrating spheres	CRYBA4-Hs00608089_m1	11.332691	#####	-4.3398056	20.2								
tissue	CRYBB2-Hs00166761_m1							0	1				
cells	CRYBB2-Hs00166761_m1					-0.9281826	1.9	4.0860233	0.059				
spheres	CRYBB2-Hs00166761_m1			10.596167	###	3.1741047	0.1	9.686258	0.001				
migrating spheres	CRYBB2-Hs00166761_m1							2.793129	0.144				
tissue	CRYGB-Hs00245463_m1					0	1	0	1	0	1	0	1
cells	CRYGB-Hs00245463_m1			-2.3785343	5.2	8.8253765	0	-4.360695	20.54	33.285618	####	8.306568	0.0032
spheres	CRYGB-Hs00245463_m1			2.6711998	0.16	11.225519	###	9.431074	0.001	24.88472	####	5.5940304	0.0207
migrating spheres	CRYGB-Hs00245463_m1	3.3851547	0.0957	0.46107864	0.73	7.1608906	0	5.1650085	0.028	33.17103	####	7.806038	0.0045
tissue	CRYGD-Hs00359815_m1									0	1		
cells	CRYGD-Hs00359815_m1							-9.88685	946.8	39.5233	####		
spheres	CRYGD-Hs00359815_m1									36.436386	####		
migrating spheres	CRYGD-Hs00359815_m1									39.408714	####		
tissue	CSF2-Hs99999044_m1			0	1	0	1			0	1		
cells	CSF2-Hs99999044_m1	-17.148384	145271	4.82831	0.04	-0.97654533	2	-4.351282	20.41	2.2502413	0.21	-0.54034424	1.4543
spheres	CSF2-Hs99999044_m1			15.252695	###	6.09939	0	3.2210903	0.107	9.730446	0		
migrating spheres	CSF2-Hs99999044_m1	11.135361	#####	10.313763	###	5.1207905	0	-1.1316452	2.191	-0.01442146	1.01		

tissue	CTGF-Hs00170014_m1					0	1	0	1	0	1	0	1
cells	CTGF-Hs00170014_m1	-5.1238422	34.868	-4.38962	21	1.3756542	0.4	1.2463131	0.422	0.6072769	0.66	0.7299881	0.6029
spheres	CTGF-Hs00170014_m1	0.002736092	0.9981	-1.8545723	3.62	0.17168713	0.9	0.030963898	0.979	-1.7085094	3.27	-1.0884457	2.1264
migrating spheres	CTGF-Hs00170014_m1	0.010846138	0.9925	-1.6196918	3.07	-1.8862314	3.7	-2.2276258	4.684	-2.5905228	6.02	-1.8493605	3.6034
tissue	CTSB-Hs00947433_m1					0	1	0	1	0	1	0	1
cells	CTSB-Hs00947433_m1	-5.68968	51.614	-7.4270477	172	-1.2324286	2.3	-1.3467445	2.543	-0.26040173	1.2	0.19530582	0.8734
spheres	CTSB-Hs00947433_m1	-0.6377516	1.5559	-3.199747	9.19	-0.094088554	1.1	-0.2898426	1.223	0.2175579	0.86	1.0863647	0.4709
migrating spheres	CTSB-Hs00947433_m1	-0.6657915	1.5864	-3.032011	8.18	0.6489992	0.6	0.33936787	0.79	-0.15367508	1.11	0.70914555	0.6117
tissue	CTSD-Hs00157205_m1					0	1	0	1	0	1	0	1
cells	CTSD-Hs00157205_m1			-6.019953	64.9	-0.037983894	1	-0.089962006	1.064	-0.6802759	1.6	-0.37884045	1.3003
spheres	CTSD-Hs00157205_m1	0.10369587	0.9306	-2.4379349	5.42	-0.43879795	1.4	-0.47543526	1.39	-1.0212479	2.03	-0.12096405	1.0875
migrating spheres	CTSD-Hs00157205_m1	0.32794094	0.7967	-2.0202675	4.06	0.31229115	0.8	0.39194393	0.762	-0.6669731	1.59	-0.17194462	1.1266
tissue	CXCL12-Hs00171022_m1					0	1					0	1
cells	CXCL12-Hs00171022_m1			-1.4138699	2.66	-2.230009	4.7	-4.899334	29.84	-0.11187744	1.08	4.105442	0.0581
spheres	CXCL12-Hs00171022_m1	1.6260023	0.324	-0.59799576	1.51	-5.0772963	34	-8.0648575	267.8	-4.4197655	21.4	-0.17451668	1.1286
migrating spheres	CXCL12-Hs00171022_m1	1.7480593	0.2977	-0.3343525	1.26	-4.064928	17	-6.496132	90.27	-5.1288013	35	-0.86528397	1.8217
tissue	DCN-Hs00370385_m1			0	1	0	1	0	1	0	1	0	1
cells	DCN-Hs00370385_m1	-8.517899	366.56	-6.7257214	106	-1.2646036	2.4	-1.1955242	2.29	0.096310616	0.94	0.4641981	0.7249
spheres	DCN-Hs00370385_m1	-3.366994	10.317	-1.863205	3.64	-2.3700113	5.2	-2.7525482	6.739	-0.1908474	1.14	-0.136549	1.0993
migrating spheres	DCN-Hs00370385_m1	-2.6411905	6.2385	-1.1961842	2.29	-1.2023859	2.3	-1.5673742	2.964	-0.4895649	1.4	-0.15568638	1.114
tissue	EFEMP2-Hs00213545_m1					0	1	0	1	0	1	0	1
cells	EFEMP2-Hs00213545_m1	-16.063051	68464	-1.4501514	2.73	-0.7521839	1.7	-0.60720444	1.523	3.322795	0.1	-1.9278793	3.805
spheres	EFEMP2-Hs00213545_m1	-1.6046762	3.0413	-0.9386902	1.92	-2.9820395	7.9	-2.9857483	7.921	2.8543282	0.14	-4.174143	18.053
migrating spheres	EFEMP2-Hs00213545_m1	-0.8784208	1.8384	-0.51659393	1.43	-2.821044	7.1	-2.4078789	5.307	1.9376602	0.26	-3.2791185	9.7076
tissue	EFNB2-Hs00970627_m1					0	1	0	1	0	1	0	1
cells	EFNB2-Hs00970627_m1			-1.4631023	2.76	4.741728	0	5.0711308	0.03	5.614849	0.02	3.003498	0.1247
spheres	EFNB2-Hs00970627_m1	6.536602	0.0108	2.7435474	0.15	4.7587643	0	4.572359	0.042	3.5032425	0.09	2.9528713	0.1292
migrating spheres	EFNB2-Hs00970627_m1	4.299362	0.0508	1.6764832	0.31	3.1492443	0.1	2.3247223	0.2	5.0088024	0.03	3.6914215	0.0774

tissue	EGF-Hs01099990_m1					0	1	0	1	0	1	0	1
cells	EGF-Hs01099990_m1					-1.2721729	2.4	2.3563366	0.195	1.4403763	0.37	10.528137	#####
spheres	EGF-Hs01099990_m1	8.615414	0.0025	7.5485935	0.01	-0.64536095	1.6	1.7205315	0.303	8.102451	0	7.8155994	0.0044
migrating spheres	EGF-Hs01099990_m1	11.289673	#####	5.7246895	0.02	-8.380776	333	1.8464584	0.278	4.848528	0.03	5.073349	0.0297
tissue	FBLN2-Hs00157482_m1					0	1	0	1	0	1	0	1
cells	FBLN2-Hs00157482_m1			-1.5301876	2.89	0.83294106	0.6	-0.39012146	1.311	-0.09682465	1.07	-0.43919373	1.3558
spheres	FBLN2-Hs00157482_m1	2.6213188	0.1625	-1.0806942	2.12	-1.8768873	3.7	-3.6314793	12.39	-2.6744995	6.38	-2.1212978	4.3509
migrating spheres	FBLN2-Hs00157482_m1	3.9922867	0.0628	0.30880737	0.81	-0.9882755	2	-2.3451614	5.081	-1.878912	3.68	-1.246769	2.3731
tissue	FDPS-Hs00266635_m1	0	1	0	1	0	1	0	1	0	1	0	1
cells	FDPS-Hs00266635_m1	1.622263	0.3248	1.6329784	0.32	1.1007328	0.5	3.2613583	0.104	3.8018684	0.07	5.134674	0.0285
spheres	FDPS-Hs00266635_m1	5.125084	0.0287	6.5932865	0.01	1.872942	0.3	3.8243847	0.071	4.421688	0.05	2.5890713	0.1662
migrating spheres	FDPS-Hs00266635_m1	4.760906	0.0369	5.802784	0.02	1.6437702	0.3	2.9025726	0.134	-0.1431694	1.1	1.1539612	0.4494
tissue	FGF1-Hs01092738_m1							0	1	0	1	0	1
cells	FGF1-Hs01092738_m1					0.086725235	0.9	3.5039272	0.088	18.05052	####	8.962667	0.002
spheres	FGF1-Hs01092738_m1	8.49416	0.0028	6.132906	0.01	0.5838108	0.7	2.5055103	0.176	14.963606	####	5.136387	0.0284
migrating spheres	FGF1-Hs01092738_m1	7.3547134	0.0061	4.6786366	0.04	-0.937891	1.9	1.2134094	0.431	7.127983	0.01	8.204939	0.0034
tissue	FGF7-Hs00940253_m1	0	1			0	1	0	1	0	1	0	1
cells	FGF7-Hs00940253_m1	0.001260757	0.9991	-5.567709	47.4	-4.0521383	17	-4.217848	18.61	3.1415825	0.11	2.3445168	0.1969
spheres	FGF7-Hs00940253_m1	7.6644783	0.0049	3.5719433	0.08	-0.63809013	1.6	-0.8016033	1.743	3.9082184	0.07	5.500845	0.0221
migrating spheres	FGF7-Hs00940253_m1	7.2646904	0.0065	3.2129555	0.11	-0.19024467	1.1	-1.0616035	2.087	3.2085285	0.11	4.232525	0.0532
tissue	GJB2-Hs00955889_m1					0	1	0	1	0	1	0	1
cells	GJB2-Hs00955889_m1					5.309017	0	4.964655	0.032	3.162712	0.11	3.2886353	0.1023
spheres	GJB2-Hs00955889_m1	7.121464	0.0072	5.0380154	0.03	11.162174	###	12.8434925	####	7.110096	0.01	6.783205	0.0091
migrating spheres	GJB2-Hs00955889_m1	9.370861	0.0015	6.690941	0.01	11.109673	###	11.606506	####	10.082422	####	8.995213	0.002
tissue	GSTA4-Hs00155308_m1					0	1	0	1	0	1	0	1
cells	GSTA4-Hs00155308_m1	-4.516035	22.88	-1.4548092	2.74	-0.4526348	1.4	-0.24713326	1.187	2.785862	0.15	1.1446304	0.4523
spheres	GSTA4-Hs00155308_m1	-1.7427702	3.3468	0.9352169	0.52	-0.8287983	1.8	-0.78554726	1.724	1.0479279	0.48	-0.46115685	1.3766
migrating spheres	GSTA4-Hs00155308_m1	-0.8916216	1.8553	1.6181011	0.33	-0.010736465	1	0.60248184	0.659	0.45552254	0.73	-0.6417999	1.5603
tissue	GSTO1-Hs00818731_m1					0	1	0	1	0	1	0	1

cells	GSTO1-Hs00818731_m1	-5.4588604	43.983	-6.656973	101	-1.873168	3.7	-2.0240288	4.067	-0.72585964	1.65	-0.5309763	1.4449
spheres	GSTO1-Hs00818731_m1	1.6246519	0.3243	-0.42285347	1.34	1.2542248	0.4	1.1062508	0.464	0.5848732	0.67	1.9486332	0.2591
migrating spheres	GSTO1-Hs00818731_m1	1.301898	0.4056	-0.7253113	1.65	1.4726696	0.4	0.9761696	0.508	0.65820885	0.63	1.493927	0.355
tissue	HES1-Hs00172878_m1					0	1	0	1	0	1	0	1
cells	HES1-Hs00172878_m1			-3.3976383	10.5	-0.5381794	1.5	-0.3743496	1.296	-0.9644356	1.95	-0.6501732	1.5694
spheres	HES1-Hs00172878_m1	3.2334557	0.1063	1.5526257	0.34	1.758955	0.3	1.6965809	0.309	-0.33644485	1.26	1.1691494	0.4447
migrating spheres	HES1-Hs00172878_m1	5.3457108	0.0246	3.4112473	0.09	3.0978603	0.1	2.5989494	0.165	0.6997967	0.62	1.4521446	0.3655
tissue	HGF-Hs00900070_m1					0	1	0	1	0	1	0	1
cells	HGF-Hs00900070_m1	-3.1013546	8.5822	-4.7654552	27.2	-2.986287	7.9	-2.6425076	6.244	-1.1688337	2.25	-1.1717329	2.2528
spheres	HGF-Hs00900070_m1	2.1483002	0.2256	0.5565071	0.68	-0.9979191	2	-0.8842201	1.846	-0.8480034	1.8	-0.38355827	1.3046
migrating spheres	HGF-Hs00900070_m1	1.0120554	0.4958	-0.8671284	1.82	-0.41359138	1.3	-0.08106232	1.058	-1.3294239	2.51	-0.86159134	1.817
tissue	ICAM1-Hs00277001_m1					0	1	0	1	0	1	0	1
cells	ICAM1-Hs00277001_m1	-4.0813656	16.928	-4.4148197	21.3	-3.906499	15	-3.603918	12.16	-0.8423662	1.79	-1.1978941	2.294
spheres	ICAM1-Hs00277001_m1	4.55085	0.0427	2.440096	0.18	-0.4853115	1.4	-0.17640114	1.13	1.673378	0.31	1.448698	0.3664
migrating spheres	ICAM1-Hs00277001_m1	4.8028603	0.0358	2.6313095	0.16	1.5029316	0.4	1.2313728	0.426	1.60812	0.33	2.1204605	0.23
tissue	ICAM3-Hs00233674_m1	0	1			0	1					0	1
cells	ICAM3-Hs00233674_m1	-12.126402	4471.1			16.931263	###	0.15649986	0.897	-2.1120796	4.32	8.093487	0.0037
spheres	ICAM3-Hs00233674_m1	6.668644	0.0098	10.660261	###	10.856297	###	-0.023504257	1.016	-8.621447	394	6.5869503	0.0104
migrating spheres	ICAM3-Hs00233674_m1	15.459114	#####			15.266777	###					15.30925	#####
tissue	IL10-Hs99999035_m1					0	1						
cells	IL10-Hs99999035_m1					8.012165	0	-2.9001598	7.465	0.95777893	0.51	1.438057	0.3691
spheres	IL10-Hs99999035_m1			10.563059	###	10.169746	###	2.9030132	0.134				
migrating spheres	IL10-Hs99999035_m1	3.56855	0.0843			12.741241	###						
tissue	IL13-Hs99999038_m1					0	1						
cells	IL13-Hs99999038_m1					10.529955	###			-0.7940407	1.73		
spheres	IL13-Hs99999038_m1					12.930098	###						
migrating spheres	IL13-Hs99999038_m1					8.865469	0			-2.955347	7.76		
tissue	IL15-Hs99999039_m1							0	1				

cells	IL15-Hs99999039_m1					-0.23101616	1.2	-0.3308468	1.258	-0.2972145	1.23	0.47439957	0.7198
spheres	IL15-Hs99999039_m1	9.644241	0.0012	7.619108	0.01	0.19538689	0.9	0.28045654	0.823				
migrating spheres	IL15-Hs99999039_m1	8.576542	0.0026	6.375717	0.01			0.7958565	0.576	1.8960857	0.27		
tissue	IL1R1-Hs00991010_m1			0	1	0	1	0	1	0	1	0	1
cells	IL1R1-Hs00991010_m1	-4.072874	16.829	-6.635874	99.4	-3.2670927	9.6	-2.902504	7.477	-1.2502432	2.38	-0.2504301	1.1896
spheres	IL1R1-Hs00991010_m1	1.5596704	0.3392	-1.7731781	3.42	-0.700407	1.6	-0.5715809	1.486	0.3092003	0.81	2.4337597	0.1851
migrating spheres	IL1R1-Hs00991010_m1	1.7889261	0.2894	-1.4788723	2.79	-0.13144493	1.1	-0.27560043	1.21	-0.24559593	1.19	1.2194138	0.4295
tissue	IL6ST-Hs01006741_m1					0	1	0	1	0	1	0	1
cells	IL6ST-Hs01006741_m1	-5.12438	34.881	-7.486559	179	-3.801015	14	-3.6950836	12.95	-3.2960577	9.82	-2.421729	5.3581
spheres	IL6ST-Hs01006741_m1	0.98315144	0.5059	-1.4260807	2.69	-1.4818583	2.8	-1.3351517	2.523	-1.4496994	2.73	0.61133766	0.6546
migrating spheres	IL6ST-Hs01006741_m1	0.19818783	0.8716	-1.8492985	3.6	-0.9251375	1.9	-0.4921751	1.407	-2.0341892	4.1	-0.7604685	1.694
tissue	IRX3-Hs00735523_m1					0	1	0	1			0	1
cells	IRX3-Hs00735523_m1	-4.059801	16.677	-4.3939953	21	-1.7357807	3.3	-1.8009243	3.484	-2.2431793	4.73	1.7107468	0.3055
spheres	IRX3-Hs00735523_m1	2.8000412	0.1436	1.3137512	0.4	-1.6554089	3.2	-2.0221367	4.062	-4.471195	22.2	0.5560665	0.6802
migrating spheres	IRX3-Hs00735523_m1	2.5499535	0.1708	2.0705109	0.24	-1.9126759	3.8	-2.4646797	5.52	-3.101366	8.58	0.5079918	0.7032
tissue	ITGA5-Hs01547673_m1			0	1	0	1	0	1	0	1	0	1
cells	ITGA5-Hs01547673_m1	-4.3949566	21.038	-6.957205	124	-2.452073	5.5	-1.879158	3.679	-0.8920126	1.86	-2.1738768	4.5123
spheres	ITGA5-Hs01547673_m1	0.60190487	0.6589	-2.9974937	7.99	-0.37419605	1.3	-0.0345459	1.024	-0.4691887	1.38	-1.1964741	2.2918
migrating spheres	ITGA5-Hs01547673_m1	0.1332407	0.9118	-2.869587	7.31	-1.1544809	2.2	-0.82872105	1.776	-1.0535107	2.08	-2.00134	4.0037
tissue	KERA-Hs00559942_m1					0	1	0	1	0	1	0	1
cells	KERA-Hs00559942_m1	-3.0409222	8.2302	-4.1473637	17.7	2.967146	0.1	3.1084385	0.116	0.8049698	0.57	2.8526917	0.1384
spheres	KERA-Hs00559942_m1	-1.1492224	2.2179	-1.4324608	2.7	-4.6525373	25	-4.516405	22.89	-3.8706799	14.6	-2.57333	5.9518
migrating spheres	KERA-Hs00559942_m1	-0.35615253	1.28	-1.5355129	2.9	-3.122714	8.7	-2.8597403	7.259	-4.399763	21.1	-2.6131277	6.1183
tissue	KRT12-Hs00165015_m1					0	1	0	1			0	1
cells	KRT12-Hs00165015_m1					8.9394245	0	8.670982	0.002	0.011756897	0.99	7.8922997	0.0042
spheres	KRT12-Hs00165015_m1	12.63958	#####	10.592039	###	15.35803	###	15.78067	####			9.772715	0.0011
migrating spheres	KRT12-Hs00165015_m1	10.071098	#####	8.275795	0	11.293402	###	11.514605	####	0.883337	0.54	8.961281	0.002
tissue	LAMA2-Hs01124081_m1					0	1	0	1	0	1		
cells	LAMA2-Hs01124081_m1					1.9558163	0.3	4.240732	0.053	5.4380875	0.02		

spheres	LAMA2-Hs01124081_m1	7.5939445	0.0052	4.583954	0.04	0.44634056	0.7	-0.3898182	1.31	6.8718224	0.01	-1.2916622	2.4481
migrating spheres	LAMA2-Hs01124081_m1	7.2992744	0.0063	4.609516	0.04	0.0826664	0.9	1.142868	0.453	0.50156975	0.71	-0.9774437	1.969
tissue	LCN2-Hs00194353_m1					0	1	0	1	0	1	0	1
cells	LCN2-Hs00194353_m1			-1.4125957	2.66	9.169998	0	10.904932	####	3.4246635	0.09	5.6830635	0.0195
spheres	LCN2-Hs00194353_m1					14.953651	###	22.35697	####	5.9934883	0.02	7.9950504	0.0039
migrating spheres	LCN2-Hs00194353_m1	11.363903	#####	9.617146	0	13.870083	###	1.3183317	0.401	8.965815	0	10.207058	#####
tissue	LOX-Hs00942480_m1					0	1	0	1	0	1	0	1
cells	LOX-Hs00942480_m1	-3.0581532	8.3291	-4.530634	23.1	-0.18890572	1.1	-0.5933094	1.509	-0.19764328	1.15	-0.22637558	1.1699
spheres	LOX-Hs00942480_m1	-1.6008482	3.0332	-0.3815899	1.3	-1.823801	3.5	-2.36697	5.159	-1.4742317	2.78	-1.2061596	2.3072
migrating spheres	LOX-Hs00942480_m1	-4.448413	21.833	-0.8918896	1.86	-2.3447351	5.1	-2.7610931	6.779	-2.317133	4.98	-1.9818182	3.9499
tissue	LUM-Hs00158940_m1					0	1	0	1	0	1	0	1
cells	LUM-Hs00158940_m1	-5.0751896	33.712	-7.1552544	143	-0.6874037	1.6	-0.12811661	1.093	1.1391954	0.45	0.606658	0.6567
spheres	LUM-Hs00158940_m1	-3.565236	11.837	-6.457279	87.9	-4.542342	23	-4.2870293	19.52	-1.5664406	2.96	-1.870081	3.6555
migrating spheres	LUM-Hs00158940_m1	-3.0793238	8.4522	-5.360943	41.1	-2.8309317	7.1	-2.6153421	6.128	-2.1130009	4.33	-2.4207563	5.3545
tissue	MMP12-Hs00899668_m1					0	1	0	1			0	1
cells	MMP12-Hs00899668_m1	-5.5038586	45.376	-8.122341	279	-4.8789206	29	-6.8778896	117.6	-7.6782827	205	-6.8799257	117.78
spheres	MMP12-Hs00899668_m1			10.571722	###	3.5383701	0.1	1.5046177	0.352			0.37402916	0.7716
migrating spheres	MMP12-Hs00899668_m1	10.290768	#####			6.513464	0	1.8118324	0.285	1.8441372	0.28	1.7223816	0.303
tissue	MMP3-Hs00968308_m1			0	1	0	1	0	1	0	1	0	1
cells	MMP3-Hs00968308_m1	-10.113518	1107.8	-10.206631	1182	-3.821414	14	-4.243025	18.94	-3.4880247	11.2	-3.6331797	12.408
spheres	MMP3-Hs00968308_m1	4.084797	0.0589	3.7478561	0.07	1.0502386	0.5	0.66124535	0.632	2.4931583	0.18	2.4495087	0.1831
migrating spheres	MMP3-Hs00968308_m1	3.711464	0.0763	2.8138256	0.14	3.4719887	0.1	3.1337967	0.114	1.5211315	0.35	1.4539614	0.365
tissue	MRC1;MRC1L1-Hs00267207_m1							0	1				
cells	MRC1;MRC1L1-Hs00267207_m1					0.7344799	0.6	2.9289608	0.131	1.9903564	0.25	1.466732	0.3618
spheres	MRC1;MRC1L1-Hs00267207_m1	12.731224	#####	10.638235	###	1.4359035	0.4	4.943079	0.033				
migrating spheres	MRC1;MRC1L1-Hs00267207_m1	10.848309	#####	9.370338	0			2.5241852	0.174				
tissue	MSI2-Hs00292670_m1					0	1	0	1	0	1	0	1
cells	MSI2-Hs00292670_m1			-3.7612514	13.6	-0.064668655	1	-0.18061829	1.133	0.027042389	0.98	-3.01E-04	1.0002

spheres	MSI2-Hs00292670_m1	3.6263962	0.081	0.71194077	0.61	-0.5720835	1.5	-0.87304115	1.832	0.54325867	0.69	0.30018044	0.8122
migrating spheres	MSI2-Hs00292670_m1	3.1657715	0.1114	0.6479492	0.64	0.10625267	0.9	-0.054142	1.038	-0.5170555	1.43	-0.228302	1.1715
tissue	MSN-Hs00792607_mH					0	1	0	1	0	1	0	1
cells	MSN-Hs00792607_mH	-4.0822163	16.938	-6.52055	91.8	-2.0685225	4.2	-2.3817635	5.212	-1.8429937	3.59	-1.0371122	2.0521
spheres	MSN-Hs00792607_mH	-1.0433874	2.0611	-3.1106033	8.64	-0.10832119	1.1	-0.6110344	1.527	-1.0484028	2.07	0.47550774	0.7192
migrating spheres	MSN-Hs00792607_mH	-1.5620832	2.9528	-3.3435116	10.2	-0.22467327	1.2	-0.59063816	1.506	-1.8277588	3.55	-0.65160275	1.5709
tissue	NEUROD1-Hs00159598_m1											0	1
cells	NEUROD1-Hs00159598_m1	-27.705414	#####			0.6927166	0.6			-0.6362343	1.55	11.206402	#####
spheres	NEUROD1-Hs00159598_m1					-2.4511127	5.5			-8.195951	293	8.493864	0.0028
migrating spheres	NEUROD1-Hs00159598_m1											10.705872	#####
tissue	NOTCH1-Hs01062014_m1					0	1	0	1			0	1
cells	NOTCH1-Hs01062014_m1			-1.40518	2.65	0.68577003	0.6	1.0941772	0.468	-2.4195518	5.35	-0.259243	1.1969
spheres	NOTCH1-Hs01062014_m1	4.681099	0.039	1.0780563	0.47	2.9188824	0.1	2.6568184	0.159	-2.0559425	4.16	0.95160484	0.5171
migrating spheres	NOTCH1-Hs01062014_m1	5.36948	0.0242	2.4982834	0.18	2.5258656	0.2	1.4069176	0.377	-2.2120838	4.63	0.29140472	0.8171
tissue	OGN-Hs00247901_m1							0	1				
cells	OGN-Hs00247901_m1					0.7407932	0.6	7.2235775	0.007			1.4402809	0.3685
spheres	OGN-Hs00247901_m1	2.8052979	0.1431	0.4433403	0.74	-8.468019	354	-5.636162	49.73	-3.115509	8.67	-4.946867	30.843
migrating spheres	OGN-Hs00247901_m1	3.293129	0.102	1.628191	0.32	-6.513113	91	-3.652073	12.57	-3.0917263	8.53	-4.2076797	18.477
tissue	PARD6A-Hs00180947_m1									0	1		
cells	PARD6A-Hs00180947_m1					-1.1332722	2.2	-1.2849331	2.437	0.052951813	0.96	-0.7080307	1.6336
spheres	PARD6A-Hs00180947_m1	11.690998	#####	7.620035	0.01	-0.8302479	1.8	-0.80539894	1.748	1.4371071	0.37		
migrating spheres	PARD6A-Hs00180947_m1	10.054428	#####	6.723194	0.01			-1.3124123	2.484	-0.623106	1.54	-0.04711914	1.0332
tissue	PAX6-Hs01088112_m1					0	1	0	1	0	1	0	1
cells	PAX6-Hs01088112_m1					6.505354	0	6.1205997	0.014	9.077419	0	8.520123	0.0027
spheres	PAX6-Hs01088112_m1	10.655514	#####	9.044649	0	10.93038	###	10.798693	####	5.990505	0.02	5.807585	0.0179
migrating spheres	PAX6-Hs01088112_m1	9.342201	0.0015	7.6965485	0	9.896605	0	9.58461	0.001	8.9628315	0	8.019592	0.0039
tissue	PDGFRA-Hs00998018_m1					0	1	0	1	0	1	0	1
cells	PDGFRA-Hs00998018_m1	-5.421629	42.862	-6.754719	108	-1.2993193	2.5	-1.5799828	2.99	-0.5804777	1.5	-0.54274654	1.4567
spheres	PDGFRA-Hs00998018_m1	-0.9430971	1.9227	-3.451641	10.9	-1.8249369	3.5	-2.391367	5.247	0.31901932	0.8	0.13337135	0.9117

migrating spheres	PDGFRA-Hs00998018_m1	-1.7042398	3.2586	-3.9052162	15	-1.1113825	2.2	-1.379775	2.602	-0.7874031	1.73	-0.33856297	1.2645
tissue	PITX2-Hs00374154_m1							0	1	0	1		
cells	PITX2-Hs00374154_m1					-0.15100288	1.1	4.661577	0.04	3.7225533	0.08	1.5693893	0.337
spheres	PITX2-Hs00374154_m1	9.59874	0.0013	7.6204624	0.01	-3.2565098	9.6	1.0972481	0.467	3.2569504	0.1	-2.090311	4.2584
migrating spheres	PITX2-Hs00374154_m1	10.365002	#####	7.994549	0	-0.97431755	2	3.2209663	0.107	3.4818707	0.09	-0.6841965	1.6068
tissue	PLA2G7-Hs00173726_m1							0	1			0	1
cells	PLA2G7-Hs00173726_m1					-1.6507664	3.1	-0.5775776	1.492	1.0287476	0.49	1.245964	0.4216
spheres	PLA2G7-Hs00173726_m1	11.405315	#####	9.216623	0	-0.6993351	1.6	-1.4179764	2.672			4.8345737	0.035
migrating spheres	PLA2G7-Hs00173726_m1	11.322563	#####	8.635883	0	-0.93525124	1.9	-1.511013	2.85			7.0465813	0.0076
tissue	POU5F1;POU5F1P3-Hs01895061_u1	0	1	0	1	0	1	0	1	0	1	0	1
cells	POU5F1;POU5F1P3-Hs01895061_u1	1.5976009	0.3304	0.8152962	0.57	4.0751266	0.1	4.4699783	0.045	6.979986	0.01	7.3796005	0.006
spheres	POU5F1;POU5F1P3-Hs01895061_u1	12.787098	#####	12.345823	###	6.359661	0	6.6231976	0.01	6.2967587	0.01	8.008123	0.0039
migrating spheres	POU5F1;POU5F1P3-Hs01895061_u1	11.461048	#####	11.162691	###	8.174065	0	7.756481	0.005	8.610424	0	8.664307	0.0025
tissue	PROM1-Hs01009250_m1			0	1								
cells	PROM1-Hs01009250_m1			22.45132	###	0.76096916	0.6						
spheres	PROM1-Hs01009250_m1	12.644165	#####	18.059189	###			3.172491	0.111				
migrating spheres	PROM1-Hs01009250_m1	11.31292	#####	21.987366	###					-6.918154	121	-3.052803	8.2982
tissue	PRRX1-Hs00246569_m1					0	1	0	1	0	1	0	1
cells	PRRX1-Hs00246569_m1	-6.060953	66.762	-7.4026146	169	-2.04733	4.1	-2.3752022	5.188	-1.1994467	2.3	-2.0709867	4.2017
spheres	PRRX1-Hs00246569_m1	-0.860507	1.8157	-3.1033764	8.59	-1.5645819	3	-1.9151955	3.772	-0.1348629	1.1	-0.6621895	1.5825
migrating spheres	PRRX1-Hs00246569_m1	-0.93687344	1.9144	-3.100584	8.58	-0.65926266	1.6	-1.3720675	2.588	-0.82803345	1.78	-1.435504	2.7048
tissue	PRRX2-Hs00212537_m1					0	1	0	1	0	1	0	1
cells	PRRX2-Hs00212537_m1	-3.0796795	8.4543	-3.8497334	14.4	-2.4135723	5.3	-1.6427746	3.123	-0.01531982	1.01	0.48566437	0.7142
spheres	PRRX2-Hs00212537_m1	2.7125664	0.1526	1.7189236	0.3	-0.98026085	2	-0.32235336	1.25	-0.7839165	1.72	-0.22406197	1.168
migrating spheres	PRRX2-Hs00212537_m1	2.607174	0.1641	1.6890697	0.31	-0.5325794	1.4	-0.3147545	1.244	0.07060051	0.95	0.7481346	0.5954
tissue	PTGDS-Hs00168748_m1					0	1	0	1	0	1	0	1
cells	PTGDS-Hs00168748_m1	-7.619211	196.61	-9.146032	567	-0.8070688	1.7	-0.8643017	1.82	0.9926176	0.5	0.9295664	0.525
spheres	PTGDS-Hs00168748_m1	-1.4287672	2.6922	-3.6767426	12.8	-0.12893581	1.1	-0.43615723	1.353	0.68632317	0.62	0.955534	0.5157

migrating spheres	PTGDS-Hs00168748_m1	-0.20450115	1.1523	-2.37051	5.17	0.28931332	0.8	0.20761585	0.866	1.6579876	0.32	1.9954977	0.2508
tissue	RAC1-Hs01025984_m1					0	1	0	1	0	1	0	1
cells	RAC1-Hs01025984_m1					3.5269794	0.1	3.5957584	0.083	3.6999817	0.08	4.192768	0.0547
spheres	RAC1-Hs01025984_m1	5.042698	0.0303	2.567402	0.17	2.3138103	0.2	2.104025	0.233	3.662159	0.08	0.39523125	0.7604
migrating spheres	RAC1-Hs01025984_m1	4.3369713	0.0495	1.962595	0.26	2.3960514	0.2	1.6640587	0.316	0.43966293	0.74	-0.4641838	1.3795
tissue	ROCK2-Hs00178154_m1					0	1	0	1	0	1	0	1
cells	ROCK2-Hs00178154_m1	-3.1316051	8.7641	-5.4411488	43.4	-0.5880804	1.5	-0.7397499	1.67	0.7357569	0.6	-1.0159178	2.0222
spheres	ROCK2-Hs00178154_m1	2.2078438	0.2165	0.58470917	0.67	1.1658459	0.4	0.9770546	0.508	0.8920822	0.54	0.27784538	0.8248
migrating spheres	ROCK2-Hs00178154_m1	0.9433336	0.52	-0.48075676	1.4	0.6989794	0.6	1.2715263	0.414	0.29873085	0.81	-0.7284937	1.6569
tissue	SC4MOL-Hs00932159_m1					0	1	0	1	0	1	0	1
cells	SC4MOL-Hs00932159_m1			-3.7412357	13.4	3.483204	0.1	3.3419743	0.099	4.370533	0.05	3.1240578	0.1147
spheres	SC4MOL-Hs00932159_m1	1.6260653	0.324	-1.230402	2.35	2.6659431	0.2	2.2530727	0.21	1.379673	0.38	0.9293194	0.5251
migrating spheres	SC4MOL-Hs00932159_m1	0.36028957	0.779	-2.378378	5.2	1.1626673	0.4	1.080802	0.473	-0.41806793	1.34	-0.480052	1.3948
tissue	SHOX2-Hs00243203_m1												
cells	SHOX2-Hs00243203_m1					-1.599741	3	-1.8956394	3.721			0.4172554	0.7488
spheres	SHOX2-Hs00243203_m1	10.614498	#####	8.853548	0	2.1163807	0.2	1.2040195	0.434				
migrating spheres	SHOX2-Hs00243203_m1			9.654072	0								
tissue	SOX10-Hs00366918_m1							0	1				
cells	SOX10-Hs00366918_m1			-2.4168415	5.34	1.115282	0.5	1.8177776	0.284	0.011348724	0.99	-1.5238647	2.8756
spheres	SOX10-Hs00366918_m1	7.8517838	0.0043	6.1320286	0.01	-2.887617	7.4	2.356554	0.195				
migrating spheres	SOX10-Hs00366918_m1	10.345093	#####	7.3654213	0.01			6.013626	0.015	0.74746513	0.6		
tissue	TGFBI-Hs00932734_m1			0	1	0	1	0	1	0	1	0	1
cells	TGFBI-Hs00932734_m1	-6.33494	80.725	-6.7561893	108	0.7914915	0.6	1.0670853	0.477	1.008893	0.5	0.46072102	0.7266
spheres	TGFBI-Hs00932734_m1	-2.3495474	5.0966	-2.1633625	4.48	-0.06927776	1	-0.24081993	1.182	0.7583847	0.59	1.0180492	0.4938
migrating spheres	TGFBI-Hs00932734_m1	-1.238658	2.3598	-0.8995056	1.87	1.6353846	0.3	1.2788153	0.412	0.8734436	0.55	0.3939638	0.761
tissue	TJP2-Hs00910541_m1					0	1	0	1	0	1	0	1
cells	TJP2-Hs00910541_m1			-3.581152	12	0.38420677	0.8	0.68554306	0.622	-0.4663887	1.38	0.17453384	0.8861
spheres	TJP2-Hs00910541_m1	5.6352425	0.0201	3.442686	0.09	4.2111263	0.1	4.2051735	0.054	1.8690338	0.27	7.405119	0.0059
migrating	TJP2-Hs00910541_m1	3.7911263	0.0722	1.6679955	0.31	3.2478313	0.1	3.3277283	0.1	1.7234325	0.3	2.5632973	0.1692

spheres													
tissue	TKT-Hs01115545_m1					0	1	0	1	0	1	0	1
cells	TKT-Hs01115545_m1	-3.0747242	8.4253	-4.4121532	21.3	0.88203144	0.5	0.5571251	0.68	0.6860609	0.62	1.252717	0.4197
spheres	TKT-Hs01115545_m1	0.3612051	0.7785	-1.1347065	2.2	2.6504602	0.2	2.0413322	0.243	0.001272202	1	0.50359154	0.7053
migrating spheres	TKT-Hs01115545_m1	-0.6449747	1.5637	-1.9494438	3.86	2.0701704	0.2	1.7693682	0.293	-0.55319786	1.47	0.27716732	0.8252
tissue	TP63-Hs00978349_m1			0	1	0	1	0	1	0	1	0	1
cells	TP63-Hs00978349_m1			-0.6638279	1.58	7.288622	0	1.5836582	0.334	7.9335938	0	7.1844597	0.0069
spheres	TP63-Hs00978349_m1	11.495438	#####	7.953001	0	2.5276546	0.2	-1.3202667	2.497	4.8466797	0.03	4.471922	0.0451
migrating spheres	TP63-Hs00978349_m1	11.324905	#####	7.348648	0.01	8.630995	0	4.8968277	0.034	2.2187138	0.21	-1.8317909	3.5598
tissue	WISP1-Hs00365573_m1											0	1
cells	WISP1-Hs00365573_m1					0.12688255	0.9	0.32591438	0.798			7.5609856	0.0053
spheres	WISP1-Hs00365573_m1	4.2617264	0.0521	2.3183537	0.2	-3.7789822	14	-1.6420002	3.121	-2.0165863	4.05	4.848448	0.0347
migrating spheres	WISP1-Hs00365573_m1	6.326954	0.0125	4.680626	0.04	-0.90587425	1.9	-1.0032768	2.005	1.8775806	0.27	7.0604553	0.0075